Temporal Control over Self-Assembly and Helicity of Supramolecular Polymers

A Thesis

Submitted in partial fulfillment for the degree of

Master of Science

as a part of

Integrated Ph.D. Programme (Chemical Sciences)

By

Shikha Dhiman

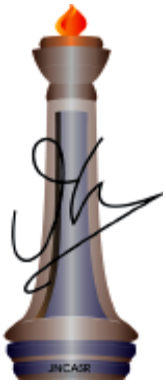

New Chemistry Unit

Jawaharlal Nehru Centre for Advanced Scientific Research

(A Deemed University)

Bangalore - 560064 (INDIA)

MARCH 2017

Dedicated to my Family

DECLARATION

I hereby declare that the matter embodied in the thesis entitled "**Temporal Control over Self-assembly and Helicity of Supramolecular Polymers**" is the result of investigations carried out by me at the New Chemistry Unit, Jawaharlal Nehru Centre for Advanced Scientific Research, Bangalore, India under the supervision of Prof. Subi J. George and that it has not been submitted elsewhere for any degree or diploma.

In keeping with the general practice in reporting scientific observations, due acknowledgement has been made whenever the work described is based on the findings of other investigators. Any omission that might have occurred by oversight or error of judgment is regretted.

March 2017 Shikha Dhiman

Jawaharlal Nehru Centre for Advanced Scientific Research

Prof. Subi J. George
New Chemistry Unit
Jawaharlal Nehru Centre for Advanced Scientific Research (JNCASR)
Bangalore-560064,India
Phone : +91 80 2208 2964
Fax: + 91 80 22082627
Date:
March, 2015

CERTIFICATE

I hereby certify that the work described in this thesis titled "**Temporal Control over Self-assembly and Helicity of Supramolecular Polymers**" has been carried out by Ms. Shikha Dhiman at the New Chemistry Unit, Jawaharlal Nehru Centre for Advanced Scientific Research, Bangalore, India under my supervision and it has not been submitted elsewhere for the award of any degree or diploma.

Prof. Subi J. George

(Research Supervisor)

ACKNOWLEDGEMENTS

Firstly I would like to thank my research supervisor Prof. Subi J. George for his constant guidance and support throughout the course of my research. I am very grateful to him for suggesting such an interesting project and encouraging me towards new explorations. His ever-enthusiastic nature, constant encouragement and support has helped me in successful completion of this work. He always inspired me in my research work and also taught how to become a good researcher and successful person in life. I also acknowledge the academic freedom that I enjoyed in the lab.

I would also like to thank the Chairman of New Chemistry Unit, Prof. C. N. R. Rao, F.R.S., for being a source of constant inspiration. I am also thankful to him for providing necessary facilities to carry out this work.

I express my sincere gratitude to Dr. Mohit Kumar and Dr. Ankit Jain for their fruitful discussions and guidance during the course of this work and manuscript writing. I would also like to thank Mr. Aritra Sarkar for his help during the synthesis of molecules and Ms. Ananya Mishra for her excellent training photophysical studies.

I would like to thank all the faculty members of NCU, CPMU and MBGU for the various courses which were extremely helpful to me. I express my sincere gratitude to Prof. Sridhar Rajaram for fruitful discussion.

It is my great pleasure to thank my other lab mates Chidambar Kulkarni, Bhawani Narayan, Krishnendu Jalani and Suman Kuila for many fruitful discussions that we had all through my research.

I am privileged to have wonderful friends Ekashmi, Chaitali, Sruthi, Sreemayi, Pavitra and Ananya. I thank them for all the help during my ups and downs in research life and also for their friendship that makes JNCASR a special place to live.

I would also like to thank Mahesh, Shiva, Usha ma'am and Suma ma'am for their help in characterization techniques. I thank all the academic, library, technical, and complab staff at JNCASR.

I would also like to thank my college teachers and school teachers for their encouragement and blessings.

I express my deepest love for my dear friends Mona, Sumedh, Ashima, Nikhil and Kabir for being there whenever I needed.

Finally I thank my family members and specially my grandparents for their encouragement, support and love.

TABLE OF CONTENTS

CHAPTER-1 (*Introduction)*

Temporally Programmable Supramolecular Polymers

CHAPTER-2

Temporally Controlled Conformational Switching in a Supramolecular Polymer

CHAPTER-3

Chemical Fuel-Driven Temporal Control on Self-assembly

CHAPTER-4

Transient Helicity: Temporally Modulated Helical Self-assembly

OUTLOOK

Temporal Control on Supramolecular Assemblies and their Functions

Chapter 1 (Introduction)

Temporally Programmable Supramolecular Polymers

Chapter 1 (Introduction)

Temporally Programmable Supramolecular Polymers

Abstract

Supramolecular polymerization has been inspired from biological systems such as microtubules and actin filaments that self-assemble from small monomers and are functional in their aggregated state. In synthetic systems, self-assembly of small molecules to construct supramolecular polymers has been well investigated for understanding the mechanism of polymerization and role of the non-covalent interactions. These understandings has enabled us to pre-program monomers to attain a variety of morphologies and properties under thermodynamic control and however they lack in temporal programming. On the other hand, biological systems which are the source of inspiration for self-assembly have spatio-temporal control over their self-organization owing to the non-equilibrium instability of these self-organized state. Herein, we discuss conventional thermodynamic self-assembly based on their mechanism and a comprehensive review of various strategies utilized to obtain assemblies under non-equilibrium and for a temporal control over their self-organization.

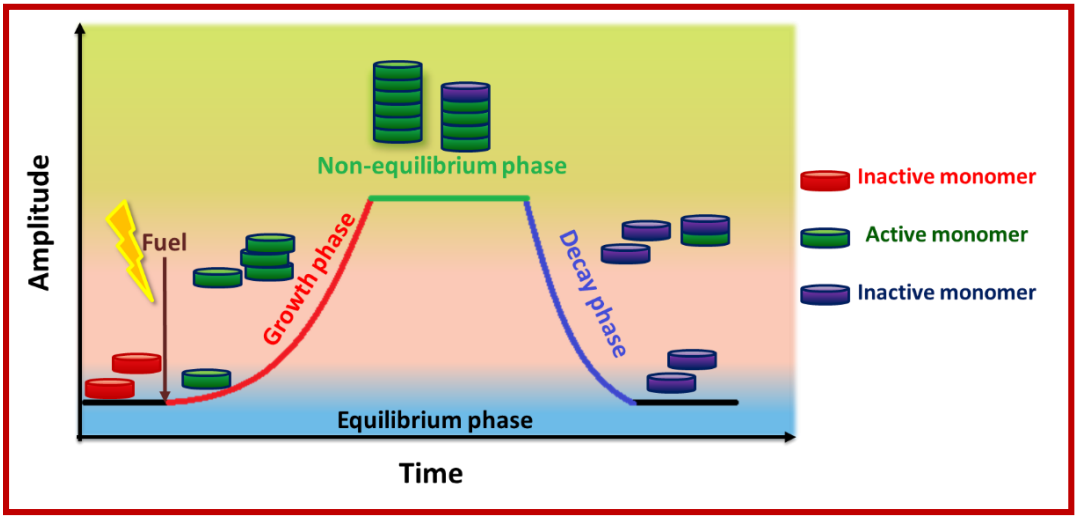

1.1 Introduction

Supramolecular chemistry has led to several novel ideas to develop a variety of applications which majorly concern the morphology and organization in spatial domains.[1-5] These supramolecular motifs have also been developed to form dynamic systems which are responsive to stimuli. However, supramolecular systems are inspired from biological systems but in reality mimicking natural systems is still a challenge to overcome.[6] This key challenge is because natural systems are complex matter and have perfect spatial and temporal control over their self-organization.

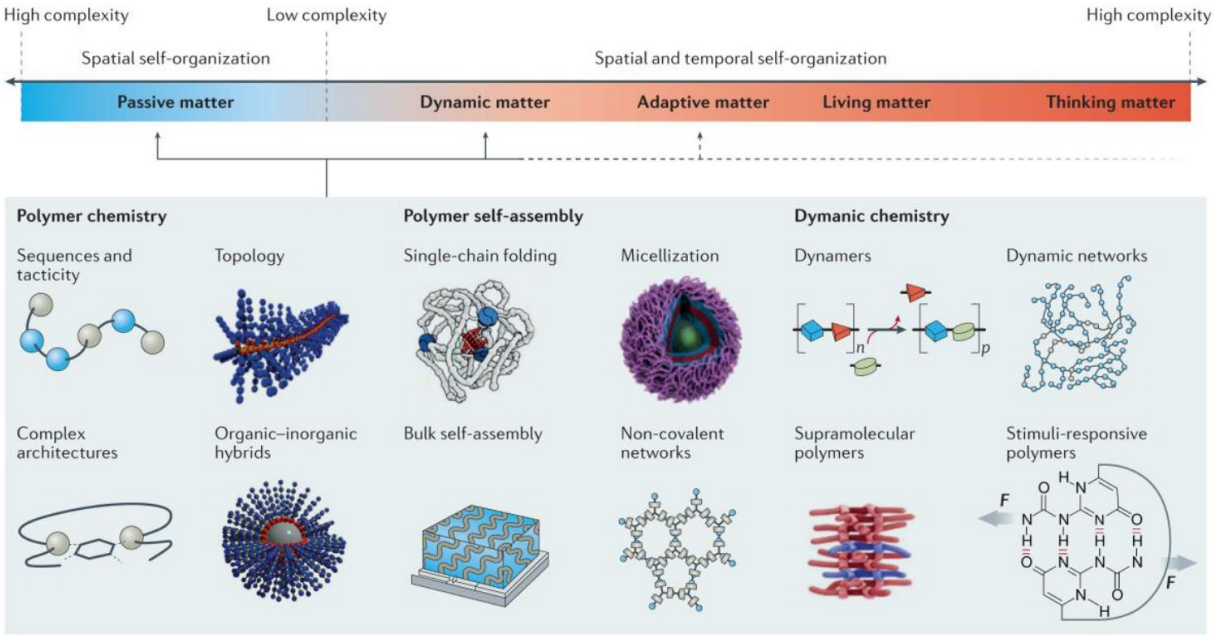

Figure 1.1*: Schematic showing the shift from conventional self-assembled materials to complex soft matter. The figure shows the current state of (supra)polymeric materials and the challenges ahead for soft matter differentiated by their spatial and temporal degrees of freedom (Figure reprinted with permission from Ref. 8).*

This differentiates living beings from animate matter as we can think, adapt to environment etc. The biological system is more than a structure in fact it is the basis of its functions.[7] The key to solve this challenge owes to the property of natural systems to work under non-equilibrium, also known as far-from-equilibrium state. Understanding non-equilibrium systems is a step towards building up life-like systems with a spatio-temporal control. Since we have been able to achieve spatial control over self-organization as in case of dynamic matter such as conventional supramolecular polymers, stimuli responsive polymers and so on that are generally in

thermodynamic equilibrium and metastable (kinetic equilibrium) (Figure 1.1). It is a need to design strategies to have time control over self-organization of matter and their properties that work out-of-equilibrium. [8]

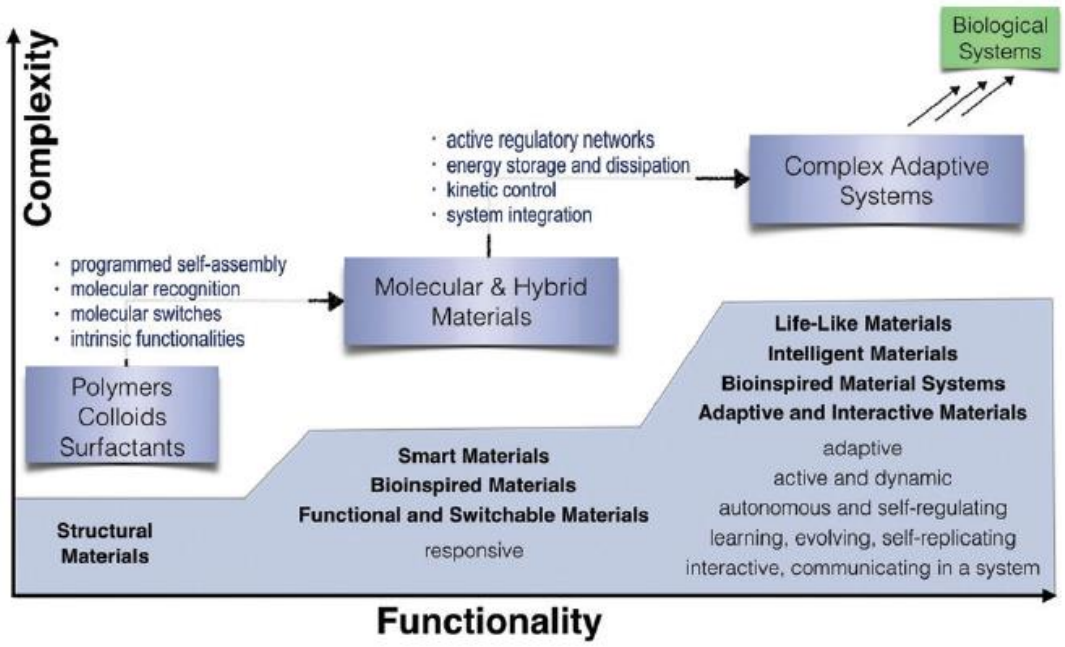

Figure 1.2: *Schematic correlates the present structural materials to responsive materials to active/adaptive systems (Figure adapted with permission from Ref. 18).*

The temporal control in the property profiles of soft matter require the development of out-of-equilibrium, fueled and feedback-controlled molecular systems. These can show programmable and autonomous dynamicity in the temporal regime which will be able to function as life-like systems with ability to sense, adapt, communicate, learn, evolve and replicate (Figure 1.2).[8-14] This needs to be addressed for the intellectual challenge it possesses. Additionally, building of complex systems with the desired control and precision shall bring down the curtain on the true potential of supramolecular assemblies towards prospective applications.[15-18]

This thesis aims at understanding biological systems which work under non-equilibrium to attain temporal control over self-organization with design strategies employing chemical fuels and enzymes.

1.2 Temporal State of System

A key difference between synthetic and natural system is its temporal state. Synthetic systems are at equilibrium and are referred as passive system. In contrast, natural systems are under non-equilibrium and are thus active in behaviour.[19] Following are the important difference between these two states.

Passive materials which are at equilibrium can be sub-classified as system under thermodynamic equilibrium and system under kinetic equilibrium. System under thermodynamic equilibrium are in the global minima of energy and the states are defined by Boltzmann distribution (Figure 1.3a). Since these systems are at energy minima, they are highly stable and do not change their state with time. A very high energy is required for system to undergo any change due to high activation barrier. These systems are pathway independent as every system has only one global minima. In case of system under kinetic equilibrium (Figure 1.3b), the system is at higher energy state other than the global energy minima or thermodynamic equilibrium state. Even though the system is at higher energy state and has tendency to fall into thermodynamic equilibrium state, there is a high activation energy barrier that traps this kinetic state and prohibits its energy dissipation and falling into global minima. Thus, system doesn't change its state with time but the system is pathway dependent, which means identical system when are subjected to different ambient conditions may lead to different kinetic equilibrium.

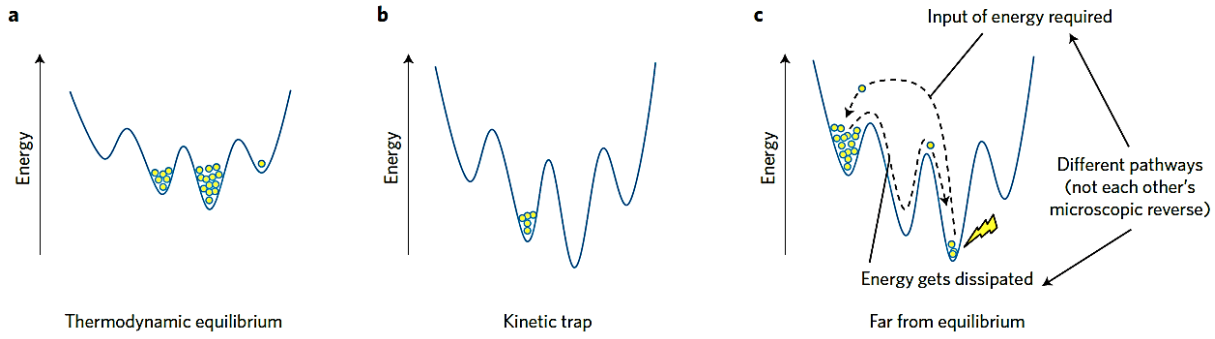

***Figure 1.3**: Temporal states of system: a) Thermodynamic equilibrium- System is at global minimum energy state determined by the Boltzmann distribution. b) Kinetic control- System is at higher energy state than thermodynamic equilibrium determined by synthetic pathway. c) Far-from-equilibrium- Systems at higher energy state than thermodynamic equilibrium with low energy barrier, the final state is determined by balance between input of energy and energy dissipation (Figure reprinted with permission from Ref. 19).*

Active systems reside under non-equilibrium state (Figure 1.3c). When a system at thermodynamic equilibrium is given sufficient energy to go to a higher energy state and the activation barrier to come back to thermodynamic equilibrium is small enough to be crossed at ambient conditions, this high energy state is referred as non-equilibrium state. Although it is similar to kinetic equilibrium state but there is a key difference of activation barrier. Kinetic equilibrium state has high energy barrier that prohibits its falling into thermodynamic equilibrium, whereas, non-equilibrium state has low energy barrier and it dissipates energy and falls into thermodynamic equilibrium. As the name suggests active systems require energy source to stay under non-equilibrium, so energy shut down leads to equilibrium state. Moreover, amount of energy provided determines the time lapse when the system is under non-equilibrium. Thus, energy source becomes an important parameter to keep system under non-equilibrium and to modulate the lifetime of non-equilibrium state.

1.3 Conventional Supramolecular Polymerization

Conventional supramolecular polymerization occurs under thermodynamic control[20] and are at equilibrium. However, to design systems under non-equilibrium we need to understand the conventional self-assembly which act as pillars for further strategies. Based on mechanism of growth, supramolecular polymerization is divided into two types, namely, Isodesmic growth and Cooperative growth.[21] Molecular designs with different non-covalent interaction leads to different growth mechanism which has constraints over equilibrium states.

1.3.1 Isodesmic Growth Mechanism

Isodesmic growth, also known as equal K growth model is defined as mechanism of growth that occurs via identical energy steps (Figure 1.4a). This means that the association constants of $(i+1)^{th}$ monomer with the self-assembled polymer is same as i^{th} monomer that assembled before it. As mentioned, equal association constant refers to the system where successive addition of monomers leads to a constant decrease in the free energy i.e. every monomer has equal affinity to assemble independent of the length of the polymer (Figure 1.4b). The length of polymer increases with higher availability of monomers and the number average degree of polymerization id given

as $C_t^{0.5}$, where C_t is the monomer concentration (Figure 1.4c). However, there are two limitations of this type of growth. Firstly, independency of monomers on polymer length results in high polydispersity index (PDI) of about 2, which is high enough to limit its material applications.

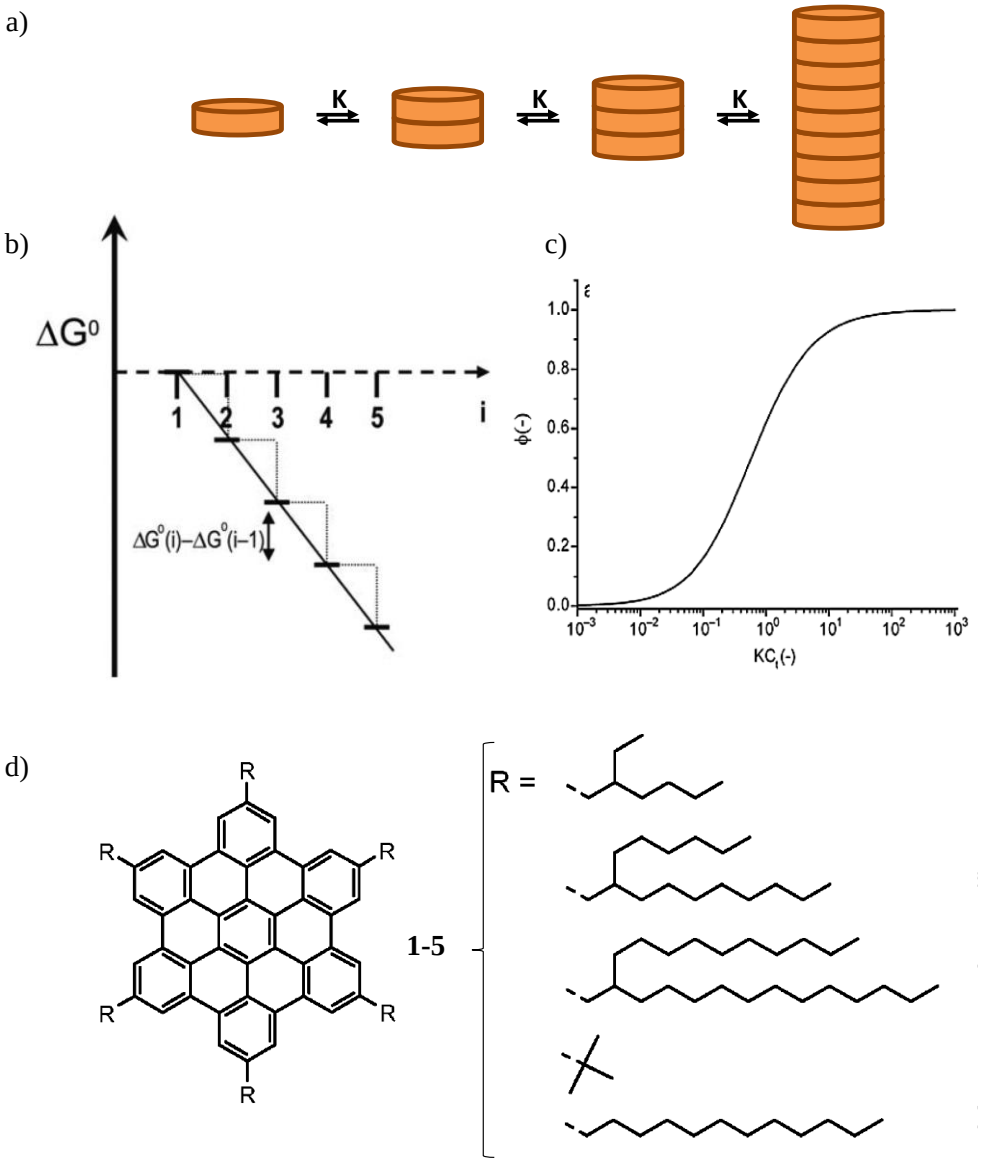

Figure 1.4*: Isodesmic growth mechanism. a) Schematic representation of the equal-K isodesmic growth mechanism. b) Graphical representation of change in Gibbs free energy with increase of aggregate size. c) Effect of concentration on increase in fraction of monomers in aggregated state. d) Molecular structures of various HBC derivatives which show isodesmic growth (Figure 1.4b,c reprinted with permission from Ref. 20 and Figure 1.4d from Ref. 22).*

Secondly, to have high number average degree of polymerization, the association constant of monomers should be very high (>10^6 M^{-1}). Molecules such as hexa-peri-hexabenzocoronene

(HBC) shows isodesmic growth behavior (Figure 1.4d). Literature reports suggest that isodesmic growth could be due to lack of molecular rigidity and/or a macro-dipole along the growth axis.[23]

1.3.2 Cooperative Growth Mechanism

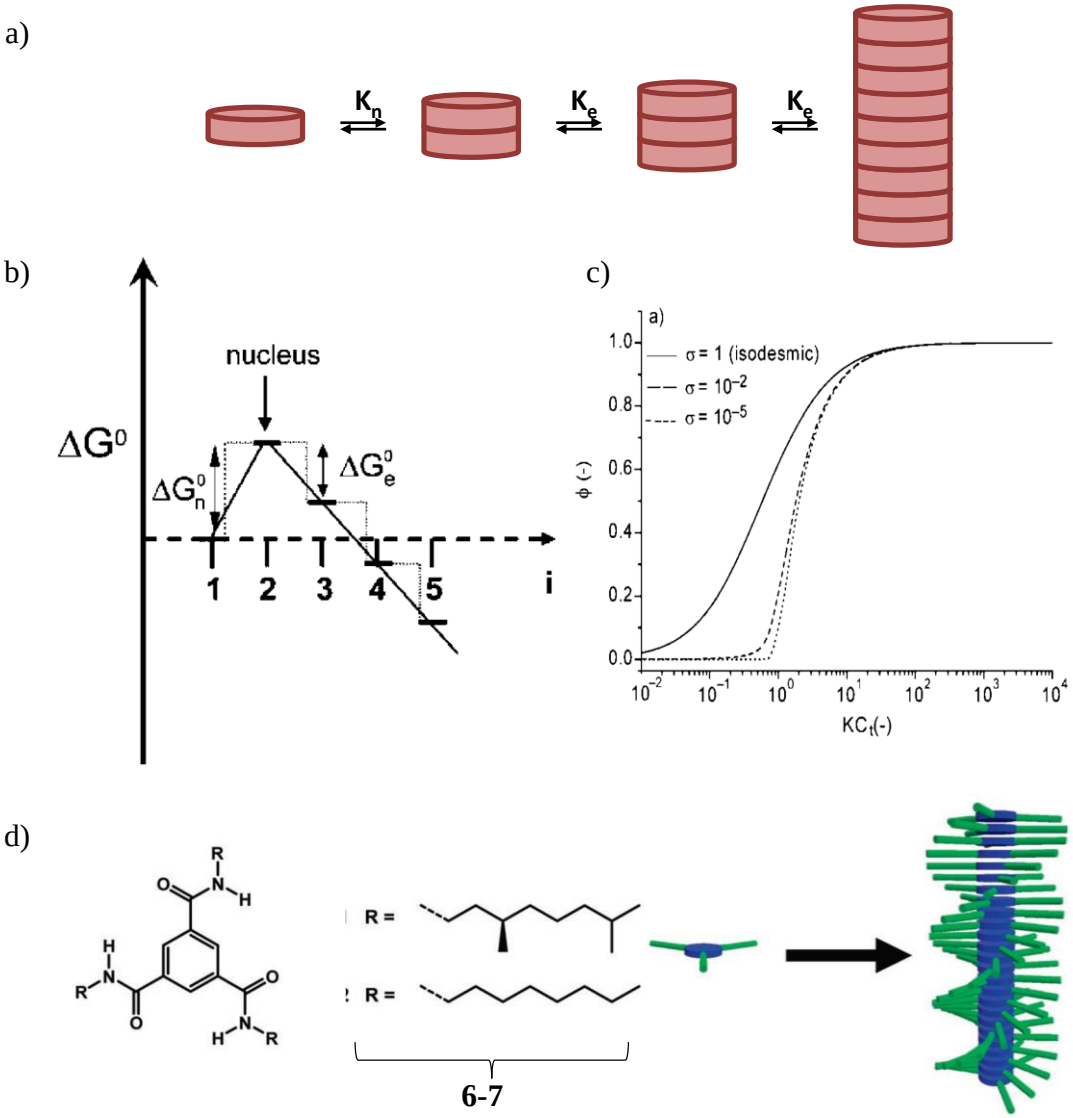

Figure 1.5*: Cooperative growth mechanism. a) Schematic representation of the nucleation-elongation cooperative growth mechanism. b) Graphical representation of change in Gibbs free energy with increase of aggregate size. c) The effect of concentration on increase in fraction of monomers in aggregated state. d) Molecular structures of various BTA derivatives which show co-operative growth (Figure 1.5b,c reprinted with permission from Ref. 20 and Figure 1.5d from Ref. 24).*

Cooperative growth mechanism, also known as nucleation-elongation growth model is defined as mechanism of growth that occurs *via* two distinct energy steps (Figure 1.5a). The first energy stage is isodesmic growth to reach critical polymer length referred as critical nuclei size with association constant K_n, known as nucleation equilibrium constant. The second energy stage is linear isodesmic growth of monomers over the nuclei formed with association constant of K_e, known as elongation equilibrium constant. The second stage is referred as growth phase. This means that the association constants of $(n+1)^{th}$ monomer with the self-assembled polymer is different than that of as n^{th} monomer that assembled before it, where n is critical nuclei size. Thus, in nucleation phase there is an increase in free energy which is energetically unfavourable and is the least prevalent species in the system (Figure 1.5b). After formation of nuclei, there is a constant decrease in free energy with subsequent addition of monomers. An important parameter of cooperative growth mechanism is cooperativity factor (σ) defined as ratio of nucleation to elongation equilibrium constant i.e. K_n/K_e. In general, cooperativity factor is less than 1 and lower the value of σ indicates higher cooperativity in the system. Important advantage of cooperative system is higher degree of polymerization can be achieved by lower σ value and/or higher association constant (Figure 1.5c). There is a bimodal distribution in size due to presence of monomers (less than critical nuclei size) and polymers of significant length. Molecules such as C3-symmetrical trialkylbenzene-1,3,5-tricarboxamides (BTA) undergo cooperative growth and have σ value $2.3x10^{-2}$ (Figure 1.5d).[24,25] Reports suggests that macro-dipole created by Hydrogen bonding is considered to be responsible for this cooperativity.[26] These basic mechanisms define thermodynamically controlled polymerization which constitute passive self-assemblies which are dynamic but are stable, however, to mimic biological systems we need to have polymerization under non-equilibrium which are unstable under ambient conditions.

1.4 Temporal Control in Natural Systems

The goal of temporal control can be addressed by understanding the strategies employed by natural systems which have a plenty of synchronized or disconnected time-regulated functions. Amongst these are the pumping of blood by heart with rhythmic pacemaker activity, the synchronization of day and night cycle on earth with metabolic functions and periodic growth and division of cells. The efficiency of these periodicity and oscillatory networks is regulated by

chemical signals which interconnect different networks and oscillators together resulting in a synchronized communication of their functions in temporal regimes. An important characteristic of these systems is their oscillatory behavior where a feedback control of the system is a requisite. These require a negative feedback loop to act as a reset pathway to reach the initial state. One of the interesting examples is of the circadian clock which has an oscillating period of 24 hours which as discussed above control various metabolic and non-metabolic functions.[27] The circardian rhythm is maintained by several transcription-translation-regulation feedback loop that simulates the peripheral circardian rhythm in synchrony to modulate the macroscopic functions in temporal regime (Figure 1.6).

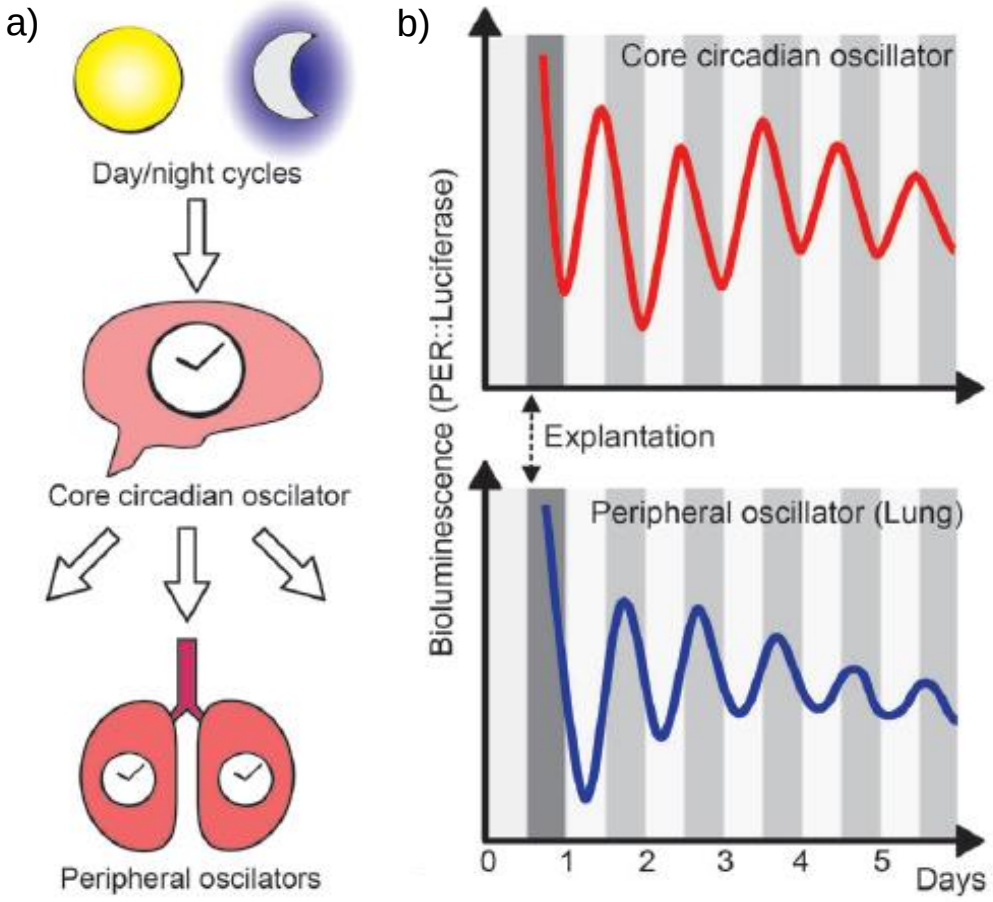

Figure 1.6: *a) Schematic representation of the regulation of day and night cycles on earth to the core circardian clock and its synchrony to the metabolic clock and peripheral oscilators. b) Real time visualization of time delay between core circardian clock and peripheral oscillators (Figure adapted with permission from Ref. 18).*

Circadian rhythms show a periodicity of 24 hours, on the other extreme transmembrane potentials have a periodicity in second regime. Transmembrane potentials in nerves stimulate muscle contractions and maintain the pacemaker activity for cardiac contraction and therefore pumping of blood by heart. Each cycle of transmembrane potential begin with cooperative opening of sodium and potassium channels which act as the positive feedback upon depolarization that allow propagation of electrical impulse.[28,29] Then hyperpolarization-activated ion channels result in a negative feedback mechanism driving the autonomous oscillations. Hence, engineering time delays is essential to obtain autonomous oscillations. Also, these networks involve adaptation mechanism to change in external parameters such as environment.

In transmembrane proteins, ATP acts as the molecular cue for conformational changes, these proteins are classified under ATP-binding cassette transporters (ABC transporters). They utilize ATP as chemical fuel to drive non-equilibrium conformational switching to facilitate the translocation of a variety of different substrates such as ions, toxins etc. across the membranes by the consumption of ATP binding and hydrolysis energy (Figure 1.7).[30]

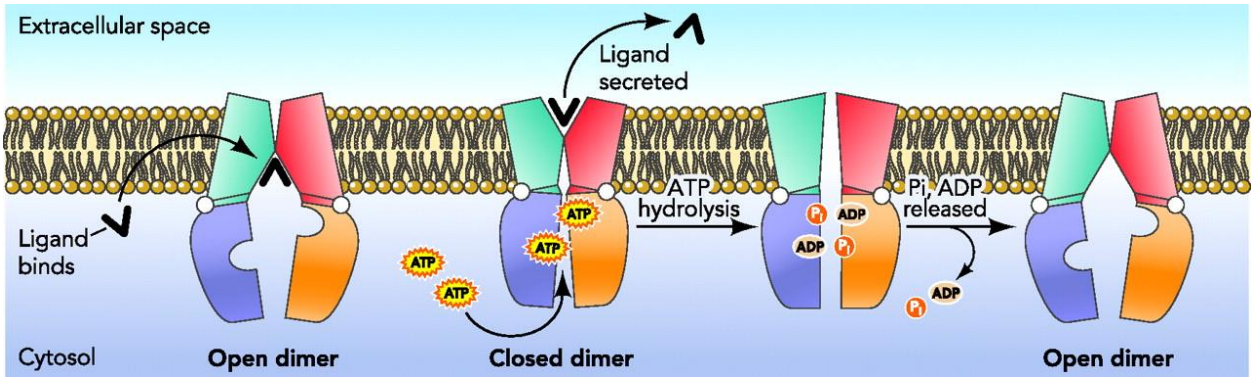

Figure 1.7: *Schematic representation of conformational switching in ATP-Binding cassette transporters fuelled by ATP (Figure reprinted with permission from Ref. 30).*

Another important biological system working under non-equilibrium state for temporal regulations are cytoskeleton proteins. Amongst these cytoskeleton proteins are microtubules and actin-filaments which form out-of-equilibrium supramolecular assemblies undergoing constantly polymerization and depolymerization.

The microtubules undergo a chemical fuel-driven transient self-assembly with high dynamics. Microtubules consist of assembly of hetero-dimeric tubulin protein consisting of a α/β-tubulin activated by binding of guanosine triphosphate (GTP).[32] Microtubulin undergo two

processes: first is the binding of GTP to activate the tubulin forming GTP-tubulin building block that add to the microtubule end and second is the hydrolysis of GTP-tubulin into GDP-tubulin that undergo disassembly (Figure 1.8). Former is the energy uptake step and latter is energy dissipation step. A simultaneous polymerization and depolymerization result in dynamic instability that allow for a quick reorientation in the cellular space. Microtubule have important functions such as chromosomal sorting during cell division and it also serves as tracks for molecular motors to transport large cellular components. Since microtubule undergo chemical fuel-driven dissipative self-assembly, thus, structures only form till there is energy (GTP) in the system. Therefore, the lifetime of the transient steady-state microtubule self-assembly is determined by GTP. Complete consumption of GTP result in decay of structure.

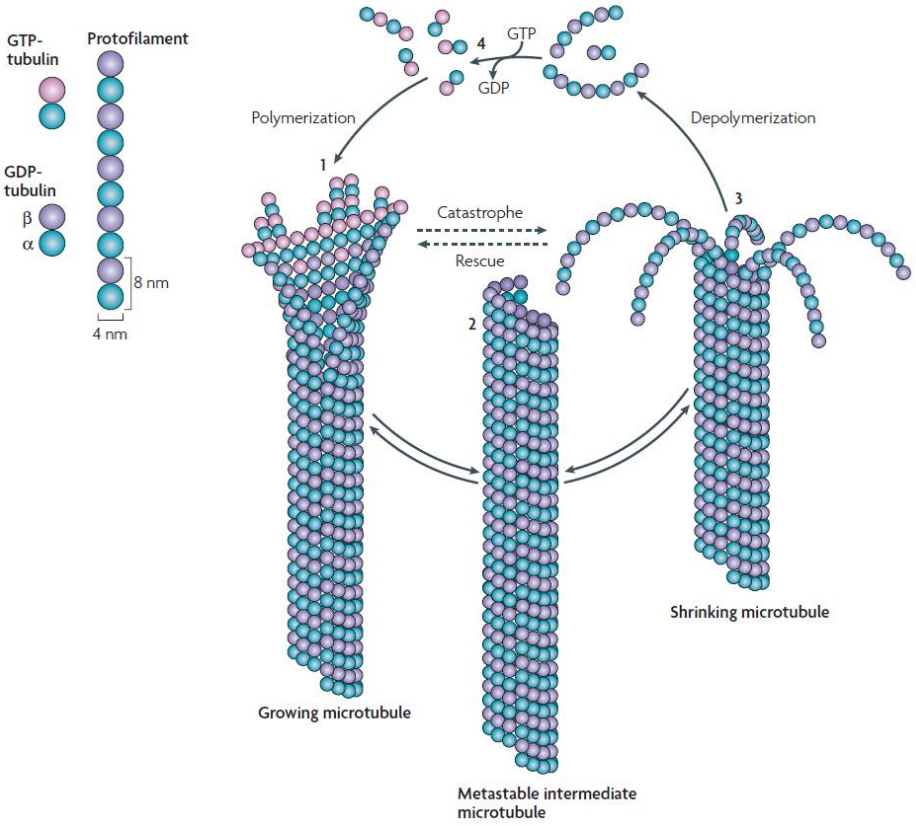

Figure 1.8*: Schematic representation of dynamic instability in microtubules fuelled by guanosine triphosphate (GTP)(Reproduced with permission from Ref. 31).*

Another such example is Actin filaments. These proteins are found in eukaryotic cells. Actin are important for cellular functions such as mobility and cell division. These actin exists in

two basic forms which are a free monomeric G-actin where G refers to globular nature and linear polymeric microfilament F-actin where F refers to filamentous form. G-actin which are free monomer gets activated on binding with chemical fuel ATP which then self-assemble to give oligomers, then nuclei and finally to linear polymeric F-actin microfilament (Figure 1.9). Thus, formation of active F-actin form is dependent on the concentration of ATP which convents inactive G-form into active F-form.[33,34] This binding kinetics of ATP to G-actin gives the time delay in formation of nuclei as opposed to fast growth that follows after.

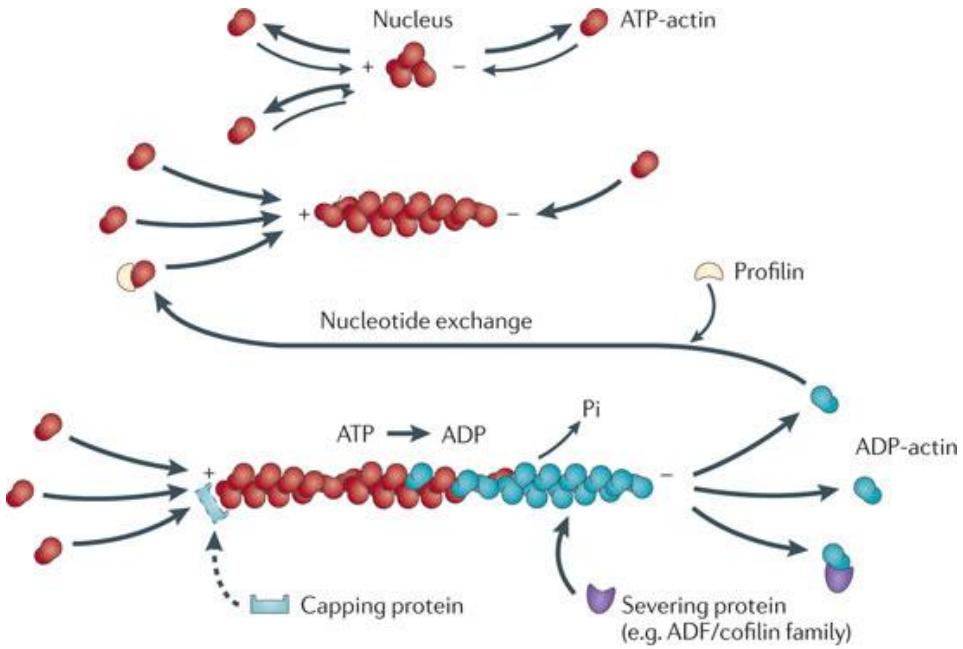

***Figure 1.9**: Schematic representation of transient self-assembly in actin filaments fuelled by adenosine triphosphate (ATP) (Reproduced with permission from Ref. 34).*

Once the F-actin filaments are formed and have performed their function of mobility and/or cell division it breaks down into monomeric G-Actin form. This happens as F-actin is inherently an ATPase which hydrolysis ATP into ADP thus deactivating the monomers of the F-actin filament which depolymerize into initial monomeric state and hence results in dynamic instability. In contrast to microtubules, Actin filaments are not designed for spatial search in cytoplasm and hence the switching between polymerization and depolymerization is slower. The dynamic instability though has immense biological relevance, but can also be a viable route to attain transient self-assembling materials which disassemble in a pre-programmed manner. These

materials are obviously advantageous in areas where the material needs to be discarded after the function such as a drug carrying matrix.

1.5 Principles for an Autonomous System

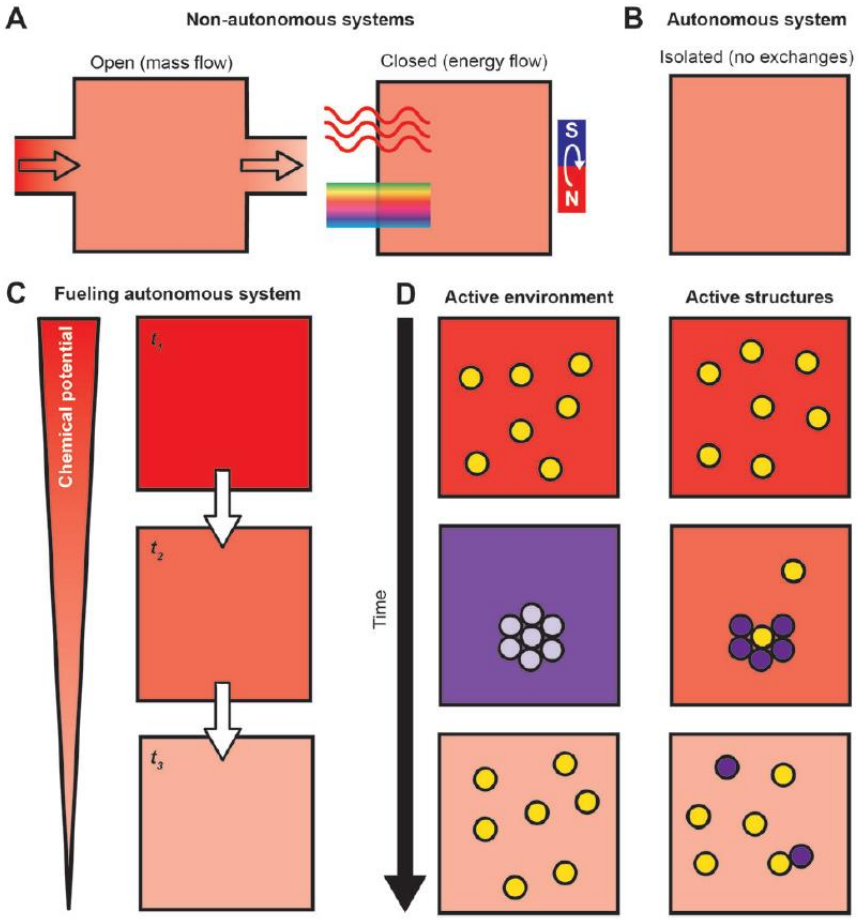

Figure 1.10: *Classification of out-of-equilibrium structural systems. Schematic representation of a) open and closed non-autonomous dissipative systems, b) an autonomous isolated system, c)-e) autonomous chemical systems: c) Temporal decrease of chemical potential, d) structural transformation by an active environment (left) or active structures (right) (Figure adapted with permission from Ref. 18).*

Systems in general are non-autonomous as they involve an exchange of either matter or energy whereas autonomous systems have an effective temporal control in isolation (Figure 1.10a, b). An example of such an autonomous system is microtubules as they can store energy in the form of GTP and use it on demand to function autonomously. For an autonomous system, self-assembly

must be driven by conversion of chemical fuel with a high chemical potential into more stable final products (Figure 1.10c).[18]

Driving of autonomous systems can be classified into two types based on the active component in the system. Active component is the element harnessing the energy by the fuel transformation (Figure 1.10d). First type of active component is the structural component itself and secondly the environment. The former is similar to tubulin where it catalyze the consumption of its own fuel. The latter involves use of structural component which is responsive to change in chemical potential of other component in the environment and therefore temporal regulation of chemical potential should bring about out-of-equilibrium structural systems. The two cases differ in their macroscopic property changes, active environment actuates the synchrony of elements present in the system resulting in changes such as gelation and dissolution. On the other end, active structural elements depict the assembly/disassembly but still have persistent properties.

1.6 Strategizing the Temporal Control

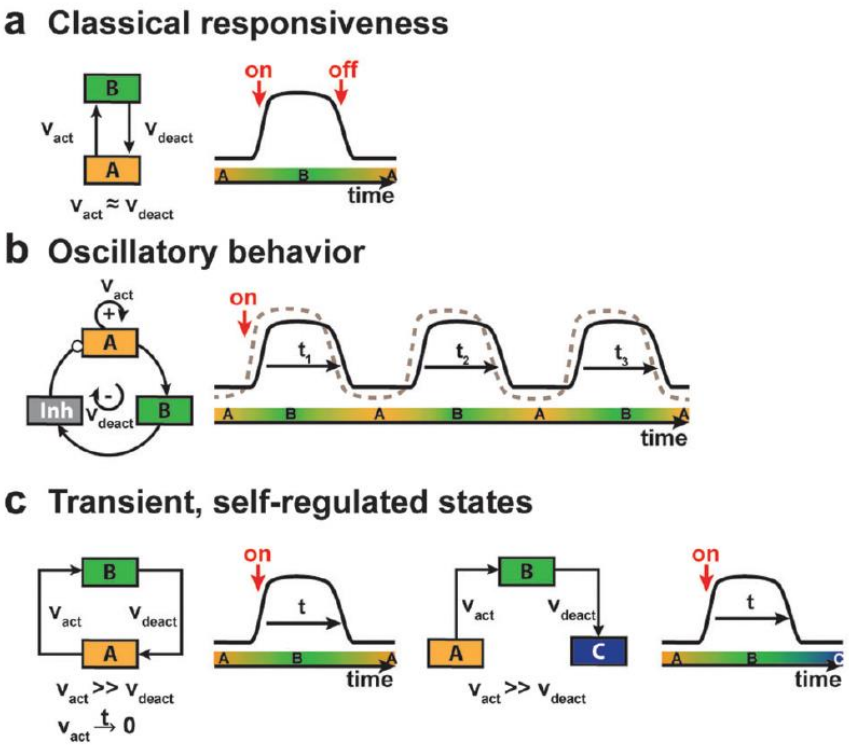

Figure 1.11: *Schematic representation of passive and active responding system. a) classical responsiveness, b) oscillatory behavior and c) transient and self-regulated stress (Figure adapted with permission from Ref. 35).*

Classical responsiveness with two reactions forward and reverse with similar reaction rates and thus require switch on and then off on subsequent addition of chemical reagents. Since state B doesn't have any control over time, these are classified as temporally passive systems (Figure 1.11a).

Transient systems can be built upon by modulating switch on/off systems. If the system consists of monomer, activating agent/fuel and deactivating agent/dissipating agent such that rate of activation > rate of deactivation, then the system may show transiency (Figure 1.11b,c).[35]

Activating agent is referred to the agent which fuels the system and activates the assembly of the monomers, consumption of this activating agent brings down the system to equilibrium. Deactivating agent is referred to the agent which hydrolyses/breaks down the activating agent into form which can't reactivate the system resulting into the formation of monomers again. Amount of fuel provided to the system determines the lifetime of self-assembly.

1.7 Temporally Programmed Supramolecular Polymers

Inspired from natural systems such as microtubules which self-assemble in presence of fuel and disassemble when fuel is consumed, we can build synthetic transient systems.

Temporal programming in supramolecular polymerization requires system to self-assemble in non-equilibrium state and be monomeric in equilibrium state. As mentioned in Section 1.2, system working under non-equilibrium state has certain features such as system should be under thermodynamic equilibrium in absence of energy source, and when energy is supplied system goes to a higher energy non-equilibrium state. Then, with time system relaxes back to equilibrium state, may/not be same as initial state (Figure 1.11c).

Recent research shows various examples known for self-assembly processes governed by templates and bond formation, however the reports of a self-assembling system showing the characteristics of biological self-assembly as shown above are extremely rare.

1.7.1 Active Environment

Autonomous materials can be obtained by coupling responsive self-assembly to an active environment.

Walther and coworkers employed this strategy to build a time modulated pH transition and pH responsive system that undergo self-assembly at low pH and disassembles on increasing pH.

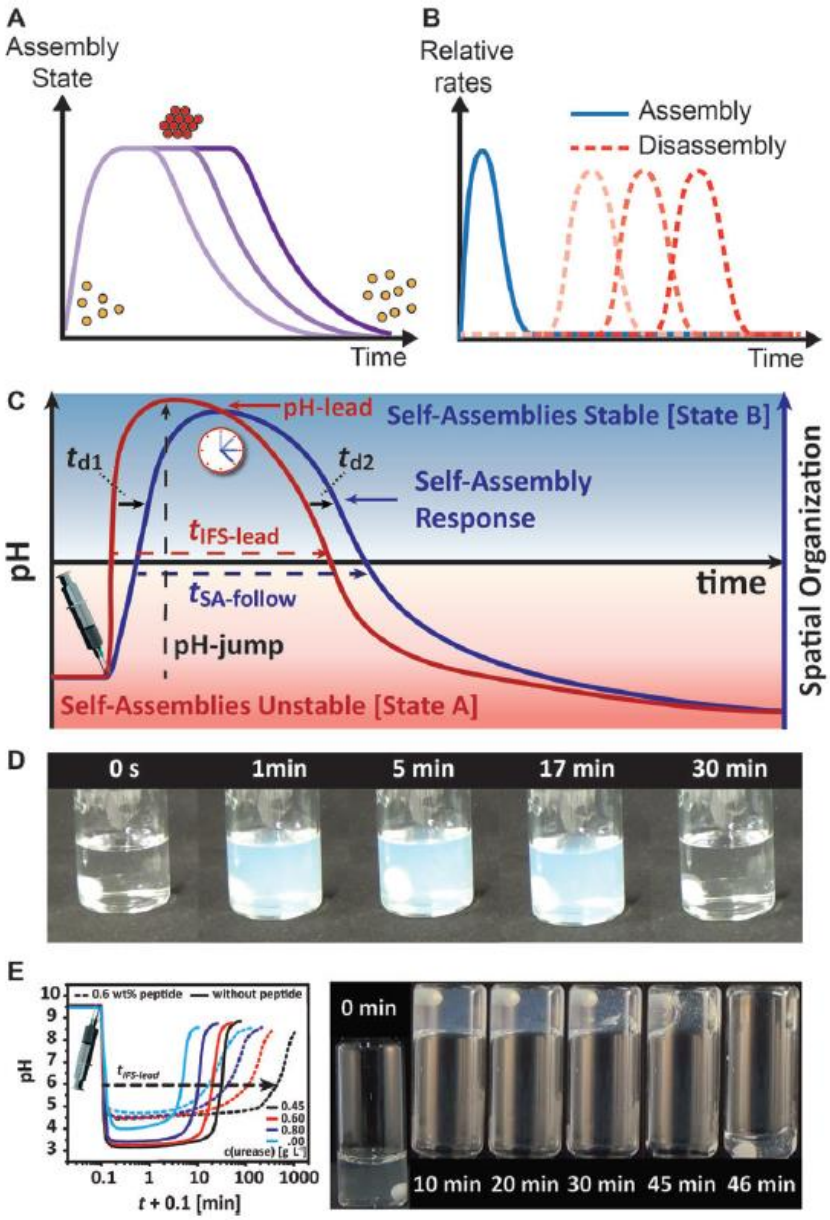

Figure 1.12: *pH-feedback systems as an active environment for transient assembly. a) Effect of the amount of activator/dormant deactivator on temporal profile of assembly. b) The corresponding dominance of assembly and disassembly rates with time. c) Schematic representation of temporal regulation of pH-responsive assemblies employing internal pH feedback as an active environment. d) Photographs of corresponding transient self-assembly depicted by the turbid dispersion. e) pH temporal profile obtained by combining urease/urea with an acidic buffer (left) and transient self-assembly of peptide hydrogel responsive to pH profile its application to the temporal control of a peptide hydrogel assembling at low pH (Figure adapted with permission from Ref. 18).*

The system consists of alkaline buffer (TRIS buffer as promoter) with ester (dormant deactivator) and pH-responsive block copolymer (Figure 1.12a-d). Aqueous solution of block co-polymer at pH ~ 6 exists in protonated form, hence dissolved state prior to addition of alkaline buffer. Addition of ester in alkaline buffer solution instantaneously increases the pH of solution to ~8.5 that deprotonates the block co-polymer resulting in its reduced solubility and therefore it assembles to stabilize hydrophobicity signified by gelation.[36] The ester depending on its electronic factors hydrolyze at a specific rate and thereby result in delayed feedback. Simultaneous hydrolysis of ester consumes hydroxyl ions and a gradual decrease of pH to ~6 is observed. This pH increases solubility of the polymer and its disassembly is observed. This non-linear hydrolysis of ester can be varied in rate and extent of pH changes by the chosen cyclic ester and hence its hydrolytic stability. The amount/ratio of ester and buffer gives another parameter to tune the lifetime of the self-assemblies with time scales from minutes to days.

Another approach by Walther and coworkers is a bio-catalytic urease/urea feedback driven transient state at low pH. In this case, acidic buffer acts as activator. Temporal profile can be tuned by variation of urease concentration that act as feedback-regulated pH reversal (dormant deactivator) and the activator buffer concentration.[37] This active environment is then coupled to peptide hydrogelators which form solid gels at low pH, for widely tunable lifetimes from a few minutes to several hours (Figure 1.12e). This chemistry has been applied to temporally block microfluidic channels and reroute fluid flow in simplistic vascular network models.

1.7.2 Active Structural Components

van Esch and coworkers have employed dibenzoyl-(l)-cystine moiety for demonstration of their chemical fuel driven transient assembly.[38] This molecule is soluble in neutral pH where these molecules are in carboxylates in nascent form, however as soon as methylating agent methyl iodide which act as fuel for the system is added, the carboxylates start to get methylated and are finally converted into esters. This formation of ester neutralizes the anionic charge of the molecule which decreases the solubility of ester form of the monomer in the aqueous media resulting into aggregation of monomers. However the esters are susceptible to hydrolysis in neutral pH which results in dynamic instability of ester aggregates and thus they hydrolyze back into carboxylates which are soluble and in monomeric state (Figure 1.13). The whole temporal map starts with free

monomers and moves to aggregate formation with finally shedding methanol as a bi-product to give the free monomers back again.

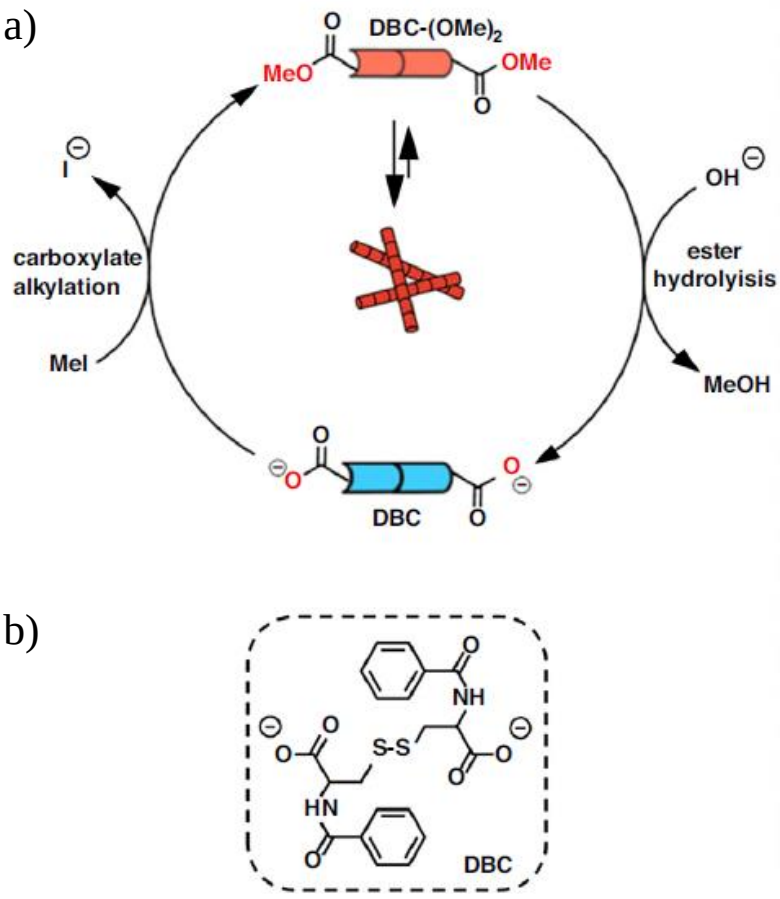

Figure 1.13: *a) MeI driven transient self-assembly in presence of alkaline buffer via active structural element autonomous system. b) Molecular structure of dibenzoyl-(l)-cystine (Figure adapted with permission from Ref. 40).*

The transient self-assembly resembles the transient formation of aggregates in biological systems and thus is therefore ground breaking in synthetic systems. This work was further extended to show generality of this concept in other carboxylate derivatives with similar transient assemblies which can be achieved with dimethyl sulphate as the methylation agent/fuel. For this particular system the pH of the solution was kept to be 11 (Figure 1.14).[39] This alkaline pH was necessary to deactivate hydrolyse the esters that are formed due to the consequent methylation. Interestingly in this work the authors could also visualize the growth and decay of the aggregates that occur at the opposite end.

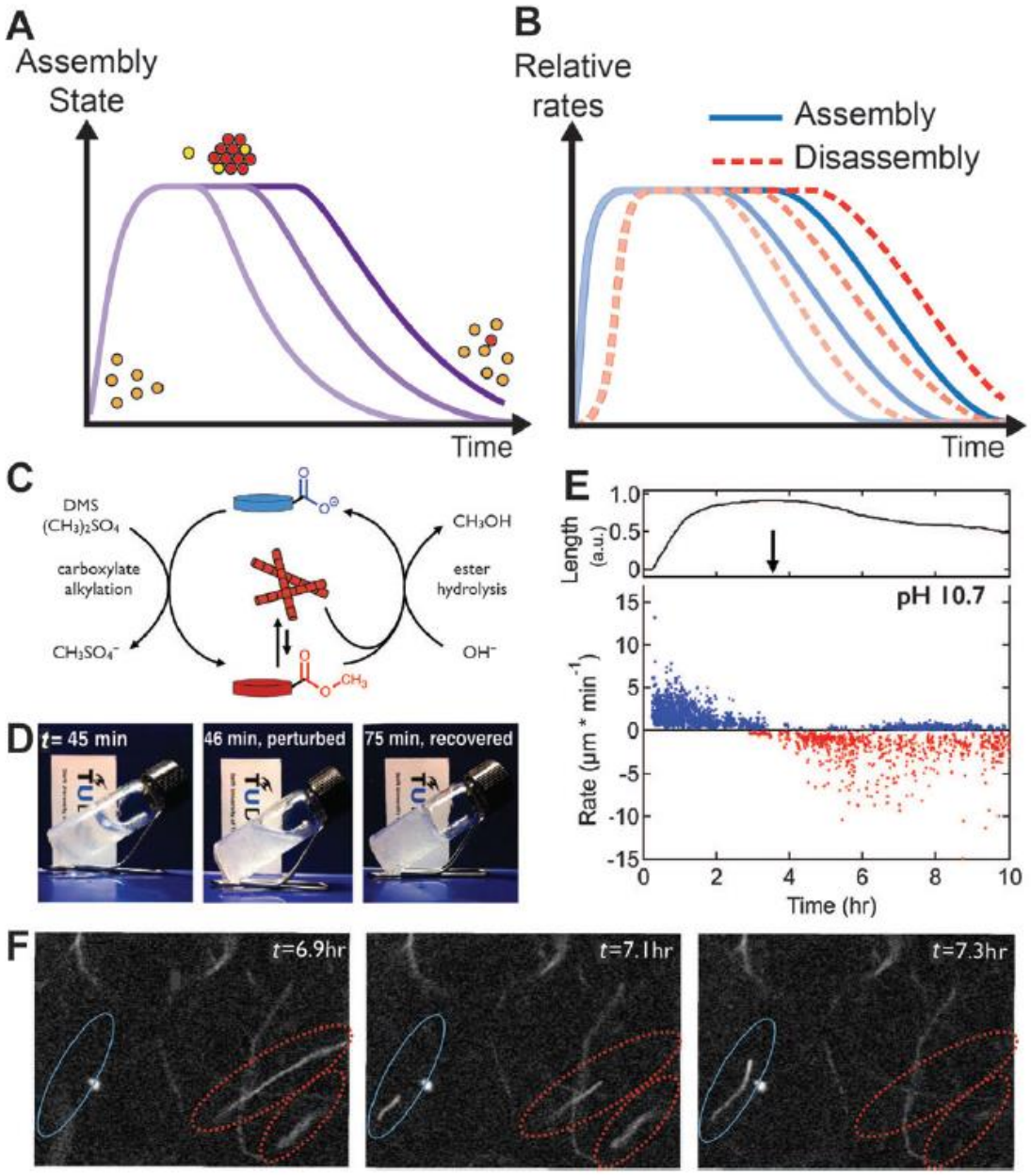

Figure 1.14. *Transient self-assembly via active structural elements: a) Temporal change in aggregation as a function of the amount of fuel introduced. b) Corresponding relative rates of assembly/disassembly. c) Schematic representation of transient assembly with active building blocks where methylation and hydrolysis compete. d) Photograph depicting the transient self-assembly signified by gelation. e) Corresponding length and relative growth rate of fibrils measured by confocal microscopy. f) Visulization of the simultaneous growth and shrinkage of the fibrils by confocal microscopy at pH 10.7. Image length is 30 mm (Figure adapted with permission from Ref. 18).*

After frame by frame analysis of the sample's confocal microscopy images they deduced that various fibers are growing and decaying at the same time bringing the whole system a step closer to biological systems. Not only a transient self-assembly, a temporal control over lifetime of self-assembly is an important parameter. For this, they varied the pH from 9 to 11 and buffer concentrations to get various lifetimes.[40]

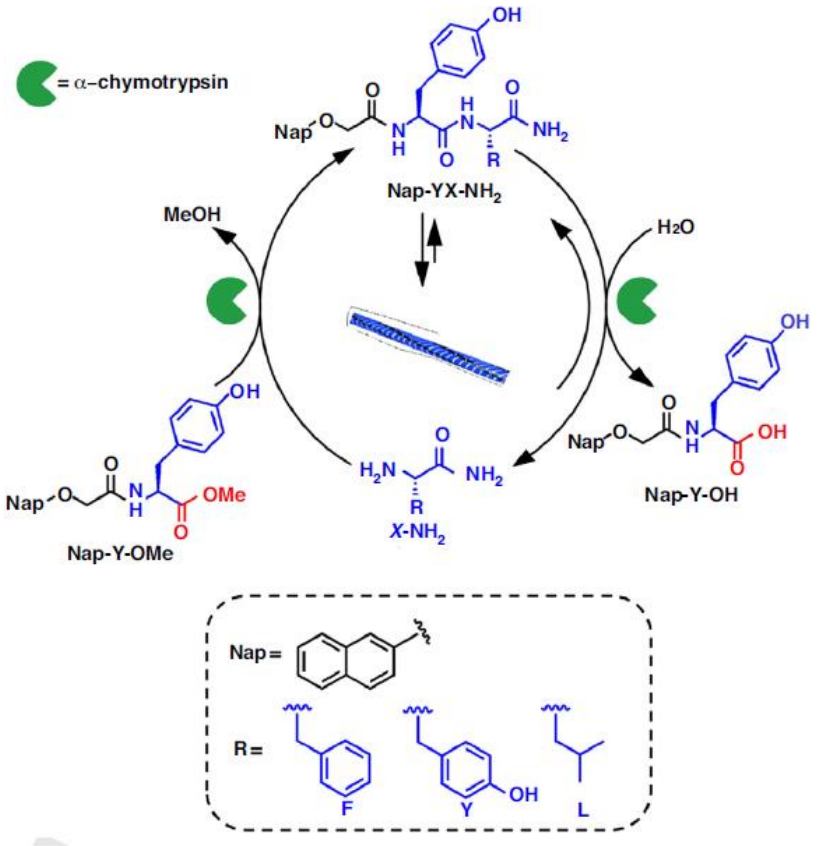

Figure 1.15: *Schematic representation of biocatalytic approach towards transient self-assembly by α-chymotrypsin (Figure adapted with permission from Ref. 40).*

Ulijn and coworkers employed a different approach and utilized enzymes to dissipate the fuel generating transient assemblies. The system relied on gelating properties of naphthalene-dipeptides and employed α-chymotrypsin enzyme which form and hydrolysis amide bonds.[41] This enzyme catalyses the transacylation of hydrophobic amino acids by acyl-donor methyl ester of tyrosine derivative. The former is the structural element and latter is the chemical fuel driving the self-assembly (Figure 1.15). The activation of molecule initiate self-assembly forming a gel state above critical gelation concentration (CGC), further α-chymotrypsin hydrolyses amide bond into

non-gelating species. The lifetime of gel was modulated by varying enzyme amounts as well pH changes.

Another biocatalytic approach was applied for transient hydrogelation using sucrose-fueled CO_2 production using microorganism.[42] Baker's yeast hydrolyses sucrose into CO_2 which upon dissolution in water decreased the pH. On acidifying carboxylate molecule become carboxylic acid forming hydrogel. With time CO_2 gets eliminated from solution and reverts the pH changes and thereby result in dissolution of acid.

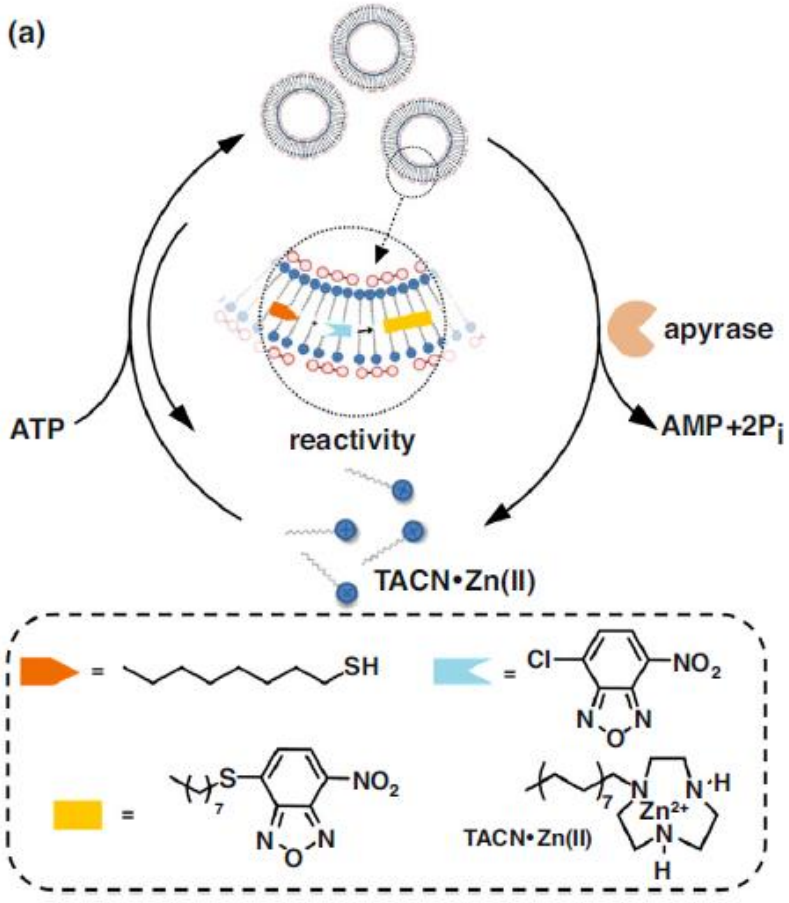

Figure 1.16: *Transient vesicle formation fuelled by ATP in presence of apyrase (Figure adapted with permission from Ref. 40).*

Although a variety of strategies have been employed by researchers but a more biologically mimicking system has not been investigated much. One of the works closer to biological system is done by Prins and coworkers.[43] His group presented the transient vesicular aggregation fuelled by ATP in presence of apyrase enzyme that hydrolyses ATP (Figure 1.16). The cationic surfactant

with zinc (II) complex as head group undergo charge neutralization on interacting with ATP electrostatically and form vesicular aggregates below critical micelle concentration (CMC).[44] On Hydrolysis of ATP to AMP decreases the multivalent interaction and therefore doesn't stabilize the vesicle. This vesicles were then employed as transient nanoreactors. The formation of vesicle facilitates the hydrophobic molecules to react. Depletion of ATP by apyrase breaks down the vesicles and reaction is disfavoured in solution. This is an example of applying transient self-assembly to temporally modulable reaction. The system was refueled multiple times by subsequent addition of ATP.

1.8 Conclusion and Outlook

We in this Chapter looked at the control that nature has over space and time of systems owing to the working of these systems under non-equilibrium. With inspiration from dynamically instable microtubules and actins which polymerize in presence of fuel and depolymerize after fuel consumption. We discussed how conventional supramolecular polymers are formed under thermodynamic equilibrium and are passive materials.

We also presented a discussion based on recent scientific reports that temporally programmable supramolecular polymers form the future of supramolecular systems in order to make controlled aggregates. We also reviewed different strategies adopted to attain transient self-assemblies that involve control over activation and deactivation step. Role of activating agent/fuel on the modulation of temporal control was surveyed in different systems. Transient systems can be built with light driven, chemical reaction driven and enzyme driven.

The problem to be investigated is to achieve bio-mimicking systems that utilize biological fuels and dissipating mechanism with a temporal control over self-organization. The biological systems utilize fuels that non-covalently interact and not as reacting species. Important parameter is control over their organization to form 1D structures similar to actin and microtubules. Not only mimicking transient self-assemblies but other functions which nature does such as transient conformational change and contraction. Going a step further, we need to modulate these systems to have materials applications.

1.9 References

1. L. Brunsveld, B. J. B. Folmer, E. W. Meijer, R. P. Sijbesma, *Chem. Rev.* **2001**, *101*, 4071-4098.
2. F. J. M. Hoeben, P. Jonkheijm, E. W. Meijer, A. P. H. J. Schenning, *Chem. Rev.* **2005**, *105*, 1491-1546.
3. A. P. H. J. Schenning, E. W. Meijer, *Chem. Commun.* **2005**, *26*, 3245-3258.
4. A. P. H. J. Schenning, P. Jonkheijm, F. J. M. Hoeben, J. van Herrikhuyzen, S. C. J. Meskers, E. W. Meijer, L. M. Herz, C. Daniel, C. Silva, R. T. Phillips, R. H. Friend, D. Beljonne, A. Miura, S. De Feyter, M. Zdanowska, H. Uji-I, F. C. De Schryver, Z. Chen, F. Würthner, M. Mas-Torrent, D. den Boer, M. Durkut, P. Hadley, *Synt. Met.* **2004**, *147*, 43-48.
5. T. Aida, E. W. Meijer, S. I. Stupp, *Science* **2012**, *335*, 813-817.
6. R. F. Service, *Science* **2005**, *309*, 95.
7. J.-M. Lehn, *Proc. Natl. Acad. Sci. U.S.A.* **2002**, *99*, 4763-4768.
8. J.-F. Lutz, J.-M. Lehn, E. W. Meijer, K. Matyjaszewski *Nat. Rev. Mater.* **2016**, *1*, 16024.
9. E. Roduner, S. G. Radhakrishnan, *Chem. Soc. Rev.* **2016**, 45, 2768-2784.
10. D. van der Zwaag, T. F. A. de Greef, E. W. Meijer, *Angew. Chem. Int. Ed.* **2015**, *54*, 8334-8336.
11. I. R. Epstein, B. Xu, *Nat. Nanotechnol.* **2016**, *11*, 312-319.
12. G. Clixby, L. Twyman, *Org. Biomol. Chem.* **2016**, *14*, 4170-4184.
13. S. Mann, *Nat. Mater.* **2009**, *8*, 781-792.
14. A. Pross, *J. theor. Biol.* **2003**, *220*, 393-406.
15. V. K. Praveen, C. Ranjith, E. Bandini, A. Ajayaghosh, N. Armaroli, *Chem. Soc. Rev.* **2014**, *43*, 4222-4242.
16. D. G. Rodriguez, A. P. H. J. Schenning, *Chem. Mater.* **2011**, *23*, 310-325.
17. S. S. Babu, V. K. Praveen, A. Ajayaghosh, *Chem. Rev.* **2014**, *114*, 1973-2129.
18. R. Merindol, A. Walther, *Chem. Soc. Rev.* **2017,** DOI: 10.1039/c6cs00738d
19. E. Mattia, S. Otto, *Nat. Nanotechnol.* **2015**, *10*, 111-119.
20. T. F. A. de Greef, M. M. J. Smulders, M. Wolffs, A. P. H. J. Schenning, R. P. Sijbesma, E. W. Meijer, *Chem. Rev.* **2009**, *109*, 5687-5754.

21. D. Zhao, J. S. Moore, *Org. Biomol. Chem.* **2003**, *1*, 3471-3491.
22. M. Kastler, W. Pisula, D. Wasserfallen, T. Pakula, K. Müllen *J. Am. Chem. Soc.* **2005**, *127*, 4286-4296.
23. C. Kulkarni, K. K. Bejagam, S. Senanayak, K. S. Narayan, S. Balasubramanian, S. J. George, *J. Am. Chem. Soc.* **2015**, *137*, 3924-3932.
24. M. M. J. Smulders, A. P. H. J. Schenning, E. W. Meijer, *J. Am. Chem. Soc.* **2008**, *130*, 606-611.
25. A. J. Markvoort, H. M. M. ten Eikelder, P. A. J. Hilbers, T. F. A. de Greef *ACS Cent. Sci.* 2016, **2**, 232-241.
26. C. Kulkarni, S. Balasubramanian, S. J. George, *ChemPhysChem* **2013**, *14*, 661-673.
27. J. A. Mohawk, C. B. Green, J. S. Takahashi, *Annu. Rev. Neurosci.* **2012**, *35*, 445-462.
28. B. P. Bean, *Nat. Rev. Neurosci.* **2007**, *8*, 451-465.
29. A. L. Hodgkin, A. F. Huxley, *J. Physiol.* **1952**, *117*, 500-544.
30. K. J. Linton, *Physiology* **2007**, 22, 122-130.
31. A. Akhmanova, M. O. Steinmetz, *Nat. Rev. Mol. Cell Biol.* **2008**, *9*, 309-322.
32. T. Mitchison, M. Kirschner, *Nature* **1984**, *312*, 237-242,
33. E.D. Korn, *Physiol. Rev.* **1982**, *62*, 672-737.
34. A. Nürnberg, T. Kitzing, R. Grosse, *Nat. Rev. Cancer* **2011**, *11*, 177-187.
35. L. Heinen, A. Walther, *Soft matter* **2015**, *11*, 7857-7866.
36. T. Heuser, A.-K. Steppert, C. Molano Lopez, B. Zhu and A. Walther, *Nano Lett.* **2015**, *15*, 2213-2219.
37. T. Heuser, E.Weyandt, A.Walther, *Angew. Chem. Int. Ed.* **2015**, *54*, 13258-13262.
38. J. Boekhoven, A. M. Brizard, K. N. K. Kowlgi, G. J. M. Koper, R. Eelkema, J. H. van Esch, *Angew. Chem. Int. Ed.* **2011**, *50*, 12285-12289.
39. J. Boekhoven, W. E. Hendriksen, G. J. M. Koper, R. Eelkema, J. H. van Esch, *Science* **2015**, 349, 1075-1079.
40. F. della Sala, S. Neri, S. Maiti, J. L. Y. Chen, L. J. Prins *Curr. Opin. Biotechnol.* **2017**, *46*, 27-33.
41. S. Debnath, S. Roy, R. V. Ulijn, *J. Am. Chem. Soc.* **2013**, *135*, 16789-16792.
42. A. -Pachón, A. César, J. F. Miravet, *Chem. Commun.* **2016**, *52*, 5398-5401.
43. C. Pezzato, L. J. Prins, *Nat. Commun.* **2015**, *6*, 7790.

44. S. Maiti, I. Fortunati, C. Ferrante, P. Scrimin, L. J. Prins, *Nat. Chem.* **2016**, *8*, 725-781.

Chapter 2

Temporally Controlled Conformational Switching in a Supramolecular Polymer

Chapter 2

Temporally Controlled Conformational Switching in a Supramolecular Polymer

Abstract

Assembly of proteins in biological systems have an important role in functioning for life. Amongst these, are the class of ATP-Binding Cassette Transporters (ABC transporters) that undergo transient conformational switching fuelled by ATP under non-equilibrium to translocate a variety of substance. In this regard, design of biomimetic systems can be a stepping stone to achieve life-like complex systems with spatio-temporal control over its functioning. In an attempt to alleviate this, we present ***NDPA****, napthalene diimide functionalized with dipicolylethylenediamine (DPA) motif which shows unprecedented transient conformational switching driven by ATP by employing a bio-inspired "enzyme in tandem" approach for a temporally controlled dynamic helical conformational reversal of* ***NDPA*** *assembly.*

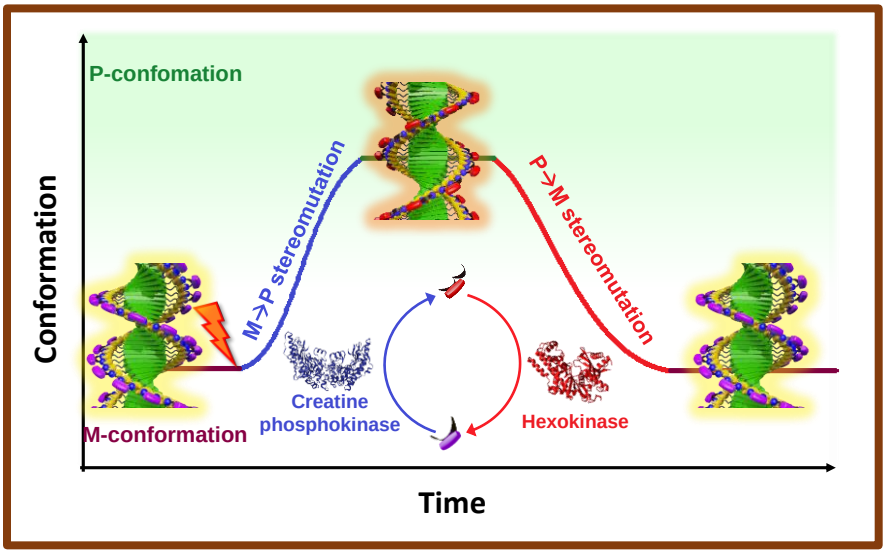

Publication based on this work: *Angew. Chem. Int. Ed.* **2017**, *129*, 1349-1353 (Hot paper), Highlighted in Nature Nanotechnology

2.1 Introduction

Biological systems work out of equilibrium also known as dissipative conditions. To operate under these conditions, energy needs to be consumed to overcome the unfavoured parameters in the energy landscape. For this, in most cases, biological systems employ chemical fuel Adenosine triphosphate (ATP), hence it's renowned as the biological energy currency.[1] This fascinating fact inspires us to understand its importance and employ in synthetic systems for future advances. One such prominent example for out-of-equilibrium functioning driven by ATP is conformational switching of a class of proteins, ATP-binding Cassette Transporters (ABC transporters).[2] These proteins are an assembly often consisting of multiple subunits with transmembrane proteins and membrane-associated ATPases. ABC transporters natively in their open conformation utilize the energy of adenosine triphosphate (ATP) binding to undergo a conformational switching to close conformation and subsequent hydrolysis of ATP energizes the translocation of various substrates across membranes such as export of toxins from cell and uptake of nutrients by cell and result in the regeneration of native open conformation of ABC transporter.

In supramolecular chemistry, however, a thorough investigation of passive conformational switching at molecular level as well as assembly state has been done over decades.[3] But, chemical fuel-driven active system with spatio-temporal conformational reorganization under non-equilibrium conditions similar to natural systems has not been investigated so far.

In this Chapter, we describe a novel bio-inspired "enzyme in tandem" strategy to appreciate a conformational change in a supramolecular polymer. For this an achiral naphthalenediimide chromophore functionalized with phosphate binding motif diethylenedipicolylamine, **NDPA** was employed (Scheme 2.1).

Detailed spectroscopic probing provided the insights into the dynamic molecular recognition, chiral induction process and stability of the assemblies. The binding of multivalent chiral phosphates resulted in high supramolecular chiral order, as evident from the excitonic, bisignated circular dichroism signals in **NDPA** assembly.[4] **NDPA** showed phosphate selective preferential helicity, forming a right-handed helical assembly (*P*-helix) on interaction with ATP and left-handed helical assembly (*M*-helix) on binding with ADP.

With this understanding, herein, we present the transient reversal of the helical handedness of **NDPA** through *in situ* transformation of guest i.e. ATP→ADP. This simple method for dynamic

switching of handedness was utilized to bring in a slow change in helicity from *M*-helix to *P*-helix to *M*-helix with an unprecedented control over lifetime of transient state and rate of transformation using an "enzyme in tandem" approach.

2.2 Design Strategy

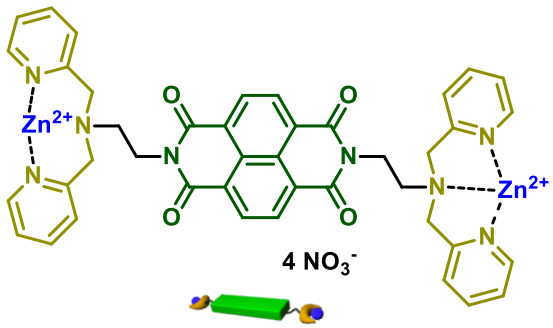

Scheme 2.1. *Structure and schematic representation of* ***NDPA****.*

The molecular recognition driven 1-D helical self-assembly of chromophores often employed non-directional electrostatic interactions for guest binding.[6] However, we envisioned that chromophore functionalization with specific guest binding groups would give a better control over the resulting self-assembly.[7] Also, use of biologically relevant guest molecules, such as adenosine phosphates,[1] would facilitate an efficient self-assembly through additional hydrophobic and π-π interactions between the base units and simultaneously act as a chiral handle for imparting chirality to the resulting assemblies. Extensive studies on molecular phosphate sensors suggest that dipicolylethylenediamine-Zinc complex (Zn-DPA) motif can specifically bind to various adenosine phosphates with high association constants.[8] Moreover, functionalization with the chromophores would provide a spectroscopic readout to various transformations. Hence we have designed **NDPA** amphiphile substituted with Zn-DPA motif (Scheme 2.1), in order to promote guest induced self-assembly and chiral induction through specific binding interactions. **NDPA** was synthesized following the literature procedure and sufficiently characterized (See Section 2.9 for details). [9]

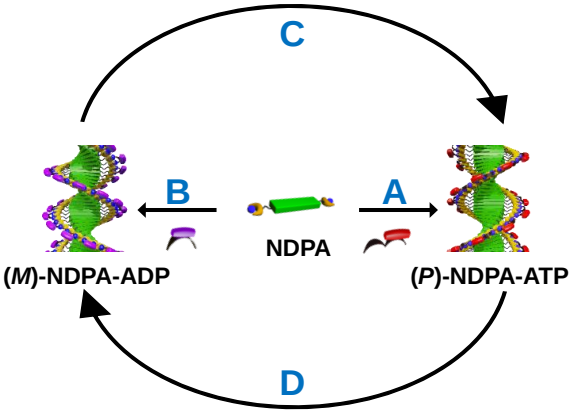

Scheme 2.2. *Schematic representation of formation of* ***NDPA*** *assemblies of opposite helicity by ATP and ADP and their inter-conversion.*

NDPA form highly dynamic assemblies that are adaptive to the guest present in the system. Such a dynamic system with control over helicity governed by phosphate recognition give an advantage to *in situ* transform the fuel and the effect should be reflected in the change in **NDPA** assembly (Scheme 2.2). ATP and ADP are biologically relevant phosphates, which further lead to employing natural enzymes that act on them for various functions.

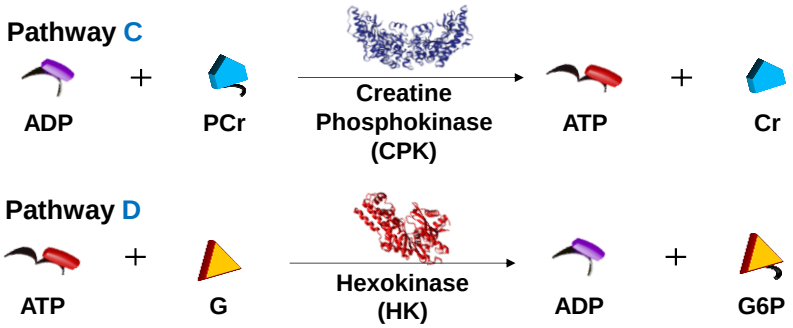

Scheme 2.3. *Schematic representation for enzymatic pathways for conversion of ADP to ATP by Creatine Phosphokinase (CPK) and ATP to ADP by Hexokinase (HK).*

Amongst various classes of enzymes phosphoryl transferase are kinases. In muscles, Creatine Phosphokinase (CPK) also known as Creatine Kinase generate ATP from ADP by using a phosphate source phosphocreatine (PCr) in order to produce energy for muscle movement till glycolysis pathway get activated for ATP synthesis.[10] Then, Myokinase consumes this energy currency ATP, hydrolysing it to ADP, to facilitate the muscle movement. Thus, enzyme in tandem, form and hydrolyse ATP for an out-of-equilibrium function of muscle movement. With this

strategy, we employed two phosphoryl transferase enzymes (Scheme 2.3) singularly as well as in tandem to achieve a transient conformational control over **NDPA** assembly. Creatine Phosphokinase, as stated above, generate ATP from ADP on consumption of PCr giving Creatine (Cr) as side product. Hexokinase, on the other hand, hydrolyses ATP to ADP by phosphorylating glucose (G) to glucose-6-phosphate (G6P).

2.3 Adenosine Phosphate Induced Helical Self-Assembly

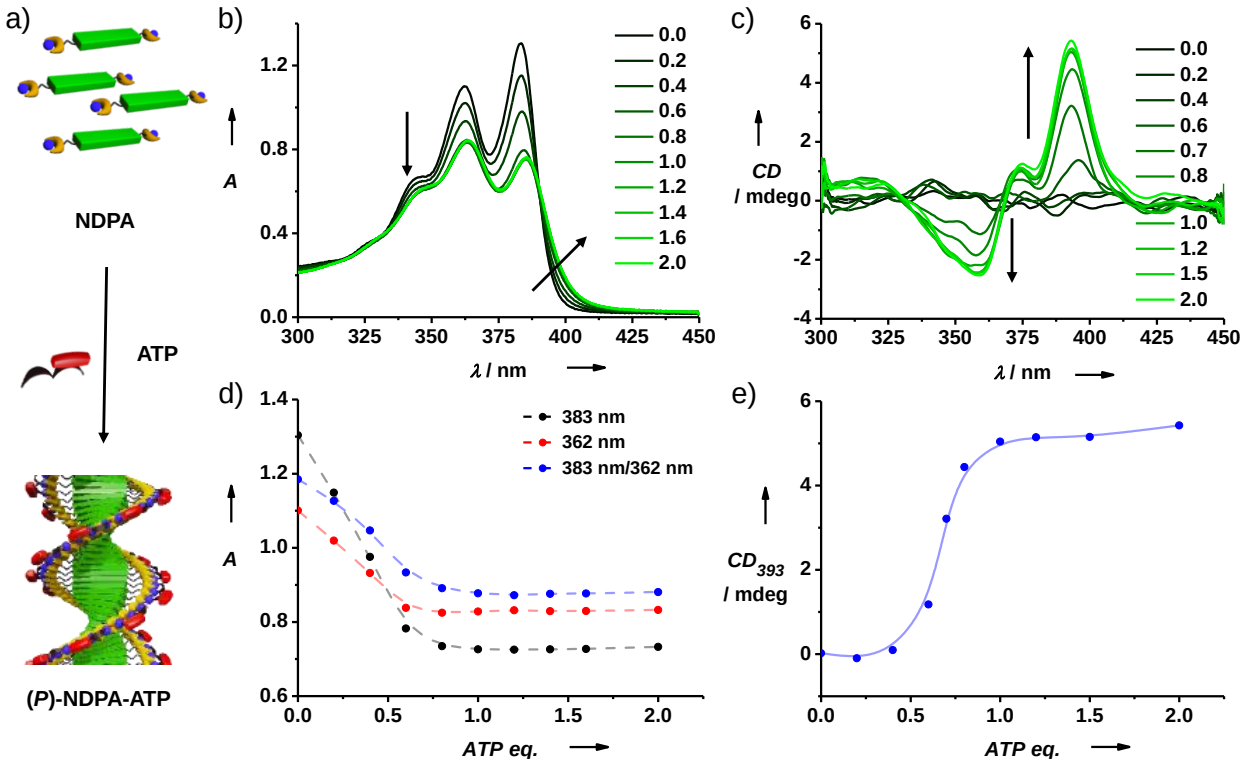

Figure 2.1. *Formation of (P)-**NDPA**-ATP self-assembly. a) Schematic representation of ATP binding induced right-handed helical assembly of **NDPA**. Changes in b) absorption, c) CD spectra of **NDPA** upon titration with ATP, corresponding changes in d) absorbance, e) CD intensity monitored at different wavelengths ([**NDPA**] = 5 x 10^{-5} M, 10 mM aq. HEPES buffer, T = 40 °C).*

The UV/vis absorption studies of **NDPA** (5 x 10^{-5} M, 10 mM aq. HEPES buffer) showed characteristic features of molecularly dissolved NDI chromophores such as sharp absorption bands (λ_{max} = 383 and 362 nm). However, titration of **NDPA** with increasing molar ratios of ATP (0-2 eq.), resulted in broadening of absorption spectra, along with reversal of relative intensity of vibronic bands at 362 nm and 383 nm characteristic of NDI chromophoric self-assembly (Figure

2.1a,b,d).[11]

Corresponding Circular Dichroism (CD) spectra showed the gradual evolution of strong Cotton effects, through an isodichroic point at the zero-crossing (369 nm), indicating that ATP binding induces a preferred helical handedness to the resulting assemblies of achiral NDIs (Figure 2.1c,e). Binding of ATP resulted in positive bisignated CD spectrum, with positive and negative maxima at 393 and 360 nm respectively, characteristic of excitonically coupled chromophores, arranged in right-handed organization.[12] The titration curve obtained by monitoring the CD intensity at 395 nm showed saturation at 1 eq. of ATP, suggesting a 1:1 stoichiometry in the co-assembly (Figure 2.1e).

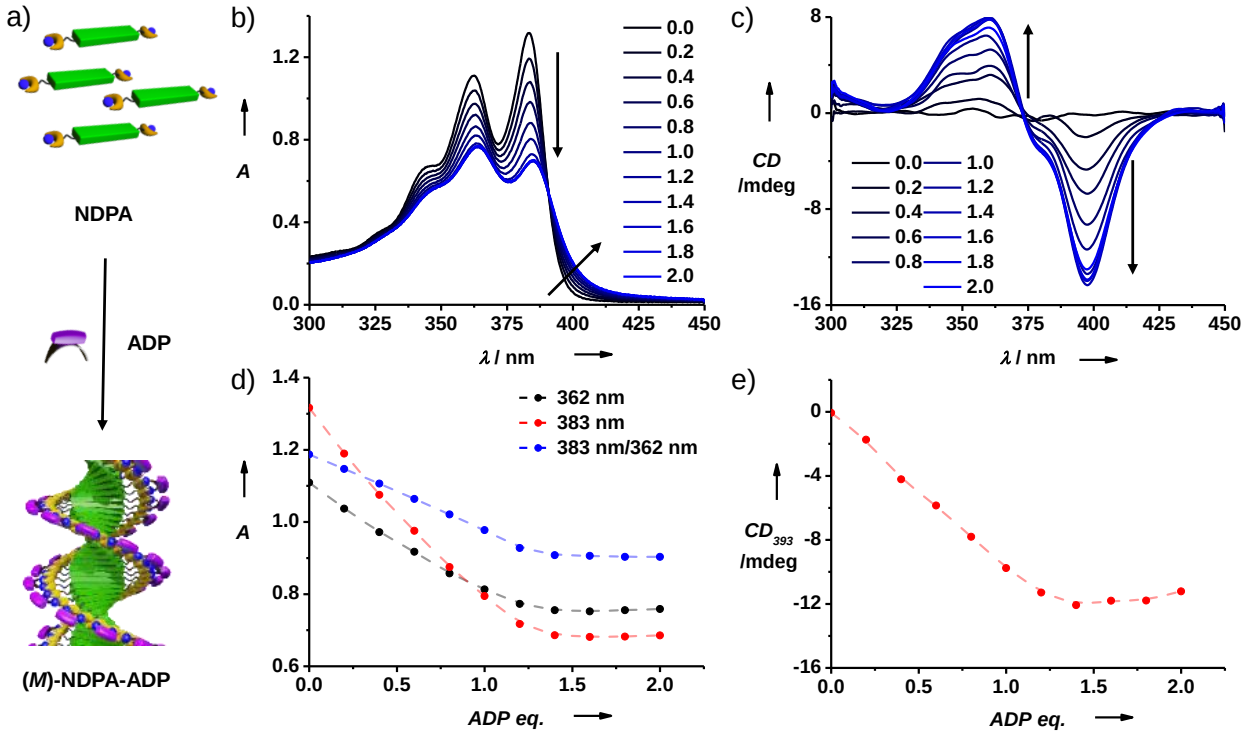

Figure 2.2. *Formation of (M)-**NDPA**-ADP. a) Schematic representation of ADP binding induced left-handed helical assembly of **NDPA**, Changes in b) absorption, c) CD spectra of **NDPA** upon titration with ADP, corresponding changes in d) absorbance and e) CD intensity monitored at different wavelengths ([**NDPA**] = 5 x 10^{-5} M, 10 mM aq. HEPES buffer, T = 40 ℃).*

NDPA showed similar assembly behaviour on titration with divalent ADP with reversal of relative intensity of vibronic bands at 362 nm and 383 nm (Figure 2.2a,b,d). However, binding of ADP induces opposite handedness to NDI assemblies as evident from the negative bisignated CD

signal, with negative and positive maxima at 393 and 360 nm, respectively (Figure 2.2c,e). The mirror image Cotton effects of **NDPA** assemblies obtained with the ATP when compared with ADP clearly suggests the induction of chirality with opposite handedness.

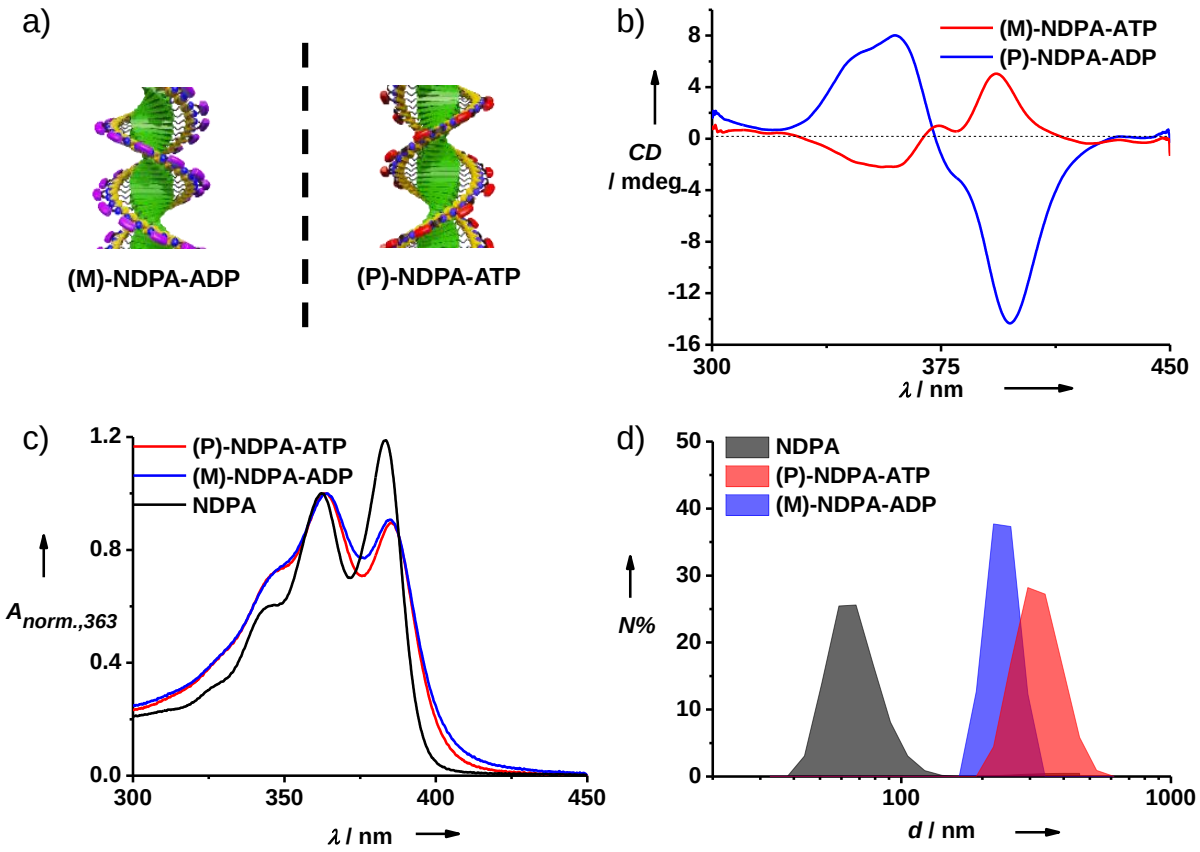

Figure 2.3. *Comparison of (P)-**NDPA**-ATP and (M)-**NDPA**-ADP assemblies. a) Schematic representation of (P)-**NDPA**-ATP and (M)-**NDPA**-ADP depicting opposite helical conformation but similar extent of self-assembly, b) CD, c) absorption and d) Dynamic Light Scattering (DLS) spectra of **NDPA** assemblies ([**NDPA**] = 5 x 10^{-5} M, [ATP] = 1 eq., [ADP] = 1 eq., 10 mM aq. HEPES buffer, T = 40 ℃).*

The ATP and ADP bound **NDPA** assemblies showed opposite helical chirality as depicted by the one equivalent of guest induced CD spectra (Figure 2.3a,b) but another aspect to be appreciated is the extent of self-assembly. The vibrational features of absorption spectra give insights to the intermolecular interaction between the two NDI cores. The ratio of intensity of two vibrational bands at 383 nm and 362 nm in absorbance spectra for monomeric **NDPA** was calculated to be 1.19, whereas for (*P*)-**NDPA**-ATP is 0.90 and (*M*)-**NDPA**-ADP is 0.91 depicting the extent intermolecular interactions are similar in presence of ATP and ADP (Figure 2.3c). The

origin of this unique guest dependent handedness was investigated through detailed molecular mechanics/molecular dynamics (MM/MD) simulations.[5] Comparison of potential energy profile confirmed the role of van der Waal's and hydrogen bonding interactions being responsible for stabilization of one form over the other.

Dynamic light scattering gave an additional proof for the extent of assembly which show self-assembly of (*P*)-**NDPA**-ATP and (*M*)-**NDPA**-ADP in the range of 200-600 nm (Figure 2.3d).

2.4 Transient Conformational Switching Mediated by Hexokinase

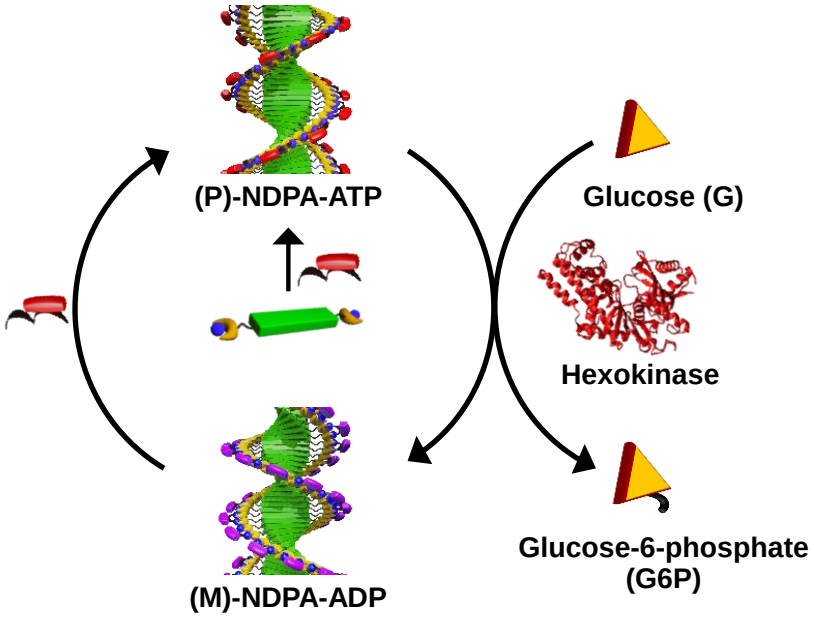

Scheme 2.4. *Schematic representation of transient conformational switching of* ***NDPA*** *assembly mediated by Hexokinase in presence of glucose.*

A transient conformational switching of **NDPA** assembly require a reaction which result in formation or degradation of any of the fuels ATP and ADP. In order to achieve this, the first attempt was made to hydrolyse ATP to ADP by the commercially available ATP hydrolysing enzyme Hexokinase (HK) (Scheme 2.4). Enzyme Hexokinase is known to phosphorylate Glucose (G) to Glucose-6-phosphate (G6P) on expense of biological energy currency ATP giving ADP as the side product. To apply Hexokinase to our system, we first investigated the effect of commercially available Hexokinase (HK) on ATP in presence of glucose using ^{31}P NMR.

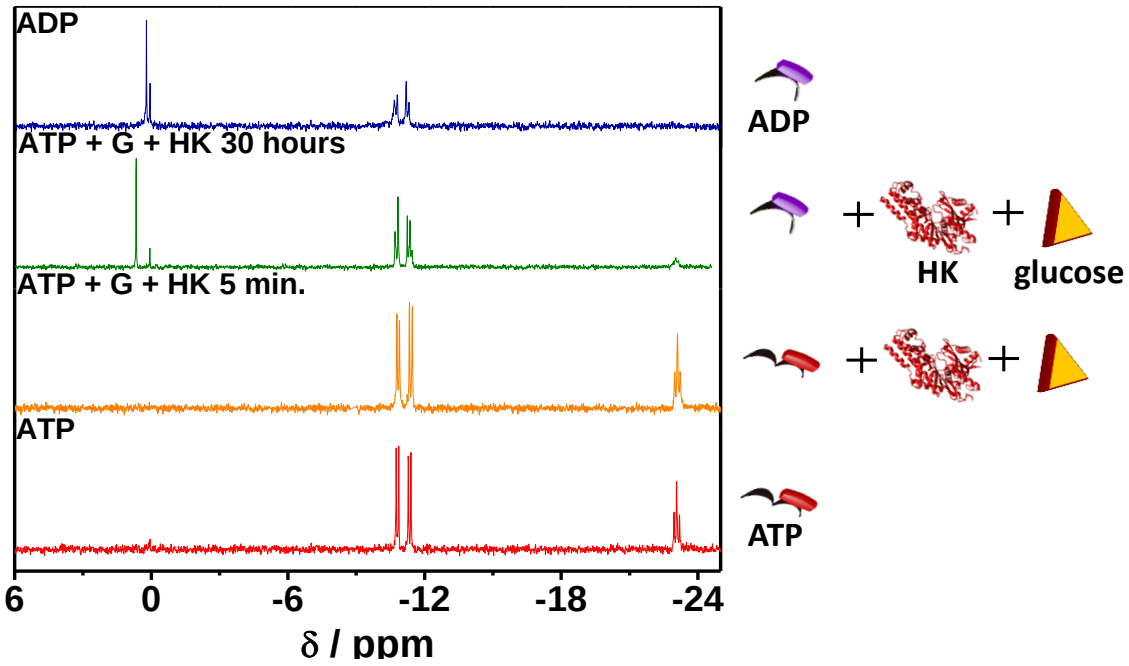

Figure 2.4. *^{31}P NMR depicting hydrolysis of ATP to ADP mediated by Hexokinase (HK) in presence of glucose (G) ([ATP] =10^{-3} M, [G] = 600 eq., 100 U/mL HK, HEPES buffer in D_2O).*

For this 10^{-3} M ATP solution in HEPES buffer in D_2O was taken and ^{31}P NMR spectra was recorded. To it 600 eq. glucose and 100 U/mL Hexokinase were added and immediately ^{31}P NMR spectra was recorded which shows no shift in ATP peaks (Figure 2.4). After 30 hours interval, ^{31}P NMR spectra showed the hydrolysis of ATP and formation of ADP suggested by disappearance of peak at δ = -23 ppm. This spectra resembled to 10^{-3} M ADP solution.

The transient conformation switching in **NDPA** assemblies mediated by Hexokinase was then investigated through CD and supported by DLS and absorption spectra. Initially no CD signal is observed for 5 x 10^{-5} M **NDPA** and corresponding absorption spectra depict molecularly dissolved **NDPA** (Figure 2.5a,b).

In a solution of **NDPA** (5 x 10^{-5} M in aq. HEPES), 1200 eq. glucose and 6.4 U/mL Hexokinase, upon addition of 1 eq. of ATP resulted in instantaneous formation of self-assembly shown by reversal of vibronic bands and broadening in absorption spectra. The CD spectra before addition showed zero signal and an instantaneous positive bisignated CD spectra on addition of ATP. This is observed signifying formation of (*P*)-**NDPA**-ATP assembly (Figure 2.5a,b).

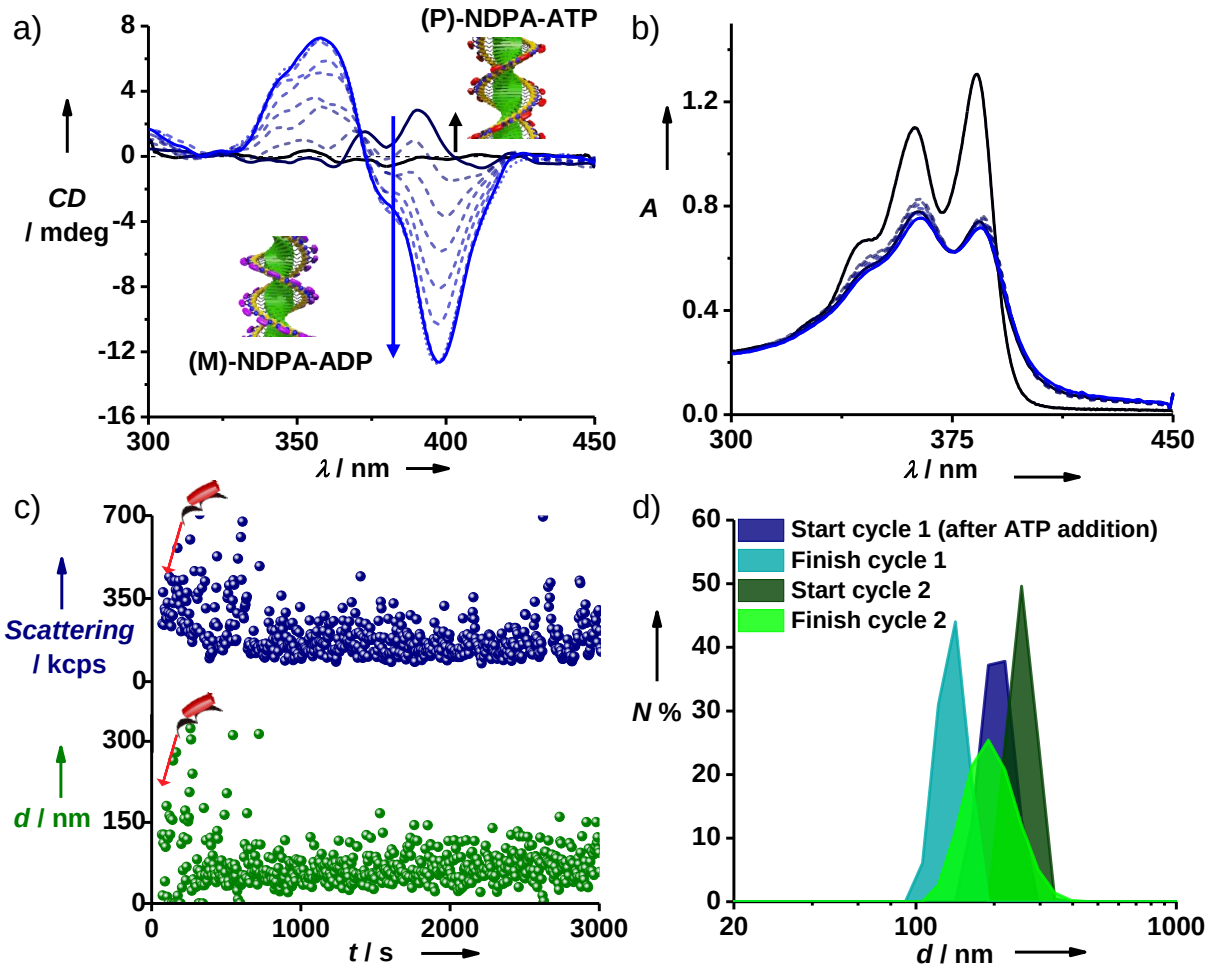

Figure 2.5. *Transient Conformational Switching mediated by Hexokinase. a) Time dependent CD spectral changes depicting gradual change from zero to positive bisignated to negative bisignated (t = 0 →50 min). b) Time dependent absorption spectral changes showing sudden decrease in absorption on adding ATP and thereafter insignificant change in vibronic features. c) Scattering and DLS size changes with time showing no change over the transient cycle. d) DLS number % size changes over the transient cycle depicting only minor change in size over time ([**NDPA**] = 5 x 10^{-5} M, [ATP] = 1 eq., [Glucose] = 1200 eq., [HK] = 6.4 U mL^{-1} 10 mM aq. HEPES buffer, T = 40 ℃).*

Time dependent spectra show a gradual change from positive bisignated to negative bisignated signifying a conformational switching in around 50 minutes. Furthermore, vibronic features in absorption spectra show there is no change in intermolecular interactions between chromophores in the self-assembly as seen in the static assembly. The dynamic light scattering data supports the insignificant change in extent of self-assembly and stack size over time as there is no change in scattering and size data over the time of the transient cycle (Figure 2.5c,d) which

correlates well with the static assembly size 200-300 nm of (*P*)-**NDPA**-ATP and (*M*)-**NDPA**-ADP (Figure 2.3d).

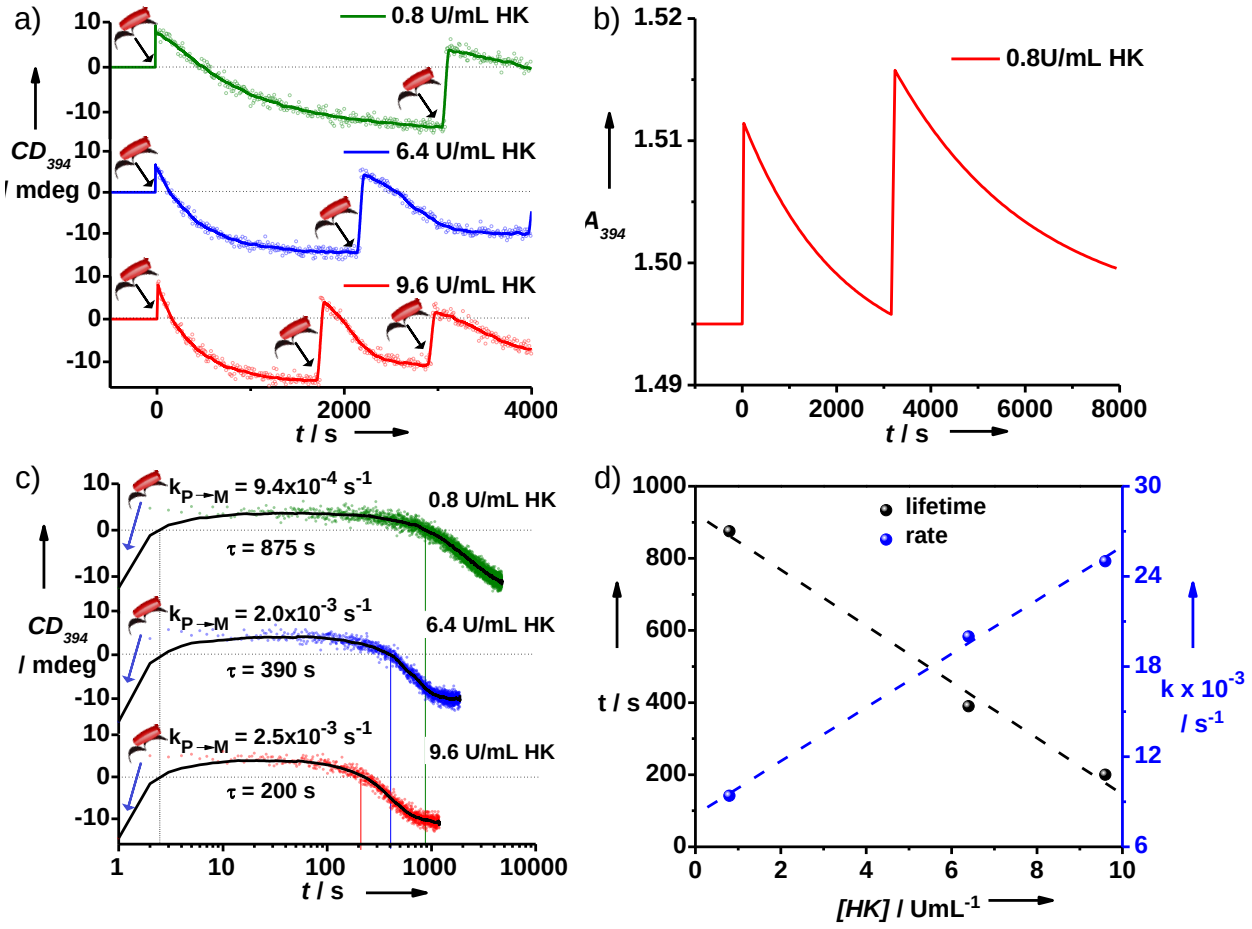

Figure 2.6. *Transient conformational switching by Hexokinase. a) Time dependent CD changes at λ = 394 nm in presence of different units of HK depicting transient cycle refueled by subsequent addition of ATP. b) Corresponding absorption changes at λ = 394 nm in presence of 0.8 U/mL HK. c) Time dependent CD changes at λ = 394 nm in presence of different units of HK with time in log scale for clearer lifetime elucidation depicting modulation of lifetime and rate. d) Plot depicting effect of variation of HK on lifetime of transient state and rate of stereomutation following a linear trend ([**NDPA**] = 5 x 10^{-5} M, [ATP] = 1 eq., [Glucose] = 1200 eq., 10 mM aq. HEPES buffer, T = 40 ℃).*

Next we monitored the transient conformation switching in **NDPA** assemblies at 394 nm for further experiments over time in CD and absorbance. At this wavelength positive and negative CD signal correspond to *P* and *M*-type assembly and in absorbance refers to aggregation band. Thus any change can be corresponded well to the spectral changes. Both CD and absorption

changes as a function of time show an instantaneous increase and then a gradual decay (Figure 2.6a-c). This rate of stereomutation could be modulated by variation of enzyme units that changes rate of enzymatic action which further is responsible for rate of stereomutation. To realize this, Hexokinase units were varied from 0.8 to 9.6 U/mL and the lifetime were measured by taking the time where **NDPA** assemblies show a positive CD signal i.e. are in *P*-type helical conformational state (Figure 2.6c). The lifetime thus varied from 200 to 900 seconds and the corresponding rates from 9.4 x 10^{-4} s^{-1} to 2.5 x 10^{-3} s^{-1} (Figure 2.6d).

Thus, system is highly dynamic and adaptive to the amount of enzyme present. Although, we could modulate the rate and lifetime of transient cycle and further refuel the system for subsequent transient cycles, but system undergoes damping in extent of change in successive cycles. Also, a slow rate of *P*→*M* stereomutation is observed. This is because of inhibition of activity of Hexokinase by its own products after phosphoryl transfer. These are glucose-6-phosphate and ADP which in glycolysis cycle maintain the balance of glucose consumption in body, but in our system, it results in damping (Figure 2.6a).[13] Furthermore, the refueling of system required subsequent addition of 2 eq. of ATP whereas 1 eq. was sufficient for the first cycle.

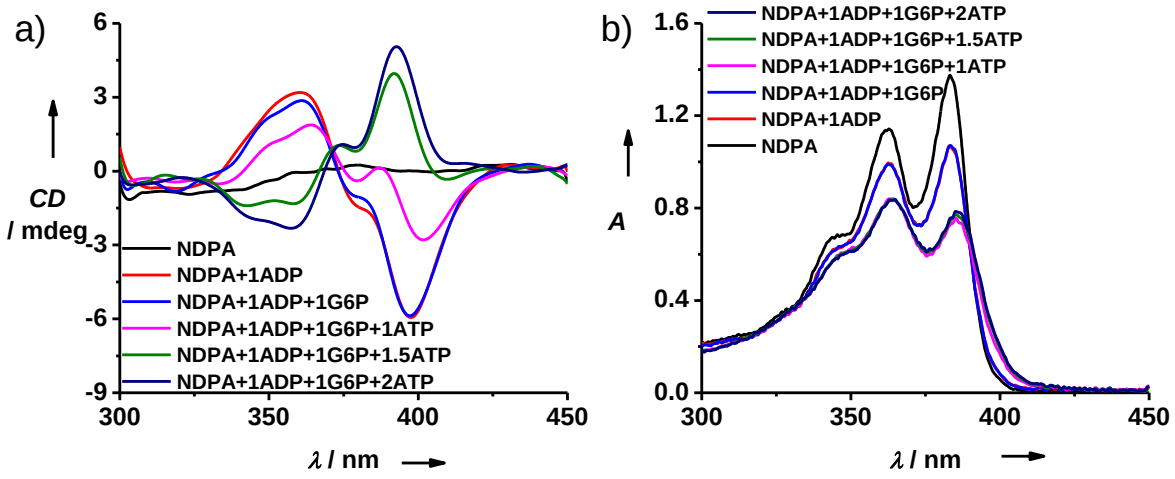

Figure 2.7. *Effect of glucose-6-phosphate on competitive binding of ATP over ADP for guest-induced self-assembly of* ***NDPA****. a) CD spectra, b) absorption spectra showing titration of (M)-****NDPA****-ADP with ATP in presence of 1 eq. glucose-6-phosphate depicting requirement of 2 eq. of ATP for refueling ([****NDPA****] = 5 x* 10^{-5} *M, [ADP] = 1 eq., [Glucose] = 1200 eq., [Glucose-6-phosphate] = 1 eq., 10 mM aq. HEPES buffer, T = 40 ℃).*

To attribute this increased requirement of ATP for refueling, a control experiment was done such that the solution depicts the completion of first cycle. Thus, it contains ADP, glucose and glucose-6-phosphate in absence of enzyme. To a solution of **NDPA** and 1200 eq. of glucose, 1 eq. ADP was added to achieve (*M*)-**NDPA**-ADP self-assembly signified by negative bisignated CD signal (Figure 2.7a,b). Further addition of glucose-6-phosphate, the side product after first equivalent of ATP hydrolysis by HK, did not result in any change in CD and absorption validating the fact that there is no change in self-assembly by addition of glucose-6-phosphate. Subsequent addition of 1 eq. of ATP, even though bought change in CD and absorption spectra, but 1 eq. of ATP was insufficient to change the CD signal to positive bisignated. On consequent addition of ATP, CD signal became positive bisignated and saturated above 2 eq. of ATP. Thus, the experiment suggests that presence of glucose-6-phosphate increases the effective binding of ADP with **NDPA** stacks which require higher equivalents of ATP to competitively replace ADP from (*M*)-**NDPA**-ADP assembly.

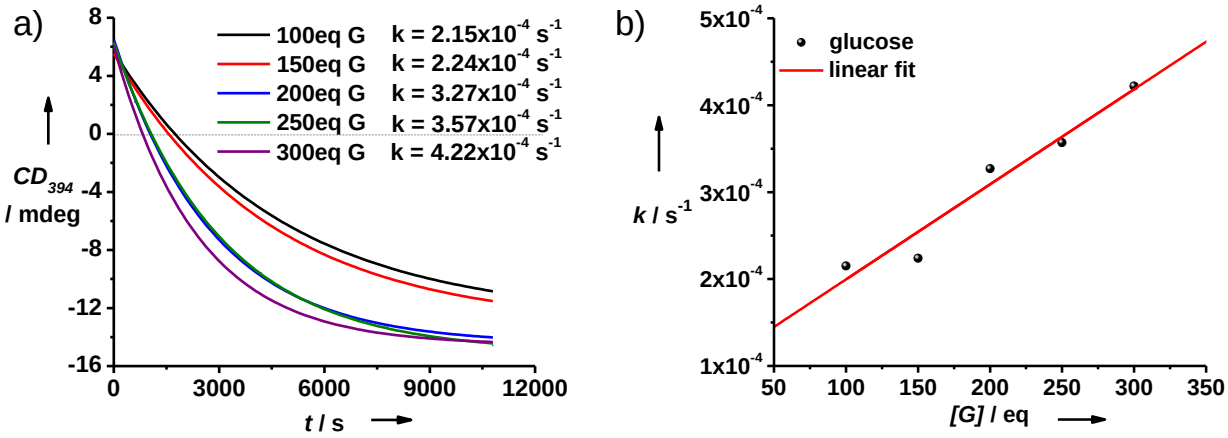

Figure 2.8. *Effect of glucose on rate of stereomutation of* ***NDPA*** *self-assembly. a) Time dependent CD changes depicting increase in rate of P→M stereomutation by increase in glucose equivalents. b) Plot of rate of stereomutation vs. eq. of glucose suggesting a linear increase in rate with increase in glucose equivalents ([****NDPA****] = 5 x 10^{-5} M, [ATP] = 1 eq., 6.4 U/mL HK, 10 mM aq. HEPES buffer, T = 40 ℃).*

Enzymes such as Hexokinase with bi-substrate reactions give an additional parameter to control the activity of the enzyme and the corresponding reaction. Utilizing this, we varied the equivalents of glucose from 100 to 300 eq. to see the effect on the stereomutation rate. As expected, increasing equivalents of glucose, enhances the rate of Hexokinase and simultaneously

acceleration in stereomutation rates is observed (Figure 2.8a). This enhancement follows a linear relationship with glucose concentrations and thus this change can be extrapolated to a wider window of glucose concentration and provides a wider regime of stereomutation rates and lifetime to be accessed (Figure 2.8b). Results so far have demonstrated that the transient conformational switching in **NDPA** assembly can be successfully modulated for rate of *P*→*M* stereomutation and lifetime of transient (*P*)-**NDPA**-ATP state.

2.5 Transient Conformational Switching Mediated by Creatine Phosphokinase

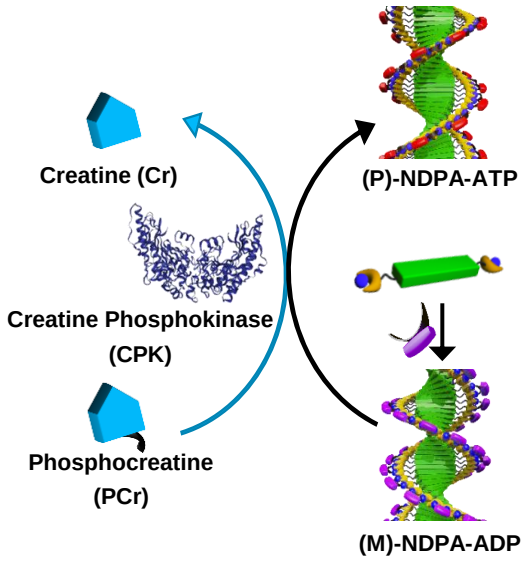

Scheme 2.5. *Schematic representation of transient conformational switching of* ***NDPA*** *assembly mediated by Creatine Phosphokinase in presence of phosphocreatine.*

In order to achieve control on rate of *M*→*P* stereomutation, which was unachieved in case where Hexokinase was employed, we attempted for the transient conformational switching of **NDPA** assembly by Creatine Phosphokinase (CPK) in presence of its substrate phosphocreatine (PCr) (Scheme 2.5). Creatine Phosphokinase is a phosphotransferase enzyme which phosphorylates ADP to form ATP in presence of phosphorylating agent phosphocreatine.

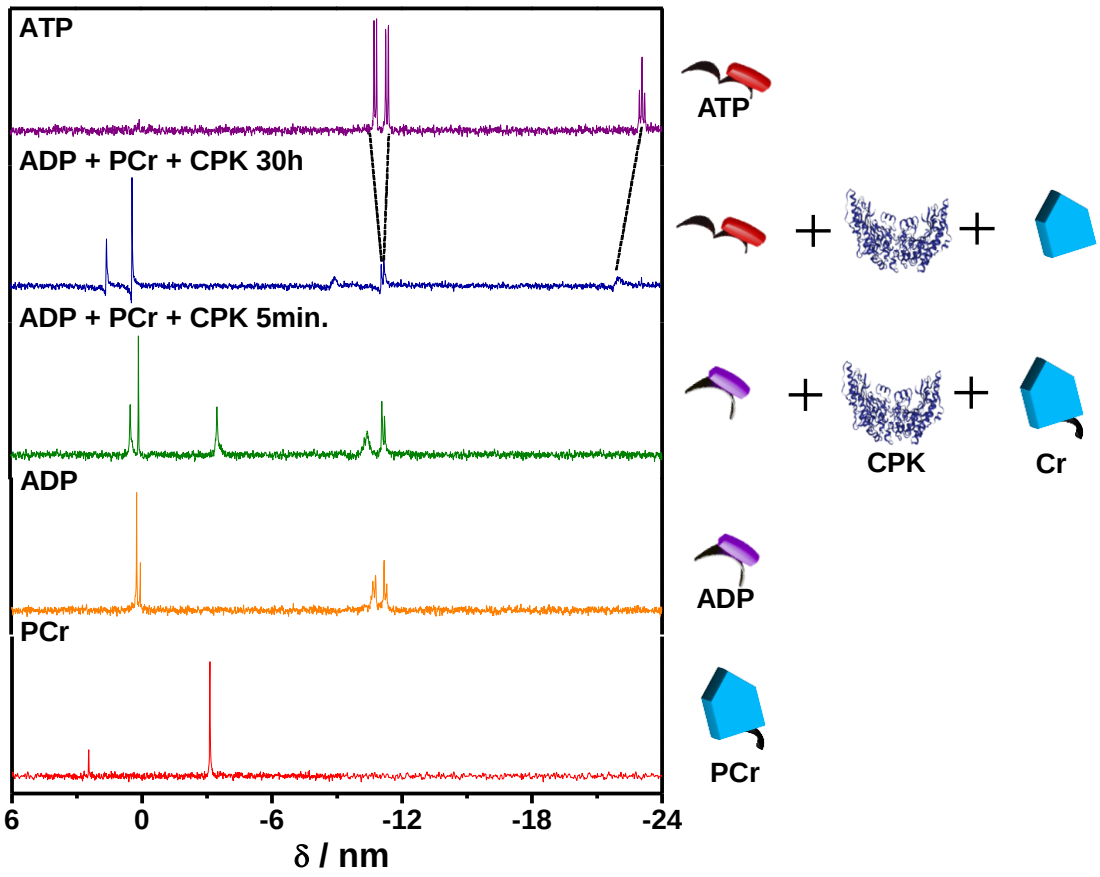

Figure 2.9. *^{31}P NMR depicting formation of ATP from ADP mediated by Creatine Phosphokinase (CPK) in presence of phosphocreatine (PCr). ([ADP] =10^{-3} M, [PCr] = 1.5 eq., 100 U/mL CPK, HEPES buffer in D_2O)*

To verify this reaction, we investigated the effect of Creatine Phosphokinase on ADP in presence of phosphocreatine. For this, separately 10^{-3} M ADP and $1.5x10^{-3}$ M PCr solution in HEPES buffer in D_2O were taken and ^{31}P NMR spectra was recorded. To 10^{-3} M ADP solution in HEPES buffer in D_2O, 1.5 eq. PCr and 100 U/mL CPK were added and immediately ^{31}P NMR spectra was recorded which shows no shift in ADP peaks (Figure 2.9). After 30 hours interval, ^{31}P NMR spectra showed the formation of ATP by appearance of δ = -23 ppm. Thus, we could confirm the activity of CPK for further investigations.

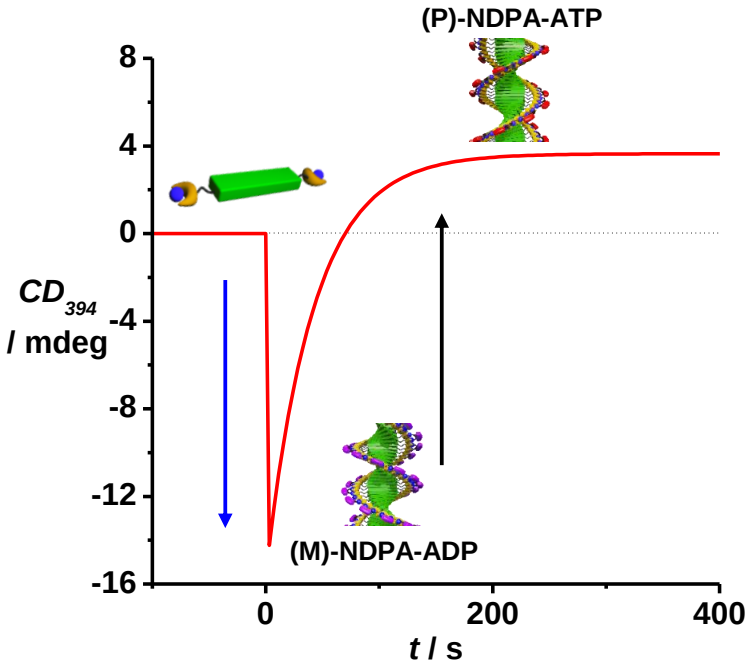

Figure 2.10. *Transient Conformational Switching by Creatine Phosphokinase: Time dependent CD changes at λ = 394 nm depicting instantaneous increase of negative CD signal and gradual change from negative to positive CD signal showing M→P stereomutation, Arrows are to guide the eye, blue showing formation of (M)-**NDPA**-ADP assembly and black M→P stereomutation ([**NDPA**] = 5 x 10^{-5} M, [ADP] = 1 eq., [PCr] = 1.5 eq., 2 U/mL CPK, 10 mM aq. HEPES buffer, T = 40 ℃).*

From the previous studies, we know that signal at 394 nm depict the sign of bisignation of CD signal and hence the type of helical conformation. Therefore, we monitored the transient conformation switching in **NDPA** assembly mediated by CPK at 394 nm over time in CD. In a solution of **NDPA** (5 x 10^{-5} M in aq. HEPES), 1.5 eq. PCr and 2 U/mL CPK, upon addition of 1 eq. of ADP resulted in instantaneous helical self-assembly shown by negative CD signal signifying formation of (*M*)-**NDPA**-ADP assembly. Then a gradual change in CD signal from negative to positive was observed due to *in situ* formation of ATP by PCr that resulted in (*P*)-**NDPA**-ATP assembly (Figure 2.10). There was no further change in CD signal as it achieved equilibrium. Hence, we could observe a slow rate of stereomutation from *M→P* that was lacking in case of Hexokinase. But, there was no control of *P→M* stereomutation that Hexokinase showed. Thus, a system with control over both *M→P* and *P→M* stereomutation rates require a two reaction steps in tandem. Which urges towards exploiting the bio-inspired "enzyme in tandem" technique to

control the kinetics of the system. This approach deals with two opposing enzymes working against each other but delayed in time by concentration of various substrates.

2.6 Transient Conformational Switching Mediated by "Enzyme in Tandem" Approach

As discussed earlier, we could achieve transient conformational switching of **NDPA** assembly by singular enzymes Hexokinase and Creatine Phosphokinase. Hexokinase was able to control *P*→*M* stereomutation whereas Creatine Phosphokinase could control *M*→*P* stereomutation. Although, rate of stereomutation could be controlled but both the enzymes lacked in complete modulation as their activity affected only in one direction. Next we envisaged to have a complete control over the system i.e. modular rate of *M*→*P* and *P*→*M* stereomutation and lifetime of transient conformational state (*P*)-**NDPA**-ATP.

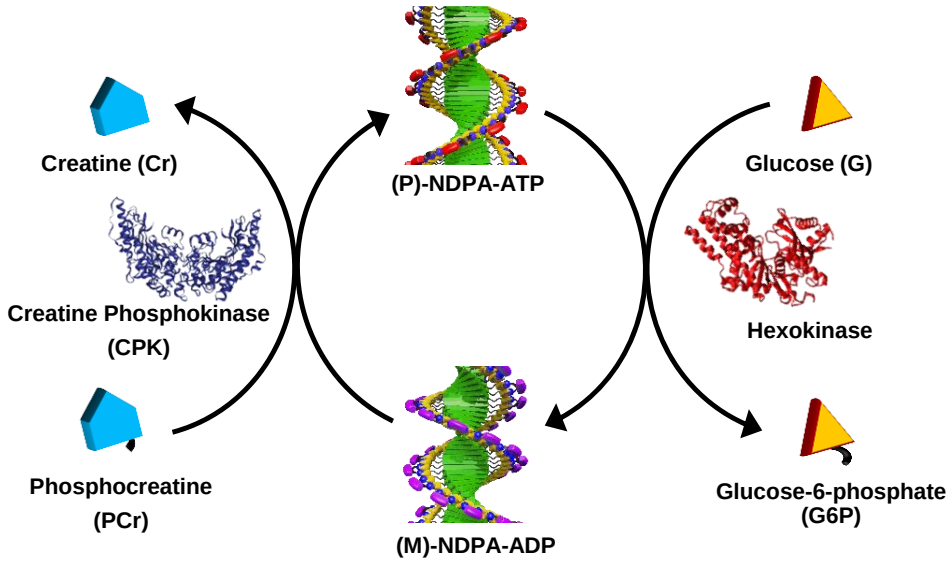

Scheme 2.6. *Schematic representation of transient conformational switching of* ***NDPA*** *assembly mediated by Creatine Phosphokinase and Hexokinase in tandem in presence of their respective substrates phosphocreatine and glucose.*

For this we used a bio-inspired "enzyme in tandem" approach (Scheme 2.6). In nature, phosphoryl transferase enzymes such as myokinase and Creatine Phosphokinase work in tandem to produce energy for muscle function. We hypothesize that control over the kinetics of the two

opposing enzymes should result in the above stated modular system. The kinetics of the system needs to be controlled such that rate of formation should be higher than rate of decay which result in significant lifetime for transient process and transient state.[14]

With this understanding, a high ratio of Creatine Phosphokinase to Hexokinase was chosen for the experiments. To a solution of **NDPA** (5 x 10^{-5} M in aq. HEPES) with 600 eq. glucose, 2 U/mL CPK and 0.8 U/mL HK, 1.5 eq. ADP was added to form (*M*)-**NDPA**-ADP assembly. Upon addition of 3 eq. of PCr, time dependent CD spectra show a gradual change from negative bisignated CD signal to positive bisignated CD signal depicting the slow stereomutation from *M*→*P* to form (*P*)-**NDPA**-ATP stacks (Figure 2.11a). This is due to *in situ* formation of ATP from ADP in presence of CPK and PCr. At this state, Hexokinase is inactivated because of unavailability of ATP for hydrolyzing, hence rate of formation of ATP is higher than rate of its hydrolysis. Rate of hydrolysis increases slowly as ATP is formed but it is always less till Creatine Phosphokinase is active. This owes to the fact that ratio of enzymatic units of CPK to HK are high.

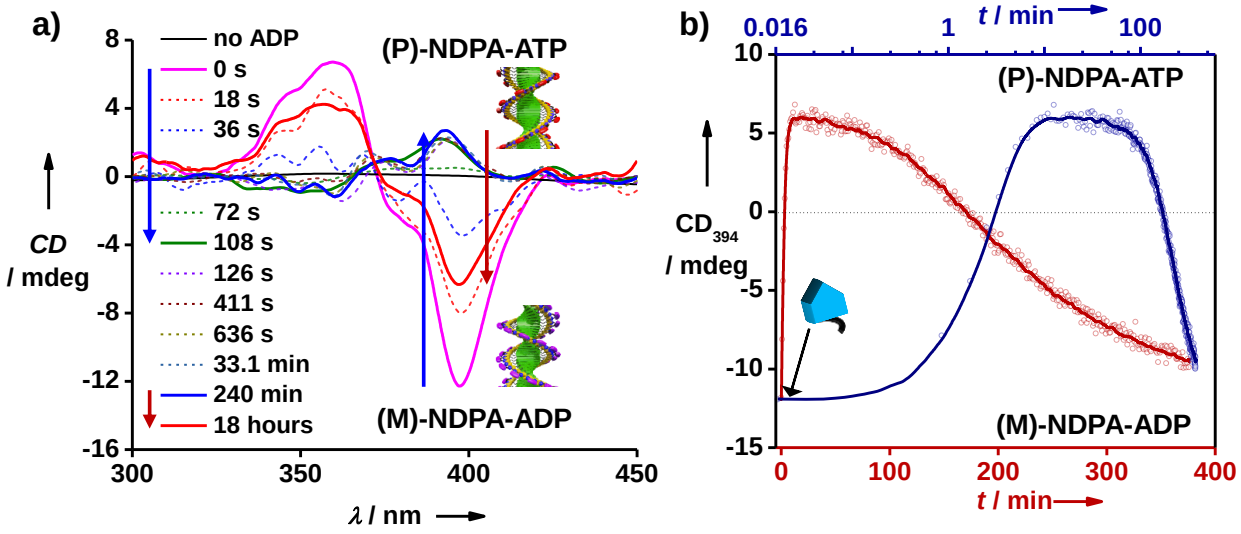

Figure 2.11. *Transient Conformational Switching Creatine Phosphokinase and Hexokinase in tandem: a) Time dependent CD spectral changes depicting gradual change from negative to positive to negative bisignated (t = 0 →108 s→18 h), b) Time dependent CD signal changes at λ = 394 nm depicting M→P→M stereomutation ([**NDPA**] = 5 x 10^{-5} M, [ADP] = 1.5 eq., [Glucose] = 600 eq., 2 U mL^{-1} CPK, 0.8 U mL^{-1} HK, [PCr] = 3 eq., 10 mM aq. HEPES buffer, T = 40 ℃).*

Next, at the transient state there is formation as well as hydrolysis of ATP in presence of two competing enzymes. The excess of phosphocreatine keeps regenerating ATP from the

hydrolyzed product ADP. Thus, a steady state (*P*)-**NDPA**-ATP is observed for 170 minutes. As PCr gets consumed, there is a change in the two rate kinetics, i.e., rate of formation of ATP decreases than rate of hydrolysis resulting in decay of the (*P*)-**NDPA**-ATP state. As soon as PCr gets consumed completely, activity of Creatine Phosphokinase gets shut and hence there is only hydrolysis of ATP to give negative bisignated CD signal confirming the formation of (*M*)-**NDPA**-ADP assembly.

The time dependent CD changes at 394 nm depict a gradual change from -12 mdeg CD signal to +6 mdeg CD signal corresponding to M→P stereomutation from (*M*)-**NDPA**-ADP assembly on addition of 3 eq. PCr (Figure 2.11b). Then, a steady state of positive CD signal depicting presence of (*P*)-**NDPA**-ATP assembly. After this a gradual decrease of CD signal from positive to negative takes place. Hence, system undergoes *P*→*M* stereomutation to revert back to its initial (*M*)-**NDPA**-ADP state.

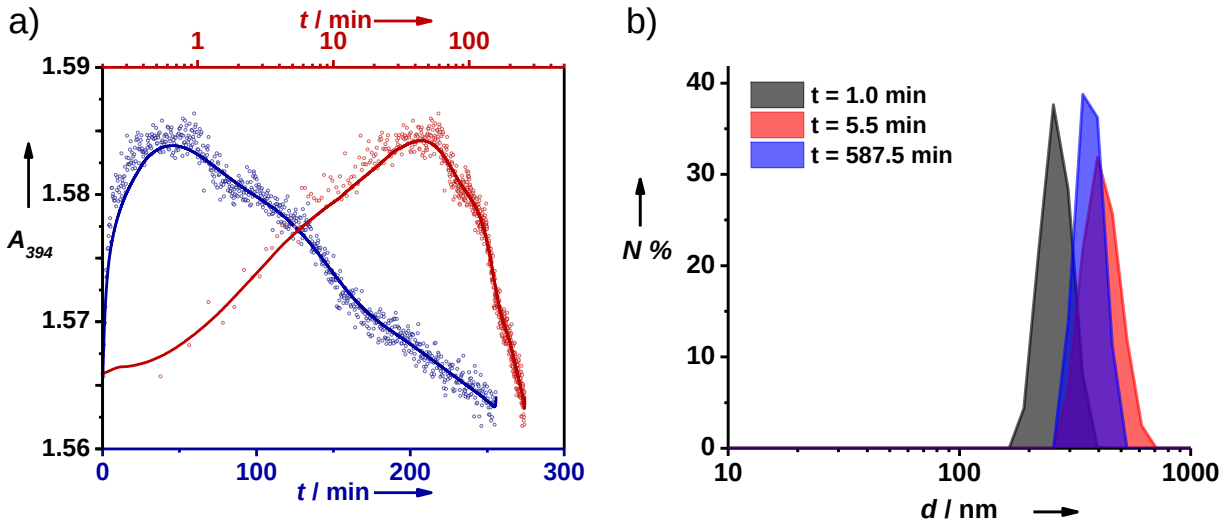

Figure 2.12. *Transient Conformational Switching mediated by Creatine Phosphokinase and Hexokinase in tandem: a) Time dependent absorption changes depicting gradual change at λ = 394 nm, b) Number percentage DLS size changes over the transient cycle showing no significant change ([**NDPA**] = 5 x 10^{-5} M, [ADP] = 1.5 eq., [Glucose] = 600 eq., 2 U mL^{-1} CPK, 0.8 U mL^{-1} HK, [PCr] = 3 eq., 10 mM aq. HEPES buffer, T = 40 ℃).*

The transient conformation switching in **NDPA** assemblies was then investigated by DLS and absorbance as a function of time. To a solution of **NDPA** (5 x 10^{-5} M in aq. HEPES) with 600 eq. glucose, 2 U/mL CPK and 0.8 U/mL HK, 1.5 eq. ADP was added to form (*M*)-**NDPA**-ADP

assembly. Upon addition of 3 eq. of PCr, time dependent absorption show a gradual increase followed by a slow decrease (Figure 2.12a). Even though absorption follow the same trend as CD changes (Figure 2.11b) but the difference is of mere 0.02 a. u. suggesting insignificant change in inter-chromophoric interactions. Furthermore, number percentage DLS size show that there is no disassembly over the cycle and thus, transient cycle majorly involves conformational switching (Figure 2.12b).

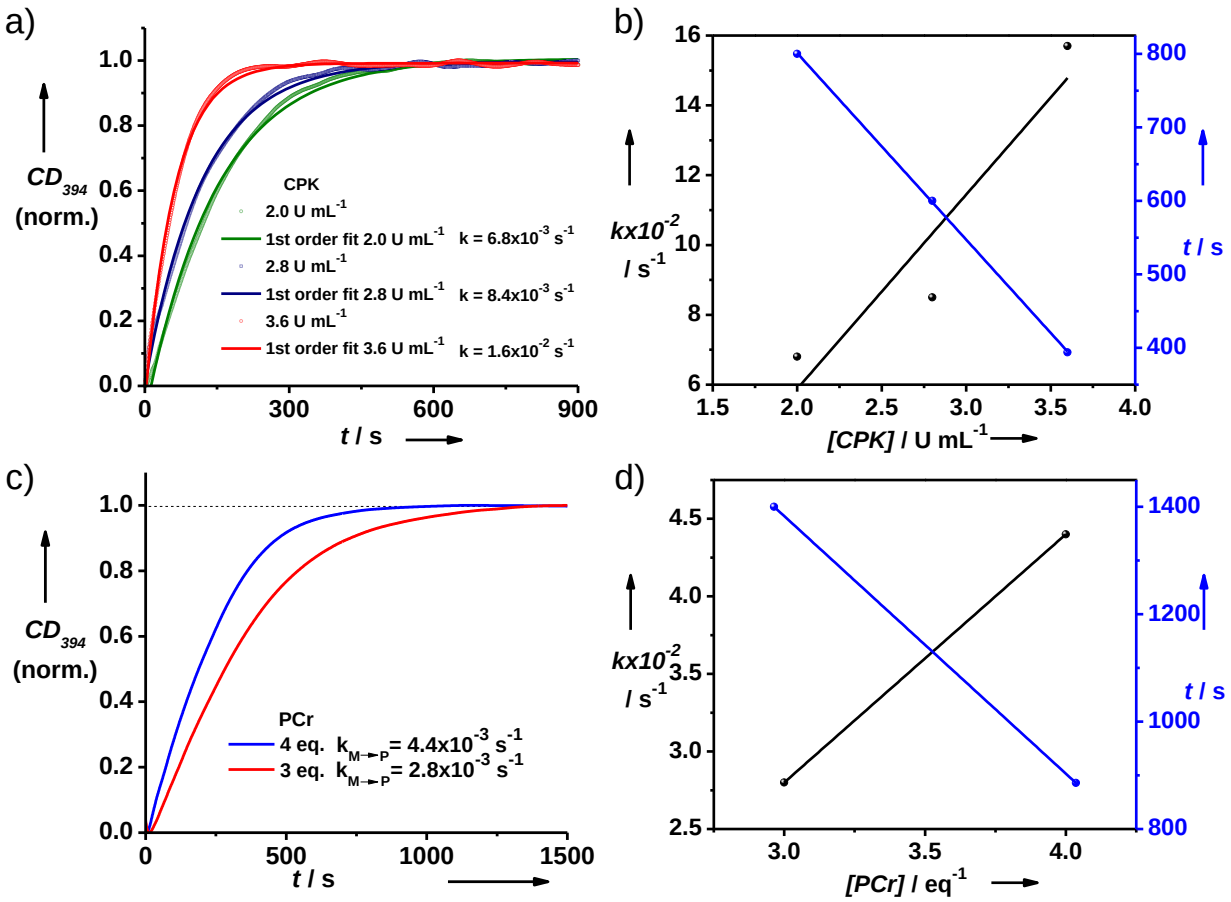

Figure 2.13. *Temporal control over M→P stereomutation by change in rate of formation of ATP in presence of Creatine Phosphokinase and Hexokinase in tandem. Time dependent normalized CD change at λ = 394 nm, a) for various units of Creatine Phosphokinase, c) for different equivalents of phosphocreatine, b) rate of stereomutation and time required for stereomutation vs. Creatine Phosphokinase units following an increase with enzyme units, d) rate of stereomutation and time required for stereomutation vs. equivalents of phosphocreatine resulting an acceleration in rate with increase in phosphocreatine equivalents ([**NDPA**] = 5 x 10^{-5} M, [ADP] = 1.5 eq., 0.8 U mL^{-1} HK, 10 mM aq. HEPES buffer, T = 40 ℃, for a) and b) [Glucose] = 600 eq., [PCr] = 3 eq., for c) and d) [Glucose] = 600 eq., 2 U mL^{-1} CPK).*

With the control over rate of *M*→*P*→*M* stereomutation, next we envisaged for modulation of the rates of stereomutation and lifetime of transient state to access different temporal regimes. For this different concentration of constituents was employed that affect the rate of formation or rate of hydrolysis of ATP and thereby result in different temporal profile.

Temporal control achieved by two opposing reaction by bi-substrate enzymes give a variety of parameters such as pH, temperature, enzyme units, substrate concentration etc. In the current system pH and temperature is chosen such that there is a sufficient high activity of both the enzymes as well as **NDPA** assemblies are of high dynamicity. Then we targeted the modulation of rates by variation of enzyme units and substrate concentration.

Firstly, we varied the parameters that directly affect the rate of ATP formation to understand the temporal control obtained for rate of *M*→*P* stereomutation. These parameters are units of Creatine Phosphokinase, concentration of ADP and concentration of phosphocreatine which accelerate the *M*→*P* stereomutation. Since appropriate equivalents of ADP need to be added for saturated CD signal, hence it was kept constant in experiments. The parameters used in initial experiments Figure 2.11 i.e. a solution of **NDPA** (5×10^{-5} M in aq. HEPES), 600 eq. glucose, 0.8 U/mL Hexokinase and 1.5 eq. ADP were kept same which formed (*M*)-**NDPA**-ADP assembly. To investigate effect of Creatine Phosphokinase, it was varied from 2 U/mL to 3.6 U/mL. Then upon addition of 3 eq. of PCr, time dependent CD changes at 394 nm were monitored. The CD signal showed a gradual change from negative to positive CD signal depicting the slow stereomutation from *M*→*P* to form (*P*)-**NDPA**-ATP stacks (Figure 2.13a). This can be attributed to the fact that the increase in enzyme units increases the rate of ADP to ATP formation and thereby stereomutation rate. The system follows a linear increase in rate with increasing enzyme units and linear decrease in time required for conversion (Figure 2.13b).

The next parameter is equivalents of phosphocreatine which affects the enzyme activity and thus changes the stereomutation rate. For this, a solution of **NDPA** (5×10^{-5} M in aq. HEPES), 600 eq. glucose, 0.8 U/mL Hexokinase, 1.5 eq. ADP and 2 U/mL Creatine Phosphokinase was taken which formed (*M*)-**NDPA**-ADP assembly. To investigate effect of phosphocreatine, two experiments were done with 3 eq. and 4 eq. PCr. To the above solution, PCr was added and time dependent CD changes at 394 nm were monitored. The CD signal followed the similar trend as in the above stated experimental conditions showing a gradual change from negative to positive CD

signal that represent a slow stereomutation from *M*→*P* to give (*P*)-**NDPA**-ATP stacks (Figure 2.13c). This can be described by the enhancement in enzymatic action on increasing concentration of its substrate and hence increase in the rate of stereomutation is observed. Increase of 1 eq. of PCr increased the rate to 1.6 times and decreased the time required for stereomutation from ~1400 to ~880 (Figure 2.13d). Thus, changes in the concentration of PCr and enzyme units result in a modulable stereomutation, even in the presence of Hexokinase which is the opposing enzyme.

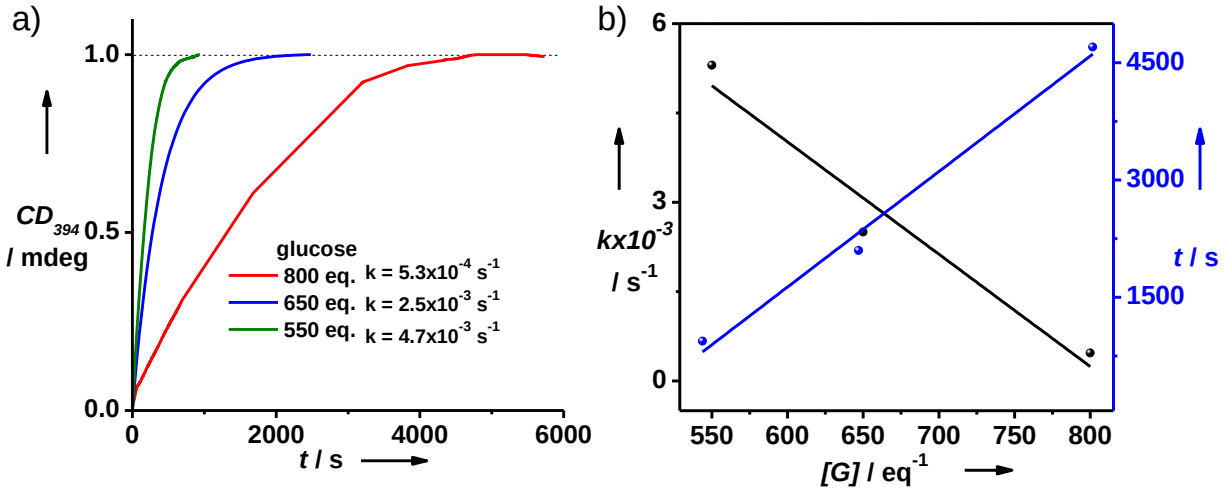

Figure 2.14. *Temporal control over M→P stereomutation by change in rate of hydrolysis of ATP in presence of Creatine Phosphokinase and Hexokinase in tandem: a)Time dependent normalized CD changes at λ = 394 nm for different equivalents of glucose and b) rate of stereomutation and time required for stereomutation vs. equivalents of glucose depicting a linear decrease on increase in glucose equivalents ([**NDPA**] = 5 x 10^{-5} M, [ADP] = 1.5 eq., 0.8 U mL^{-1} HK, 10 mM aq. HEPES buffer, T = 40 ℃, [PCr] = 3 eq., 2 U mL^{-1} CPK).*

Secondly, we varied the parameters that affects the rate of ATP hydrolysis to understand the temporal control obtained for rate of *M*→*P* stereomutation when the rate of opposite reaction i.e. ATP hydrolysis is accelerated. These parameters are units of Hexokinase and concentration of glucose which accelerate the ATP hydrolysis. A slight increase in Hexokinase did not reflect in a transient cycle and hence only glucose was varied for modulation of rate. To investigate effect of glucose on temporal variation in stereomutation, a solution of **NDPA** (5 x 10^{-5} M in aq. HEPES), with varied glucose eq., 0.8 U/mL Hexokinase, 2 U/mL Creatine Phosphokinase and 1.5 eq. ADP were taken which formed (*M*)-**NDPA**-ADP assembly. The amount of glucose was varied from 550 to 800 eq. Then 3 eq. of PCr was added to initiate the transient cycle and time dependent CD changes at 394 nm were further monitored (Figure 2.14a,b). There was a clear change in growth

of positive CD signal with glucose equivalents. This is because, increasing equivalents of glucose, accelerates ATP hydrolysis and therefore amount of ATP required to reach positive CD signal require a longer time. Therefore, increasing equivalents of glucose decelerates ATP formation and *M→P* stereomutation rate. There is an overall decrease in rate of M→P stereomutation and increase in time required for stereomutation on increasing glucose equivalents.

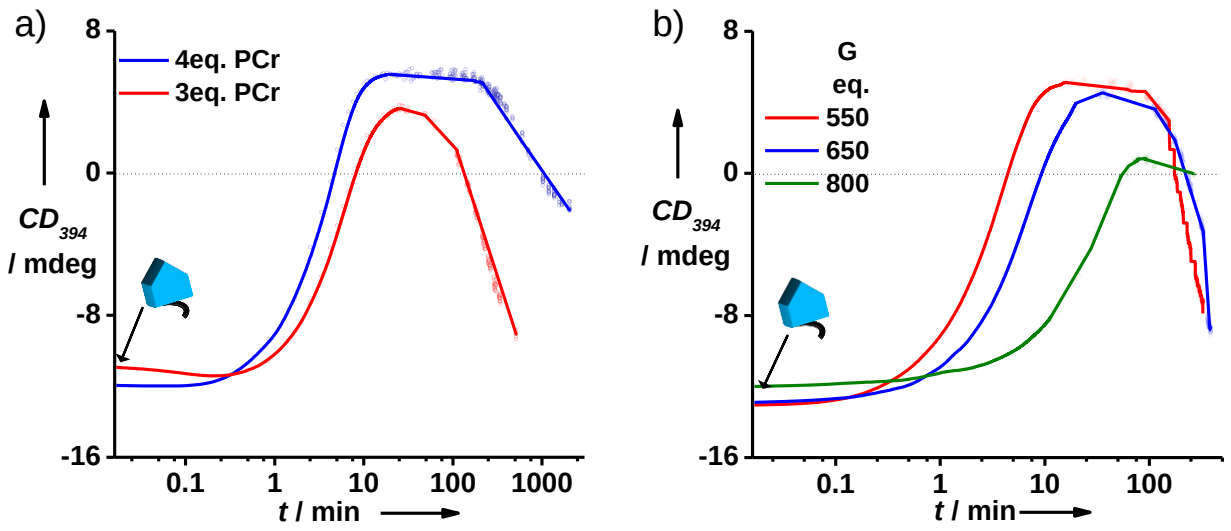

Figure 2.15. *Transient Conformational Switching Creatine Phosphokinase and Hexokinase in tandem: Time dependent CD signal changes at λ = 394 nm depicting M→P→M stereomutation a) Effect of phosphocreatine, b) Effect of glucose ([**NDPA**] = 5 x 10^{-5} M, [ADP] = 1.5 eq., 2 U mL^{-1} CPK, 0.8 U mL^{-1} HK, 10 mM aq. HEPES buffer, T = 40 ℃, for a) [Glucose] = 600 eq., for b) [PCr] = 3 eq.).*

With the investigations so far, effect of different parameters on rate of stereomutation. Then, we applied the variation of these parameters to obtain a modular transient conformational switching of **NDPA** assembly mediated by Creatine Phosphokinase and Hexokinase in tandem. First we varied phosphocreatine which acts as the primary fuel for the transient switching which (re)generates ATP from ADP. To investigate effect of phosphocreatine on transient conformational switching, a solution of **NDPA** (5 x 10^{-5} M in aq. HEPES), with 600 eq. glucose, 0.8 U/mL Hexokinase, 2 U/mL Creatine Phosphokinase and 1.5 eq. ADP were taken. Negative CD signal confirmed the formation of (*M*)-**NDPA**-ADP assembly. Then PCr was added to initiate the transient cycle and time dependent CD changes at 394 nm were monitored. The CD signal followed a gradual increase and then decrease. An increase in lifetime of transient (*P*)-**NDPA**-ATP state from 170 minutes to 940 minutes was observed (Figure 2.15a).

Finally we varied glucose equivalents, keeping initial phosphocreatine concentration to 3 equivalents. A delayed $M \rightarrow P$ stereomutation is seen as Hexokinase activity accelerates with increase in glucose equivalents. Then the system reached the transient state and stayed for 170-220 minutes of lifetime and then gradually undergo $P \rightarrow M$ stereomutation to finish the transient cycle (Figure 2.15b).

An extensive study using variation in parameters of transient cycle i.e. enzymes Creatine Phosphokinase and Hexokinase, their respective substrates phosphocreatine/ADP and glucose/ATP, we could obtain highly modular lifetime of transient state and rates of stereomutation (Table 2.1).

CPK	HK	ATP	ADP	G	PCr	$k_{M\rightarrow P}$ [a]	$t_{M\rightarrow P}$ [b]	τ_P [c]	$k_{P\rightarrow M}$ [d]
U/mL	U/mL	eq.	eq.	eq.	eq.	s^{-1}	s	s	s^{-1}
-	6.4	1	-	100	-	-	*	1753	$2.1x10^{-4}$
-	6.4	1	-	150	-	-	*	1559	$2.2x10^{-4}$
-	6.4	1	-	200	-	-	*	1071	$3.3x10^{-4}$
-	6.4	1	-	250	-	-	*	1024	$3.6x10^{-4}$
-	6.4	1	-	300	-	-	*	822	$4.2x10^{-4}$
-	0.8	1	-	600	-	-	*	875	$9.4x10^{-4}$
-	6.4	1	-	600	-	-	*	390	$2.0x10^{-4}$
-	9.6	1	-	600	-	-	*	200	$2.5x10^{-4}$
2	-	-	-	-	3	$2.4x10^{-2}$	-	-	-
2	0.8	-	1.5	600	3	$6.4x10^{-3}$	173	10165	$6.1x10^{-5}$
2	0.8	-	1.5	600	4	$5.0x10^{-3}$	260	56320	$2.5x10^{-5}$
2	0.8	-	1.5	650	3	$2.5x10^{-3}$	518	13183	-

2	0.8	-	1.5	550	3	5.2×10^{-3}	259	10188	1.5×10^{-4}
2	0.8	-	1.5	800	3	4.9×10^{-4}	-	-	-
2	1.2	-	1.5	600	4	6.9×10^{-3}	-	-	-
2	0.4	-	2	600	4	5.0×10^{-2}	-	-	2.5×10^{-5}
3.6	0.8	-	1.5	600	3	1.7×10^{-2}	75	48594	-
2.8	0.8	-	1.5	600	3	8.5×10^{-3}	197	16471	-

[a] Rate of M→P stereomutation, [b] Time required from start of cycle till CD signal at 394 nm becomes zero, [c] Lifetime of **(P)-NDPA-ATP**, [d] Rate of *P*→*M* stereomutation. [**NDPA**] = 5×10^{-5} M, equivalents of substrates are with respect to [**NDPA**]. *instantaneous

Table 2.1. Variation of parameters of transient cycle and the resulting rates of stereomutation and lifetime of transient state.

The lifetime of transient state (*P*)-**NDPA**-ATP so obtained varied from 200 seconds to 16 hours. The rate of *M*→*P* stereomutation was modulated between 5×10^{-4} s^{-1} to 5×10^{-2} s^{-1}, thus an order of 100 times was observed. The rate of *P*→*M* stereomutation was controlled between 2.5×10^{-5} s^{-1} to 10^{-3} s^{-1} by varying the above stated parameters, hence an order of 40 could be achieved. Finally, the above stated rate modulation lead to a conclusion that the ratio of rates of *M*→*P* and *P*→*M* stereomutation should be higher than 30 times for a feasible transient cycle with a significant lifetime. An increase in lifetime is observed with increasing ratio of rates.

2.7 Conclusion

To conclude, in this Chapter, we have presented a unique dynamic, helical assembly which shows adenosine phosphate binding induced supramolecular chirality with tunable handedness. We employed these distinct properties to build a chemical fuel (ATP)-driven transient conformational switching in a supramolecular polymer. We have shown a supramolecular synthetic mimic to represent non-equilibrium conformational switching in ATP-Binding Cassette Transporters. In addition, the system is highly modular in its rate of stereomutation and lifetime of

transient state owing to the use of the bio-inspired "enzyme in tandem" approach. Hence, this temporally programmed conformational switching is a stepping stone towards life-like complex systems with a high control on their function with respect to time. A helical conformation switching in a supramolecular system opens up door for a time regulated enantioselective reactions catalyzed by the concerned supramolecular motif.

2.8 Experimental Section

General Methods:

Optical Measurements: Electronic absorption spectra and Circular Dichroism measurements were performed on a Jasco J-815 spectrometer where the sensitivity, time constant and scan rate were chosen appropriately. Corresponding temperature dependent measurements were performed with a CDF – 426S/15 Peltier-type temperature controller with a temperature range of 263-383 K and adjustable temperature slope. Optical measurements were recorded in 10 mm path length cuvettes. CD spectra and time dependent CD changes were smoothened by adjacent averaging and fitted using first order kinetics to calculate rate constants. We are aware of the fact that enzymatic changes are not in theory first order changes, but a fit enables us to have a relative kinetic perspective between individual processes.

NMR Measurements: NMR spectra were obtained with a Bruker AVANCE 400 (400 MHz w.r.t. ^{1}H nuclei) Fourier transform NMR spectrometer with chemical shifts reported in parts per million (ppm).

Dynamic light scattering (DLS): The measurements were carried out using a NanoZS (Malvern UK) employing 532 or 635 nm laser at a back scattering angle of 173°. A dead time (Time between sample loading and starting of measurement by the machine) of around 45 seconds is present in all measurements.

Sample Preparation:

All solutions were prepared in 10 mM HEPES except for NMR measurements. Stocks were prepared as $5x10^{-4}$ M **NDPA**, $5x10^{-2}$ M ATP, ADP and PCr, 0.06 M G, 1 U/µL HK, 0.25 U/µL

CPK. Micropipette was used to transfer measured volumes of solution. Dead time (time between fuel injection and starting of measurement by the machine) in all the measurements were less than 60 seconds. Temperature was maintained at 40 °C to have a sufficiently high enzyme activity throughout the measurements. The samples were measured in a 10 mm quartz cuvette.

Protocol for conformational switching:

i. For only HK mediated cycles: To a solution of **NDPA**, HK and Glucose, ATP was added and measurements were done.
ii. For only CPK mediated cycles: To a solution of **NDPA**, CPK and ADP, PCr was added and measurements were done.
iii. For CPK and HK in tandem: To a solution of **NDPA**, CPK, HK, Glucose and ADP that formed (*M*)-**NDPA**-ADP, PCr was added and measurements were done.

"*(P)*-**NDPA**-ATP" term used in main text refers to 5 x 10^{-5} M solution of **NDPA** (in 10 mM aq. HEPES buffer) with 1 eq. of ATP. "*(M)*-**NDPA**-ADP" term used in main text refers to 5 x 10^{-5} M solution of **NDPA** (in 10 mM aq. HEPES buffer) with 1.5 eq. of ADP. "CPK" refers to Creatine Phosphokinase, "HK" refers to Hexokinase, "PCr" refers to phosphocreatine.

Materials: Hexokinase ex. Saccharomyces sp.(327 U/mg) (extrapure for biochemistry), Creatine Phosphate Disodium Salt Tetrahydrate (extrapure for biochemistry) and Adenosine-5-Diphosphate Disodium Salt (extrapure for biochemistry) were purchased from Sisco Research Laboratories Pvt. Ltd. India. Deuterated water (D_2O), Creatine Phosphokinase from rabbit muscle (150 U/mg), Adenosine-5-Triphosphate Disodium Salt (99%), Adenosine-5-Monophosphate Disodium Salt (99%), α-D-Glucose anhydrous (96%) were purchased from Sigma Aldrich. HEPES (4-(2-hydroxyethyl)-1-piperazineethanesulfonic acid) was procured from SD fine chemical limited.

Synthesis: NDPA was synthesized following the reported procedure and was characterized accordingly.[9]

2.9 References

1. F. H. Westheimer, *Science* **1987**, *235*, 1173.

2. T. Hayashi, S. Chiba, Y. Kaneta, T. Furuta, M. Sakurai, J. Phys. Chem. B **2014**, *118*, 12612-12620.
3. a) S. Sakurai, K. Okoshi, J. Kumaki, E. Yashima, *J. Am. Chem. Soc.* **2006**, *128*, 5650-5651; b) A. R. A. Palmans, E. W. Meijer, *Angew. Chem. Int. Ed.* **2007**, *46*, 8948- 8968; c) J. Cho, M. Tanaka, S. Sato, K. Kinbara, T. Aida, *J. Am. Chem. Soc.* **2010**, *132*, 13176-13178; d) N. Ousaka, Y. Takeyama, E. Yashima, *Chem. Eur. J.* **2013**, *19*, 4680-4685; e) J. Kang, D. Miyajima, Y. Itoh, T. Mori, H. Tanaka, M. Yamauchi, Y. Inoue, S. Harada, T. Aida, *J. Am. Chem. Soc.* **2014**, *136*, 10640-10644; f) M. Yamauchi, T. Ohba, T. Karatsu, S. Yagai, *Nat. Commun.* **2015**, *6*, 8936; g) M. Kumar, M. D. Reddy, A. Mishra, S. J. George, *Org. Biomol. Chem.* **2015**, *13*, 9938-9942; h) M. Vlatković, B. L. Feringa, S. J. Wezenberg, *Angew. Chem. Int. Ed.* **2016**, *55*, 1001-1004; i) H. K. Bisoyi, Q. Li, *Angew. Chem. Int. Ed.* **2016**, *55*, 2994-3010; j) K. Shimomura, T. Ikai, S. Kanoh, E. Yashima, K. Maeda, *Nat. chem.* **2014** , *6*, 429-434; k)D. Zhao, T. van Leeuwen, J. Cheng, B. L. Feringa, *Nat. Chem.* **2016**, doi:10.1038/nchem.2668
4. a) G. D. Pantoş, P. Pengo and J. K. M. Sanders, *Angew. Chem. Int. Ed.*, **2007**, *46*, 194; b) H. Shao and J. R. Parquette, *Chem. Commun.*, **2010**, *46***,** 4285; c) H. Shao, J. Seifert, N. C. Romano, M. Gao, J. J. Helmus, C. P. Jaroniec, D. A. Modarelli and J. R. Parquette, *Angew. Chem. Int. Ed*., **2010**, *49*, 7688; d) M. R. Molla, A. Das and S. Ghosh, *Chem. Commun.*, **2011**, *47*, 8934; e) S. V. Bhosale, S. V. Bhosale and S. K. Bhargava, *Org. Biomol. Chem.*, **2012**, *10*, 6455.
5. M. Kumar, P. Brocorens, C. Tonnelé, D. Beljonne, M. Surin, S. J. George *Nat. Commun.* **2014**, *6*, 5793
6. a) M.-A. Morikawa, M. Yoshihara, T. Endo and N. Kimizuka, *J. Am. Chem. Soc.* **2005**, *127*, 1358; b) I. O. Hirata, M. Takeuchi and S. Shinkai, *J. Am. Chem. Soc.* **2006**, *128*, 16008; c) T. Ma, C. Li and G. Shi, *Langmuir*, **2008**, *24*, 43.
7. S. Yagai, S. Mahesh, Y. Kikkawa, K. Unoike, T. Karatsu, A. Kitamura and A. Ajayaghosh, *Angew. Chem. Int. Ed.* **2008**, *47*, 4691.
8. a) A. Ojida, S.-K. Park, Y. Mito-oka, I. Hamachi, *Tetrahedron Lett.* **2002**, *43*, 6193–6195; b) O. Akio, Y. Mito-oka, K. Sada, I. Hamachi, *J. Am. Chem. Soc.* **2004**, *126*, 2454-2463; c) X. Chen, M. J. Jou and J. Yoon, *Org. Lett.*, **2009**, *11*, 2181; d) S. K. Kim, D. H. Lee, J.-

I. Hong and J. Yoon, *Acc. Chem. Res.*, **2009**, *42*, 23; e) T. Sakamoto, A. Ojida and I. Hamachi, *Chem. Commun.*, **2009**, 141.

9. H. N. Lee, Z. Xu, S. K. Kim, K. M. K. Swamy, Y. Kim, S.-J. Kim and J. Yoon, *J. Am. Chem. Soc.* **2007**, *129*, 3828-3829.
10. K. Yagi, L. Noda, *Biochim. Biophys. Acta*, **1960**, *43*, 249-259.
11. S. V. Bhosale, C. H. Jani, S. J. Langford, *Chem. Soc. Rev.* **2008**, *37*, 331.
12. J. Gawroński, M. Brzostowska, K. Kacprzak, H. Kołbon and P. Skowronek, *Chirality*, **2000**, *12*, 263.
13. A. Sols, R. K. Crane, *J. Biol. Chem.* **1954**, *210*, 597-606.
14. L. Heinen, A. Walther, *Soft matter* **2015**, *11*, 7857-7866.

Chapter 3

Chemical Fuel-Driven Temporal Control on Self-assembly

Chapter 3

Chemical Fuel-Driven Temporal Control on Self-assembly

Abstract

Biological systems such as cytoskeleton proteins function out-of-equilibrium driven by chemical fuel mediated transient self-assembly. These are microtubules and actin filaments driven by GTP and ATP, respectively. These biological systems are important examples for a spatio-temporal control over the self-organization and henceforth the function associated with the non-equilibrium state. Design of similar bio-inspired supramolecular assemblies can act as a key link between future life-like complex systems and the current passive synthetic materials. To alleviate this phenomenon, we further studied ***NDPA*** *self-assembly, which is highly dynamic and shows fuel-dependent adaptive conformations and additionally it also exhibits fuel-dependent size of the assemblies as the resultant of multivalent interactions. Hence, the hydrolysis of ATP to inorganic phosphate decreases the dimensions of the assembly. Herein, we present a unique system which undergo chemical fuel-driven transient self-assembly by employing phosphate hydrolysing enzymes.*

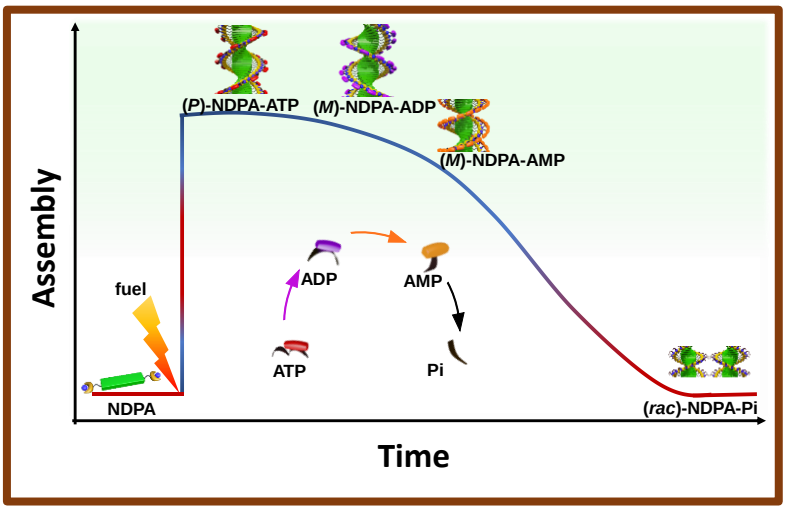

Manuscript based on this Chapter is under preparation

3.1 Introduction

Biological systems can perform thermodynamically unfavourable processes spontaneously by utilizing high energy biofuels[1] such as adenosine triphosphate (ATP) and guanosine triphosphate (GTP). These processes are ubiquitous, ranging from glycolytic pathway to translocation of substances and self-organization. The energy penalty of these unfavoured processes is provided by the binding of triphosphate and subsequent hydrolysis of their phosphodiester bonds. Amongst such unfavoured processes are self-assembly of proteins to form microtubules and actin filaments.[2,3] G-Actin protein monomers bind to ATP which activates them to undergo polymerization resulting in actin filaments (F-actin) as a non-equilibrium state which on hydrolysis of ATP to ADP undergo a spontaneous depolymerization, thus forming transient self-assembly. Self-assembly of actin filaments are selective to adenosine triphosphate and govern the movement of cell. Similarly mictotubules utilize guanosine triphosphate as the fuel to undergo transient polymerization to assist the chromosomal separation during cell division. These biological systems are important examples for a spatio-temporal control over the self-organization and hence the function associated with the non-equilibrium state.

To extend this scenario to synthetic systems, attempts have been made very recently to form transient supramolecular materials.[4] These systems involve a kinetic imbalance between activating and deactivating reactions creating a non-equilibrium state. Although, these systems show a temporally controlled self-assembly, some lack in their modulation, others in recyclability as well as a biomimetic strategy.

In this Chapter, we describe a bio-inspired approach to achieve a transient self-assembly with modular lifetime and rates. We further present the transient self-assembly of **NDPA** through *in situ* enzymatic transformation of guests i.e. ATP→ADP→AMP→Pi. This simple method of dynamic switching of bound guests, was utilized to bring a change from aggregated to disassembled state with an unprecedented control over lifetime of transient state and rate of transformation.

3.2 Design Strategy

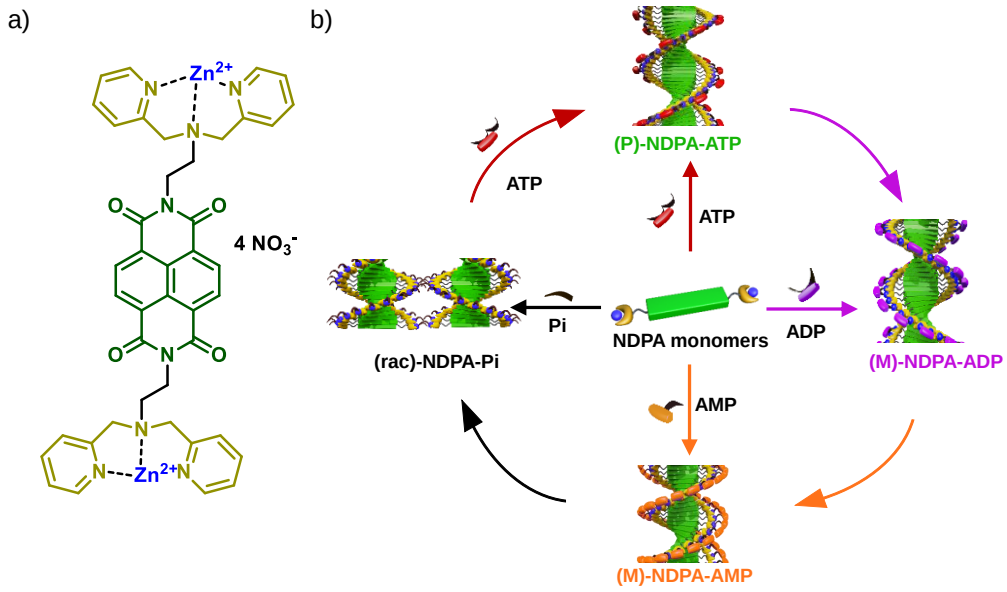

Scheme 3.1. *a) Molecular structure of* ***NDPA****. b) Schematic representation of formation and inter-conversion of ATP to Pi via ADP and AMP and the respective transformation in* ***NDPA*** *assemblies and arrows depict different probable pathways.*

As discussed in Chapter 2, the molecular recognition driven self-assembly of **NDPA** (Scheme 3.1a) employ electrostatic interactions for guest binding. The use of adenosine phosphates facilitate self-assembly of **NDPA** by inter-chromophoric π-π interactions with additional hydrophobic, hydrogen bonding and π-π interactions between the adenine units. The chiral ribose sugar act as chiral handle for imparting chirality to the resulting assemblies (Scheme 3.1b). The use of chromophore assists the understanding of self-assembly via spectroscopic probing and the phosphate receptor, dipicolylethylenediamine-Zinc complex (Zn-DPA), specifically bind to various adenosine phosphates with high association constants resulting in change in spectroscopic signatures due to the resultant self-assembly. **NDPA** was synthesized following the literature procedure.[5]

Zinc centre in **NDPA** mediates its solubility in water and its binding to phosphates. The difference in association constants arising from the multivalent phosphate electrostatic interactions and other hydrophobic, hydrogen bonding and π-π interactions between the guest phosphates makes it a highly dynamic assembly which is adaptive to the guest present in the system. The

multivalent guest molecules bind preferentially to the DPA receptors compared to monovalent or lower valent guests.[6] Such a dynamic system with control over helicity governed by phosphate recognition give an advantage for the *in situ* transformation of the fuel and the resulting effect should be reflected in the change in **NDPA** assembly (Scheme 3.1b). ATP is a biologically relevant phosphate which has compatibility to many enzyme classes which can act on it for various functions. Amongst various classes of enzymes are phosphatases which hydrolyse the phosphodiester bonds of various phosphates. Since our system is highly dynamic and adaptive to the presence of phosphate guest, it results in instantaneous formation of the stacks on addition of phosphate. A slow hydrolysis of ATP in presence of phosphatase should result in transient formation of **AXP-NDPA** (X = T, D, M) self-assembly. With this strategy, we employed two phosphoryl transfer enzymes singularly to achieve a transient **NDPA** self-assembly. Alkaline Phosphatase hydrolyses phosphodiester bonds independent of the molecular structure whereas Apyrase which constitutes ATPase and ADPase mixture has a high rate of hydrolysis of phosphodiester bond in ATP than in ADP (Scheme 3.2).

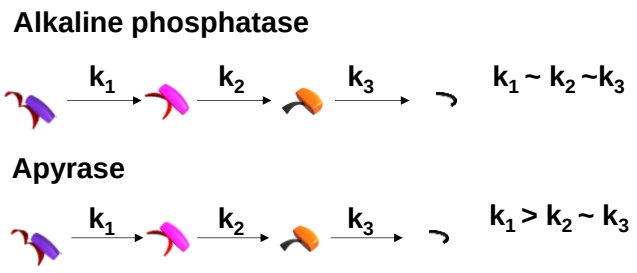

Scheme 3.2. *Schematic representation for enzymatic pathways for conversion of ATP to Pi by Alkaline Phosphatase (ALP) and Apyrase (AP).* k_1, k_2, k_3 *represents the rate constants for various hydrolysis steps.*

3.3 Adenosine Phosphate Driven Helical Self-Assembly

The absorption studies of **NDPA** (5×10^{-5} M, 10 mM aq. HEPES buffer) showed characteristic features of molecularly dissolved NDI chromophores such as sharp absorption bands (λ_{max} = 383 and 362 nm). The titrations of **NDPA** with ATP and ADP resulted in broadening of absorption spectra, along with reversal of relative intensity of vibronic bands at 362 nm and 383 nm characteristic of NDI chromophoric self-assembly (Section 2.2 and Figure 2.2). Corresponding

Circular Dichroism (CD) spectra showed the formation of *(P)*-**NDPA**-ATP and *(M)*-**NDPA**-ADP with positive and negative bisignated CD signals, respectively.

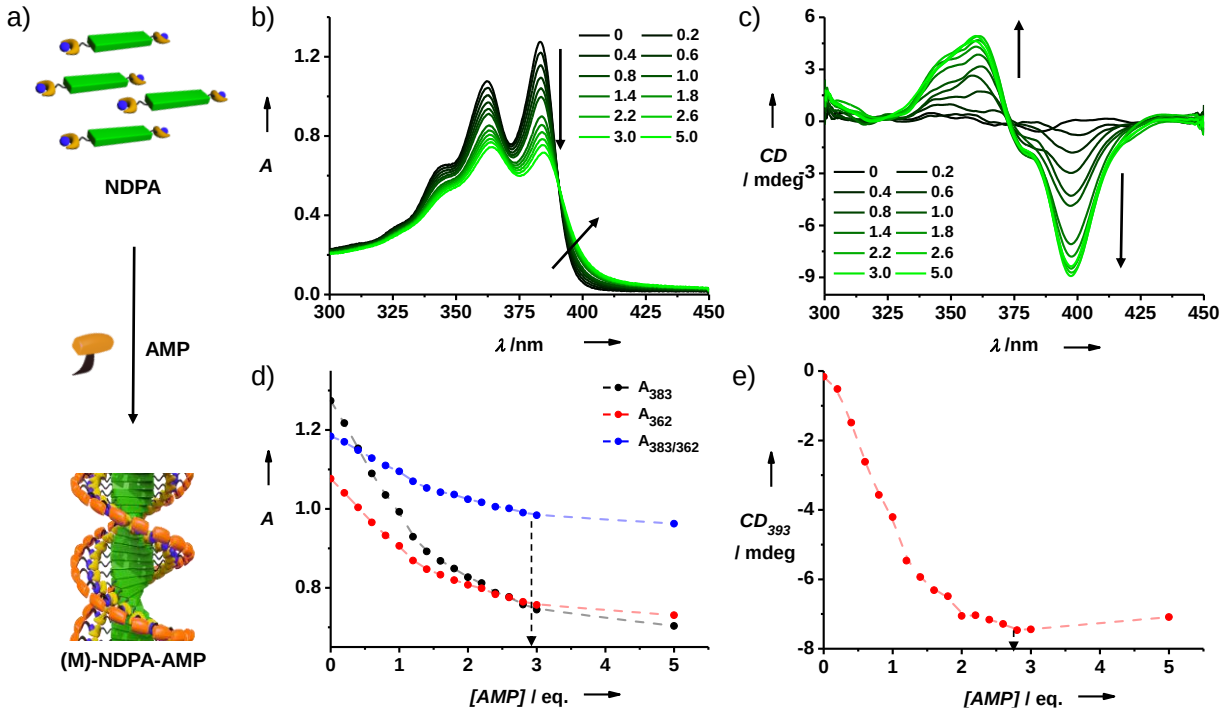

Figure 3.1. *AMP induced self-assembly of* ***NDPA****: a) Schematic representation of AMP binding induced left-handed helical assembly of* ***NDPA****. Changes in b) absorption and c) CD spectra of* ***NDPA*** *upon titration with AMP. Corresponding d) changes in absorbance and e) CD intensity monitored at different wavelengths ([****NDPA****] = 5 x 10^{-5} M, 10 mM aq. HEPES buffer, T = 40 °C).*

Binding of adenosine monophosphate (AMP) also induced similar reversal of relative absorption intensity of the two vibronic bands of **NDPA** at 362 nm and 383 nm suggesting self-assembly (Figure 3.1a,b).[7] Titration shows a gradual evolution of a strong Cotton effect resulting in negative bisignated CD spectrum, with negative and positive maxima at 393 and 360 nm respectively, characteristic of excitonically coupled chromophores, arranged in left-handed organization (Figure 3.1c). The titration curve obtained by monitoring absorption and CD intensity showed saturation at 3 eq. of AMP (Figure 3.1d,e).[8]

NDPA did not show similar assembly behaviour on titration with inorganic phosphate (Pi). However very less changes in relative intensity of vibronic bands at 362 nm and 383 nm (Figure 3.2a,b,d) on interaction with Pi suggests a weak assembly. Also, being an achiral guest binding of Pi induces no handedness to NDI assemblies as evident from the absence of CD signal (Figure

3.2c,e). Since there is no significant change in the absorption spectral features compared to adenosine bound stacks we propose that Pi bound **NDPA** assemblies exist as racemic stacks. This is also justified by presence of only one phosphate and hence it does not act as a clipper to bind to **NDPA** molecules together and also lack the additional hydrophobic stabilization of the adenosine groups.

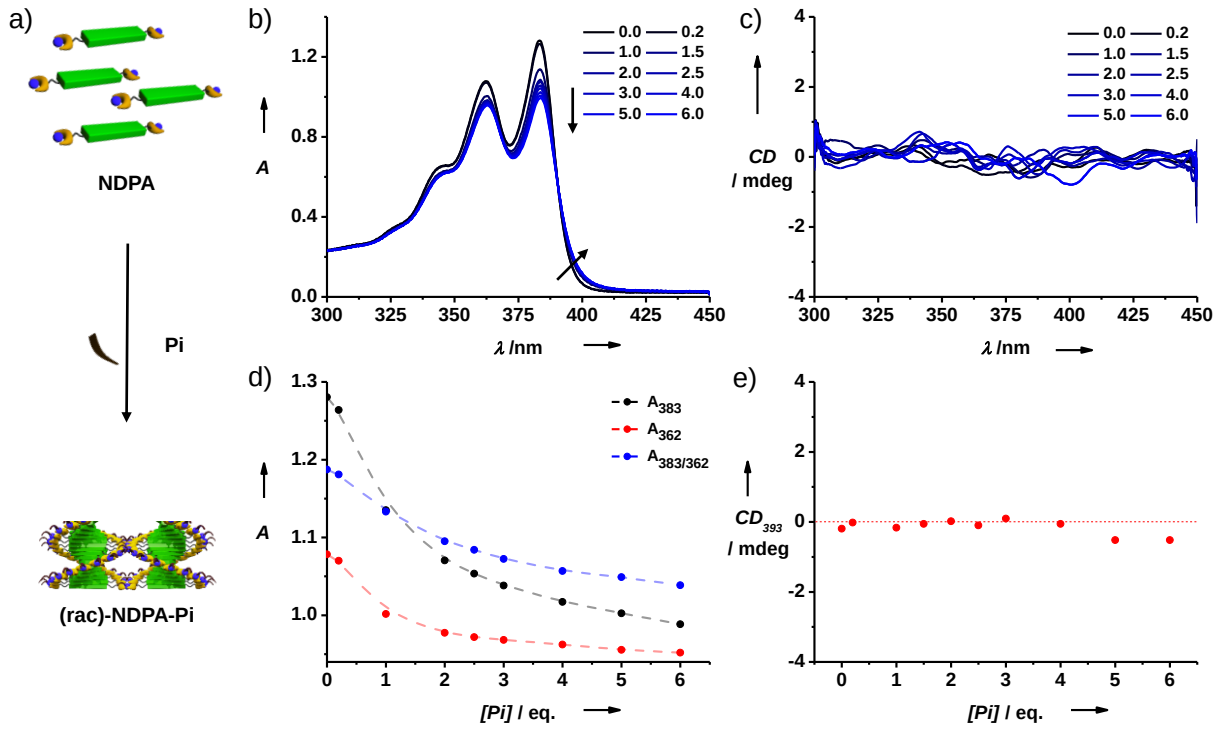

Figure 3.2. *Pi induced self-assembly of **NDPA**: a) Schematic representation of Pi binding to form short racemic assembly of **NDPA**. Changes in b) absorption and c) CD spectra of **NDPA** upon titration with Pi, corresponding changes in d) absorbance and e) CD intensity monitored at different wavelengths ([**NDPA**] = 5 x 10^{-5} M, 10 mM aq. HEPES buffer, T = 40 ℃).*

Different phosphate bound **NDPA** assemblies show differences in their helical chirality and extent of self-assembly (Figure 3.3a). Absorption spectra of saturated equivalents of phosphates show an increasing ratio of intensity of two vibrational bands at 383 nm and 362 nm from ATP bound stacks to monomeric **NDPA**. The values are 0.90 for *(P)*-**NDPA**-ATP, 0.91 for *(M)*-**NDPA**-ADP, 0.98 *for (M)*-**NDPA**-AMP and 1.06 for *(rac)*-**NDPA**-Pi compared to the 1.19 value of the NDPA monomers. This depicts that the extent of intermolecular interactions are similar in presence of ATP and ADP bound assemblies which decreases in AMP-bound stacks and the least is for inorganic phosphate bound assemblies (Figure 3.3b).

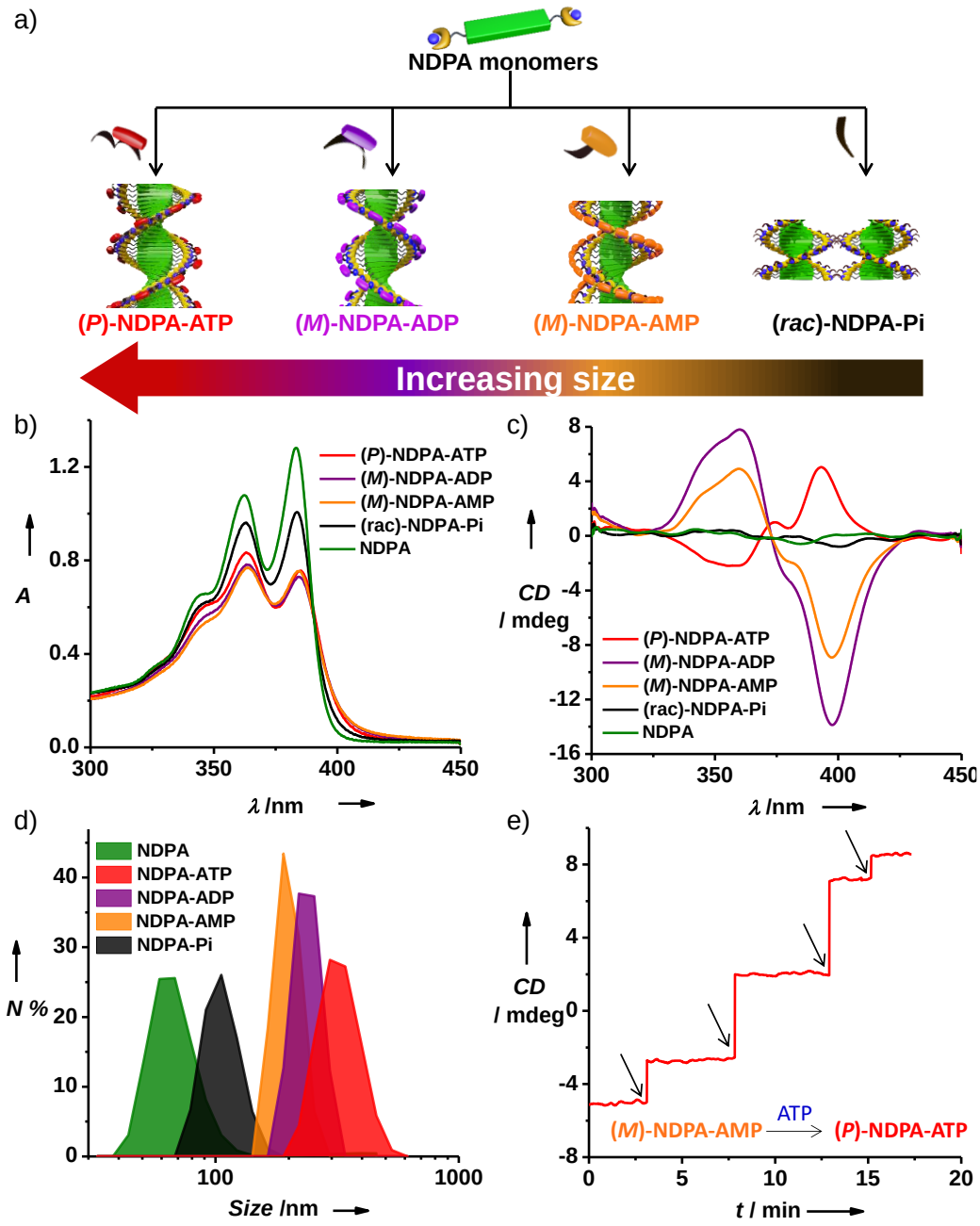

Figure 3.3. *a) Schematic representation of (P)-**NDPA**-ATP, (M)-**NDPA**-ADP, (M)-**NDPA**-AMP and (rac)-**NDPA**-Pi assemblies depicting different helical conformation and size of self-assembly. b) absorption spectra, c) CD spectra and d) dynamic light scattering (DLS) spectra of various **NDPA** assemblies. e) Dynamic conversion of (M)-**NDPA**-AMP assembly to (P)-**NDPA**-ATP assembly on addition of ATP. ([**NDPA**] = 5 x 10^{-5} M, [ATP] = 1 eq., [ADP] = 1.5 eq., [AMP] = 3 eq., [Pi] = 3 eq., 10 mM aq. HEPES buffer, T = 40 ℃).*

CD spectra of these assemblies with saturated equivalents of guest molecules show the formation of right-handed helix by ATP, left-handed helices by ADP and AMP, whereas Pi forms

racemic stacks (Figure 3.3c). The dynamic light scattering spectra further show that the length of the stacks are also dependent on the bound guest molecules as *(P)*-**NDPA**-ATP, *(M)*-**NDPA**-ADP and *(M)*-**NDPA**-AMP assemblies showed sizes in the range of 300-600 nm (Figure 3.3d) whereas the sizes of *(rac)*-**NDPA**-Pi stacks are around 100 nm. Thus, on changing the guests from ATP→ADP→AMP→Pi, there is change in chiral arrangement, extent of intermolecular interactions and also on the size of the resulting **NDPA** assemblies. The dynamic nature of these changes in the **NDPA** assembly was investigated using competitive guest binding. Thus, CD intensity of *(M)*-**NDPA**-AMP assembly (5 x 10^{-5} M in aq. HEPES) upon addition of small amounts of ATP at regular intervals were monitored at 394 nm, as a function of time. Interestingly, AMP bound stacks displayed sharp jumps in CD intensity with each successive addition of ATP (Figure 3.3e). Such instantaneous changes in Cotton effects provide strong evidence for fast switching of helicity in these dynamic supramolecular polymers.

3.4 Transient Self-assembly Mediated by Alkaline Phosphatase

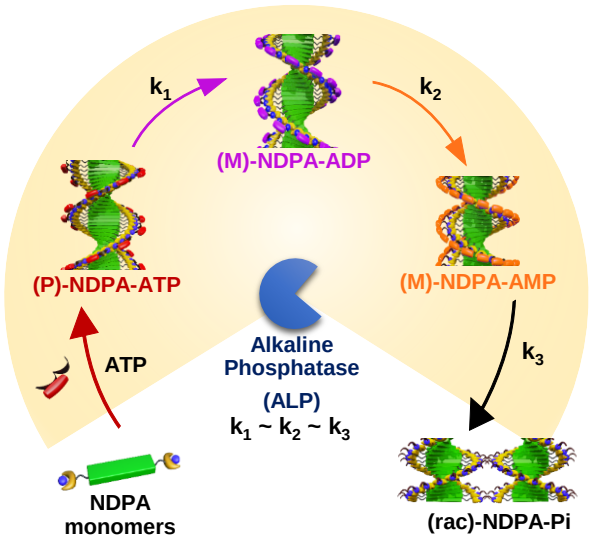

Scheme 3.3. *Schematic representation of transient self-assembly of* ***NDPA*** *assembly mediated by Alkaline Phosphatase.*

A transient self-assembly require minimum of two processes amongst which one is responsible for formation of assembly and another destroys the assembly. This formation and destruction of assembly is accountable to the addition of chemical fuel and its dissipation. The two

processes should be such that rate of formation is higher than rate of dissipation to obtain a significant lifetime of transient species. In our system, the chemical fuel responsible for driving the assembly is ATP. Thus, the first process is ATP addition to **NDPA** molecules that trigger the guest-induced self-assembly and the second process is ATP hydrolysis to inorganic phosphate that lacks in stabilizing the stacks. The first process of ATP binding to **NDPA** is instantaneous and hence rate is very high, thus enzymatic hydrolysis will always result in transient cycle. In order to achieve this, the first attempt was made to hydrolyse ATP to Pi by the commercially available Alkaline Phosphatase (ALP) (Scheme 3.3).

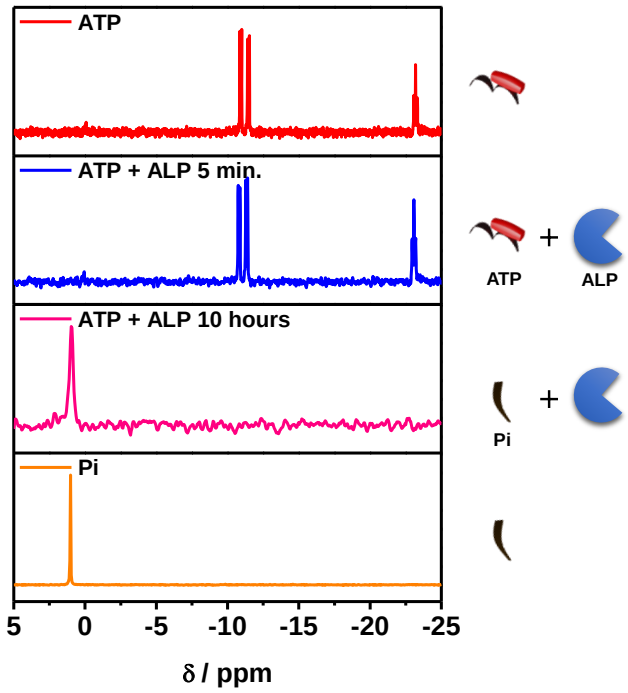

Figure 3.4. *^{31}P NMR depicting hydrolysis of ATP to Pi mediated by Alkaline Phosphatase (ALP) ([ATP] =10^{-3} M, 100 U/mL ALP, HEPES buffer in D_2O).*

Enzyme Alkaline Phosphatase in known to hydrolyse phosphodiester bonds unselectively, hence ATP undergoes hydrolysis to inorganic phosphates (Pi). To apply Alkaline Phosphatase to our system, we first investigated the effect of commercially available enzyme on ATP using ^{31}P NMR. For this 10^{-3} M ATP solution in HEPES buffer in D_2O was taken and to this solution, 100 U/mL Alkaline Phosphatase was added and ^{31}P NMR spectra was recorded. After 10 hours, ^{31}P NMR spectra showed the hydrolysis of ATP into Pi, which is suggested by the disappearance of peaks at δ = -10.8, -11.3 and -23 ppm as well as appearance of peak at δ ~ 1.0 ppm (Figure 3.4)

characteristic of Pi.

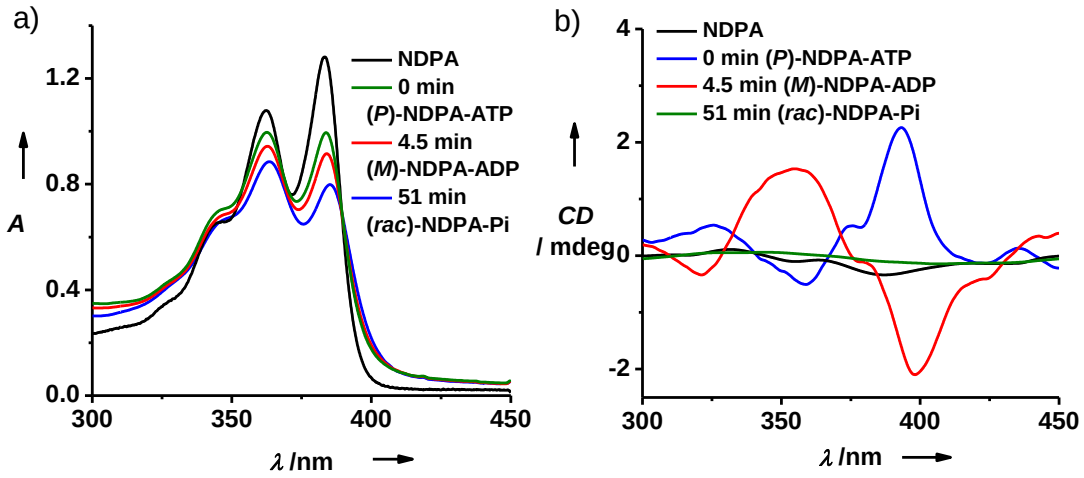

Figure 3.5. *Alkaline Phosphatase mediated transient self-assembly in* ***NDPA****:* aa. *b) Time dependent CD spectra depicting change in conformation from P→M→rac ([****NDPA****] = 5x10^{-5} M, [ATP] = 1 eq., [ALP] = 1.12 U/mL).*

The transient self-assembly process in **NDPA** assemblies was then investigated through time dependent absorption and CD spectra in presence of Alkaline Phosphatase. This enzyme will *in situ* hydrolyse the bound chiral phosphate molecule resulting in change in **NDPA** assembly. Thus, ALP (1.12 U/ml) was added to a solution of ATP bound **NDPA** assembly (5 x 10^{-5} M in aq. HEPES) and absorption and CD signal was monitored at 394 nm as a function of time. Before ATP addition, solution show monomeric vibronic features in absorption and corresponding CD spectra show no CD signal indicating no assembly (Figure 3.5a,b). Addition of ATP resulted in an instantaneous reversal in vibronic features in absorption spectra due to increased inter-chromphoric interaction and the CD spectra displayed positive bisignated CD signal reiterating the formation of (*P*)-**NDPA**-ATP assembly with excitonic coupling between chromophores. The time dependent absorption spectral changes in presence of ALP show an evolution of band at 383 nm suggesting a gradual decrease in inter-chromophoric interactions as ATP hydrolyse to Pi via ADP and AMP. Interestingly, the CD signal gradually decreases with time, indicating the decrease in ATP concentration on enzymatic hydrolysis with ALP. Remarkably, the net CD intensity reverses from positive to negative, where the signal resembles that of either ADP or AMP bound **NDPA** assemblies (Figure 3.5b).

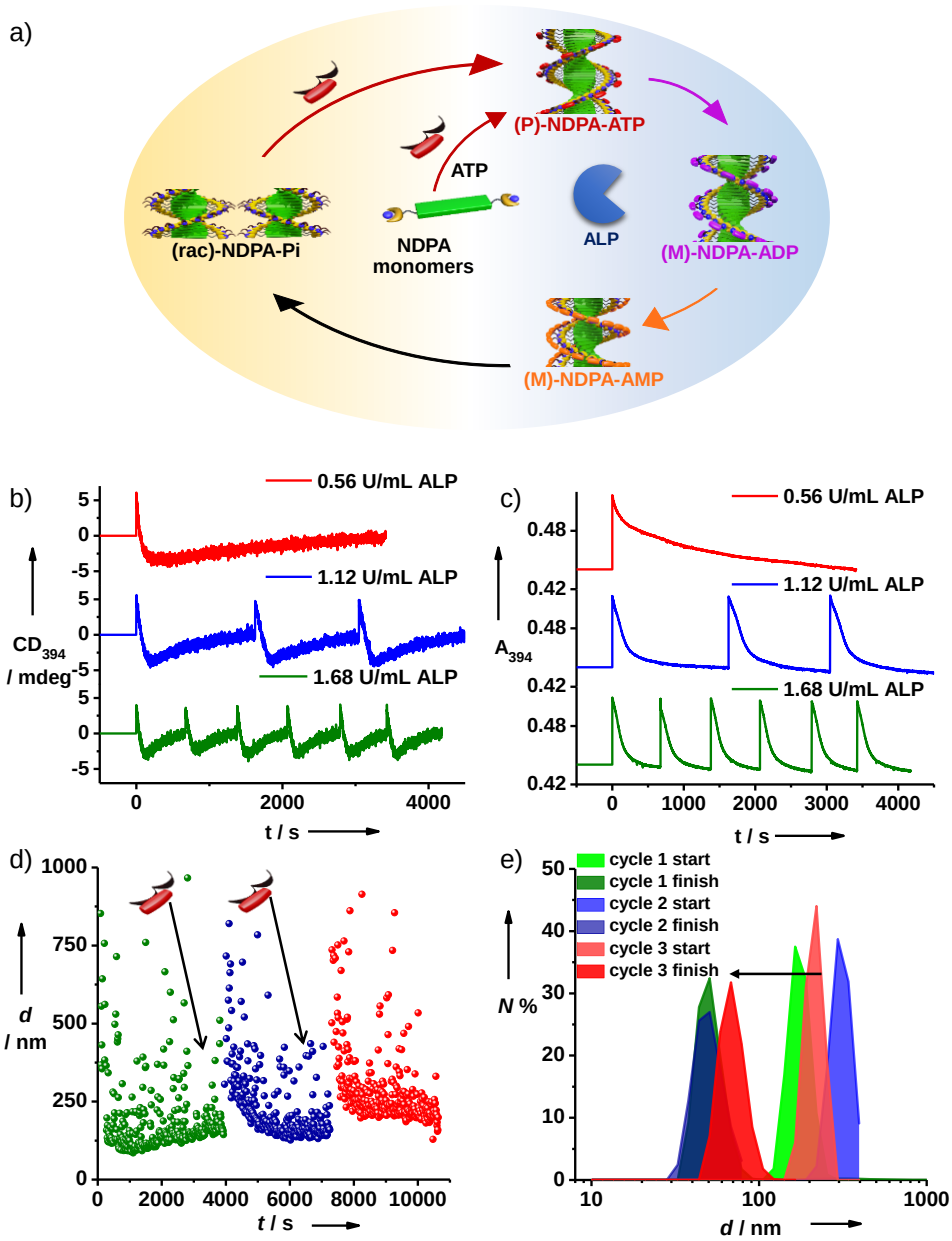

Figure 3.6. *Refuelable transient self-assembly of* ***NDPA*** *mediated by Alkaline Phosphatase: a) Schematic representation of ATP induced transient self-assembly with various states of cycle and refueling by ATP. b) Time dependent CD signal changes at 394 nm depicting gradual change from positive to negative to zero CD signal, refueling of the cycle by subsequent addition of ATP, and lifetime modulation by varying units of ALP. c) Corresponding time dependent absorption changes at 394 nm. d) Time dependent DLS size changes showing a gradual decrease in size over cycle and subsequent refueling by ATP showing instantaneous increase in size then follows the same trend, ALP = 1.12 U/mL. e) DLS number % vs size changes over the cycles showing a decrease from 300 nm to 50 nm, ALP = 1.12 U/mL. ([****NDPA****] = 5 x 10^{-5} M, [ATP] = 1 eq., [ALP] = 0.56-1.68 U/mL, 10 mM aq. HEPES buffer, T = 40 ℃).*

This inversion of CD signals with time, clearly indicates the dynamic reversal of helical handedness of **NDPA** stacks as a result of conversion of ATP to ADP/AMP through enzymatic hydrolysis. Furthermore, this negative bisignated CD signal decrease to zero over time suggesting the complete hydrolysis of adenosine phosphates to inorganic phosphate which form short racemic stacks. The lifetime of transient cycle in presence of 1.12 U/mL ALP was 51 minutes.

For further investigations of transient self-assembly, time dependent spectral properties were probed at 394 nm, which in CD data represents positive signal for (*P*)-**NDPA**-ATP, negative signal for (*M*)-**NDPA**-ADP and (*M*)-**NDPA**-AMP and lastly zero for **NDPA** monomers and (*rac*)-**NDPA**-Pi. As discussed earlier, Alkaline Phosphatase hydrolyses to ATP to Pi over time which is reflected in the **NDPA** assemblies resulting in transient self-assembly.

Next to achieve refueling of the system, ATP needs to be added to (*rac*)-**NDPA**-Pi stacks which should follow a similar trend. Here we believe that Pi lacks in clipping action to bind more than one **NDPA** molecule thus cannot form longer assemblies which is further verified by DLS data that (*rac*)-**NDPA**-Pi stacks are of 80-105 nm size whereas (*P*)-**NDPA**-ATP assemblies are of 300-500 nm. With this hypothesis, **NDPA** solution with various units of ALP was taken and to it ATP was added and time dependent CD and absorption was monitored at 394 nm. The CD signal gradually change from positive to negative and then further to zero depicting complete hydrolysis of Adenosine phosphates to Pi and finishing of the cycle. Absorption changes also follow gradual changes depicting change in inter-chromophoric interactions and therefore assembly in solution (Figure 3.6a-c). A subsequent addition of ATP resulted in an instantaneous increase in positive CD signal due to dynamic change of assembly from (*rac*)-**NDPA**-Pi stacks to (P)-**NDPA**-ATP assembly which follow the same trend in CD and absorption as the first cycle.

To further validate our hypothesis that over the cycle, the system indeed undergoes a change in size, we monitored DLS size changes as a function of time. As soon as ATP is added, the average size of the system shows 500-750 nm and gradually decrease to ~100 nm, thus verifying that there is a transient self-assembly. Furthermore, similar to CD and absorption changes, DLS sizes also follow the trend similar to the first cycle on refueling with ATP (Figure 3.6d,e). There is a sudden increase in size on ATP addition that gradually decreases over the cycle.

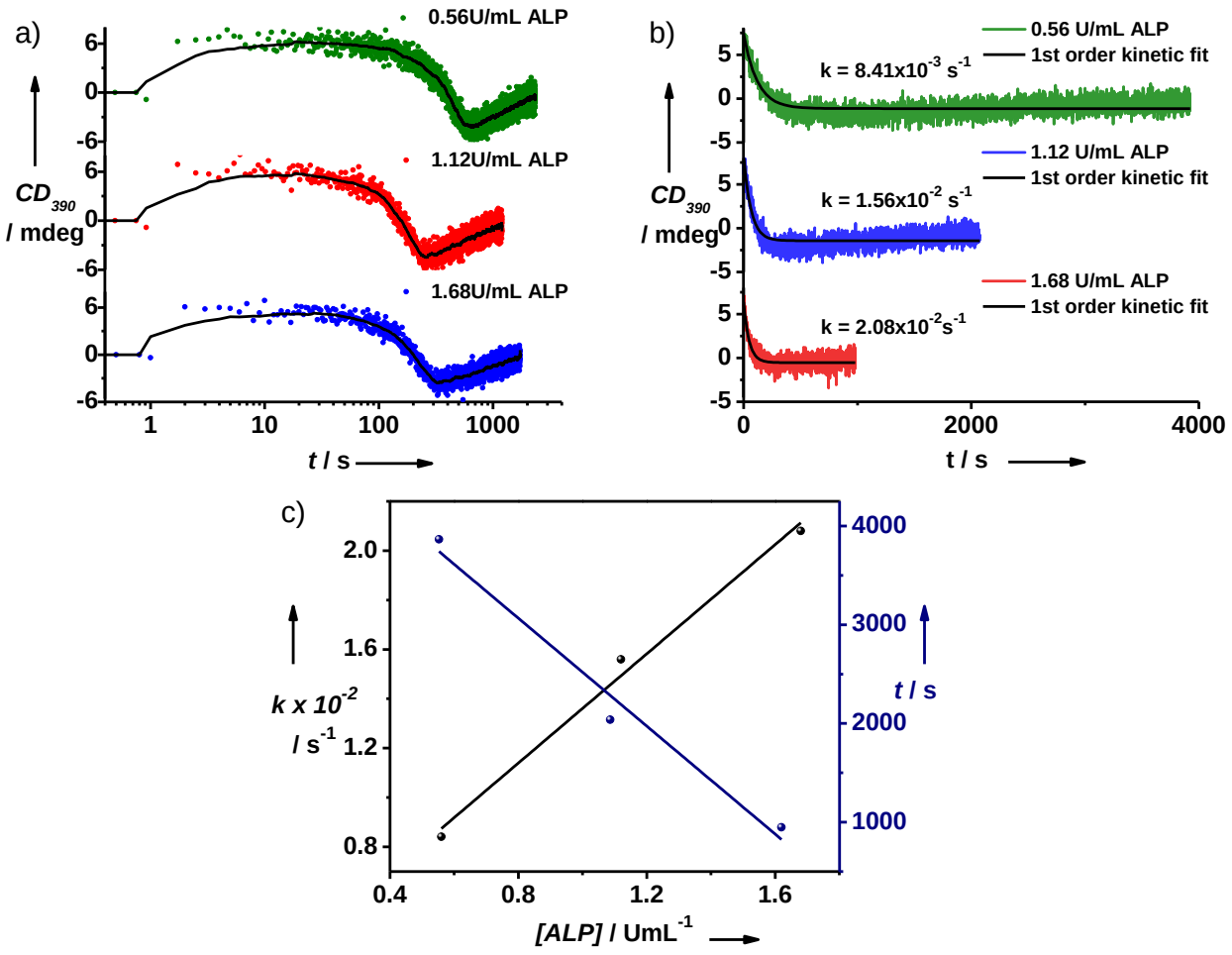

Figure 3.7. *Transient self-assembly of* ***NDPA*** *mediated by Alkaline Phosphatase: Time dependent CD changes at 394 nm in presence of different units of ALP a) time in log scale for clearer lifetime elucidation, b) acceleration of rate by increasing units of ALP and c) rate and time of disassembly with variation in ALP units. ([**NDPA**] = 5 x 10^{-5} M, [ATP] = 1 eq., [ALP] = 0.56-1.68 U/mL, 10 mM aq. HEPES buffer, T = 40 ℃).*

Transient processes makes it requisite to have a modular lifetime of transient species. For this, kinetics of the chemical reaction need to controlled. Working with enzymes give the required control over rate of reaction by a mere change of enzyme units. Applying this to the current system, the units of ALP was varied from 0.56 to 1.68 U/mL (Figure 3.7). The increase in units of ALP increases the rate of hydrolysis of adenosine phosphates which should be reflected in the **NDPA** assembly. The increase from 0.56 to 1.68 U/mL increased rate of hydrolysis from 0.8x10^{-2} s^{-1} to 2x10^{-2} s^{-1}. This rate increase follows a linear trend over these units of enzyme which can be extrapolated to a wider regime since the enzyme follows a pseudo first order kinetics. Furthermore,

rate increase is inversely proportional to the lifetime of transient cycle. Therefore, decrease in lifetime also follows a linear trend from 4000 to 1000 seconds (Figure 3.7c).

Hence, we could achieve ATP-driven transient self-assembly with control over rate and lifetime. Also, the system could be successfully refueled with insignificant damping. Although, such a control was attained by Alkaline Phosphatase enzyme but the enzyme lack in its selectivity towards hydrolysis of phosphodiester bond. Thus, there is no control over the transient states of (*P*)-**NDPA**-ATP, (*M*)-**NDPA**-ADP, (*M*)-**NDPA**-AMP and (*rac*)-**NDPA**-Pi. To overcome this, another enzyme Apyrase was used (*vide infra*).

3.5 Transient Self-assembly Mediated by Apyrase

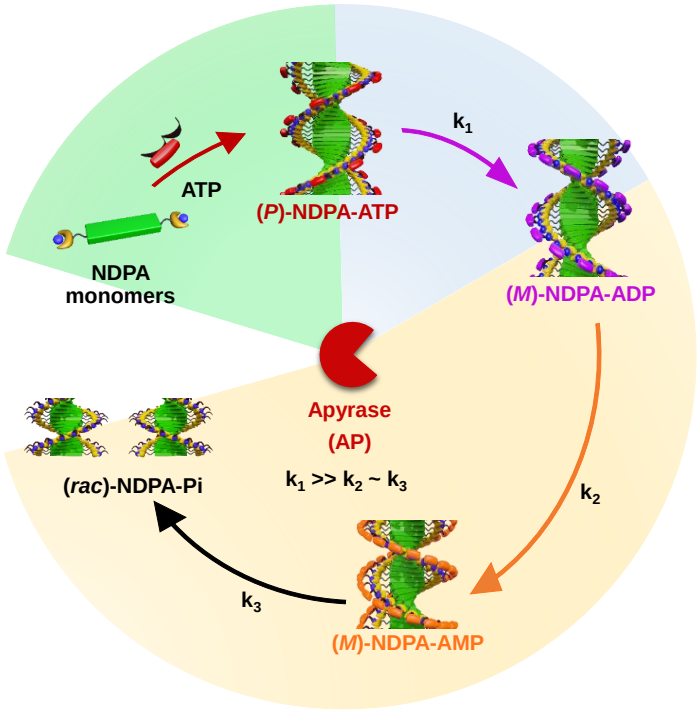

Scheme 3.4. *Schematic representation of transient self-assembly of* ***NDPA*** *assembly mediated by Apyrase.*

Amongst the plethora of adenosine phosphate hydrolyzing enzymes other than Alkaline Phosphatase is Apyrase (AP) which is constituted of ATPase and ADPase with 10:1 ratio which result in preferential hydrolysis of ATP over ADP. So, the rate constants follow the trend

k_1>>k_2~k_3 (Scheme 3.4). So we hypothesized that these rate constants allow a longer lifetime of (*M*)-**NDPA**-ADP state thereby compensating the lifetime of (*P*)-**NDPA**-ATP. Before applying Apyrase to our system, we first investigated the effect of Apyrase on ATP using ^{31}P NMR (Scheme 3.2 and 3.8).

For this 10^{-3} M ATP solution in HEPES buffer in D_2O was taken and ^{31}P NMR spectra was recorded as a control. To it 100 U/mL Apyrase was added and spectra was recorded again to see any effect of enzyme on peaks. After 10 hours incubation, ^{31}P NMR spectra resembled the NMR spectra corresponding to only Pi signifying the hydrolysis of ATP into Pi verified by disappearance of peaks at at δ = -10.8, -11.3 and -23 ppm as well as appearance of peak at δ ~ 0.8 ppm (Figure 3.8).

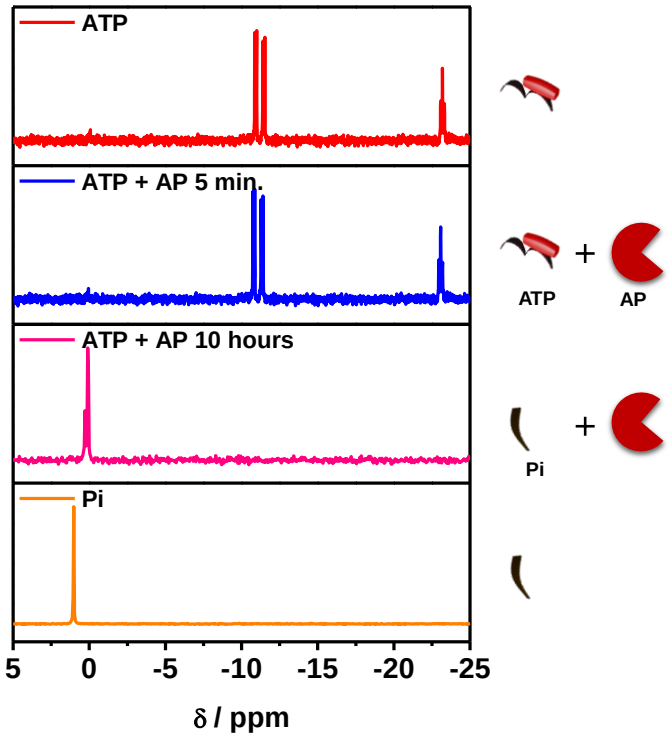

Figure 3.8. *^{31}P NMR depicting hydrolysis of ATP to Pi mediated by Apyrase (AP) ([ATP] =10^{-3} M, 100 U/mL AP, HEPES buffer in D_2O).*

For studies of transient self-assembly mediated by Apyrase, spectral measurements as a function of time were probed at 394 nm. Similar to Alkaline Phosphatase, Apyrase will also *in situ* hydrolyse the bound adenosine phosphate molecule resulting in change in **NDPA** assembly. To a solution of **NDPA** (5 x 10^{-5} M in aq. HEPES) and Apyrase, 1 eq. ATP was added to initiate the

transient cycle. Time dependent CD changes showed an instantaneous increase in positive CD signal because of formation of (*P*)-**NDPA**-ATP which transformed into (*M*)-**NDPA**-ADP indicated by negative CD signal with a fast kinetics (Figure 3.9). This was followed by a gradual disappearance of CD signal due to the formation of (*rac*)-**NDPA**-Pi. Absorbance corresponding to aggregation band show a gradual decrease in extent of assembly change until saturation because of decreased interactions on hydrolysis from ATP→Pi.

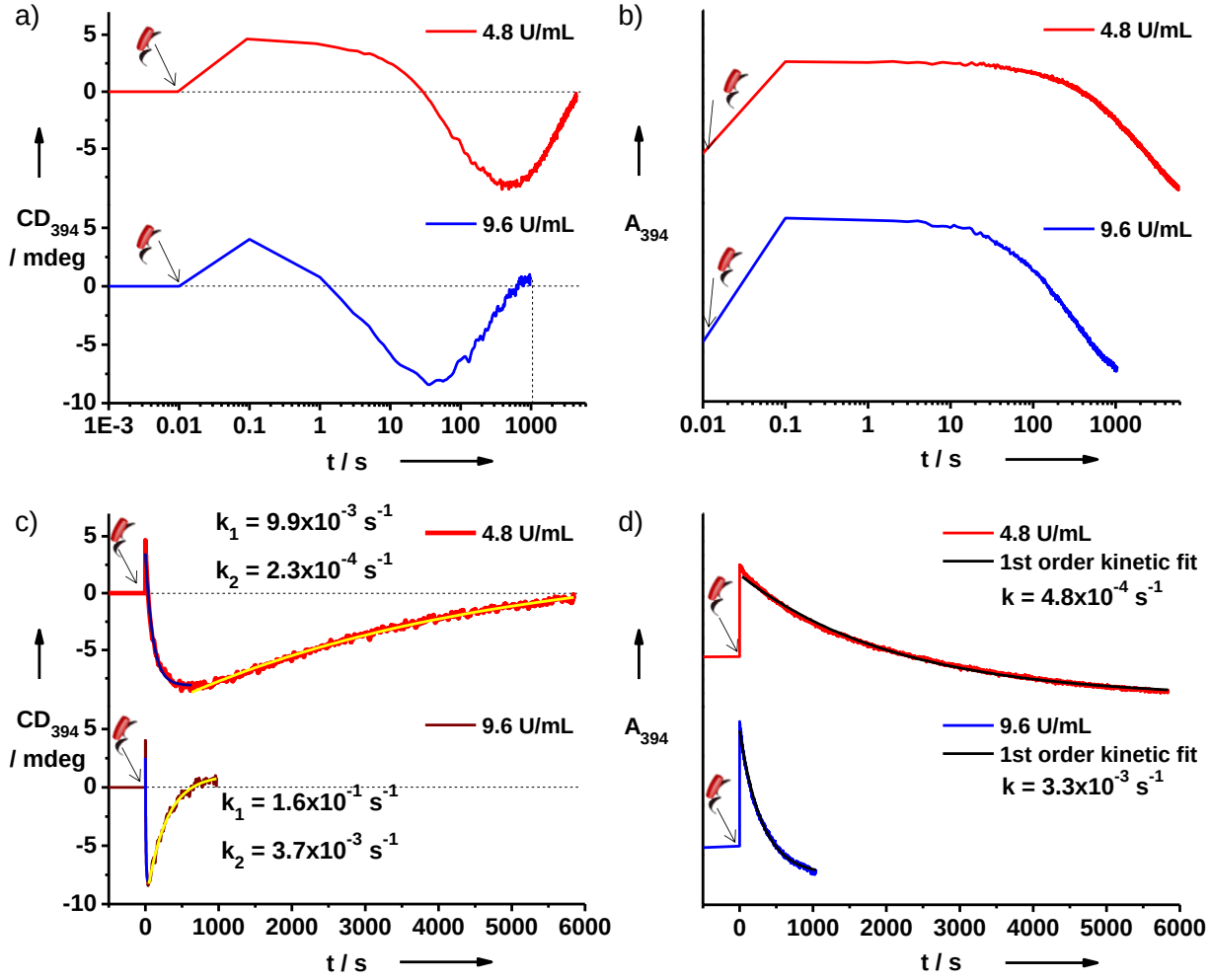

Figure 3.9. *Transient self-assembly mediated by Apyrase: Time dependent changes at 394 nm in presence of different units of Apyrase, a) CD changes with time in log scale for clearer lifetime elucidations, b) corresponding absorption changes with time in log scale, c) CD changes depicting the fast P→M and a slow M→ rac rate of stereomutations, d) corresponding absorption changes depict the rate of stereomutation showing a gradual decay ([**NDPA**] = 5x10^{-5} M, [ATP] =10^{-3} M, 4.8-9.6 U/mL AP, 10 mM HEPES, T = 40 ℃).*

An important feature of Apyrase is its ATPase: ADPase ratio of 10:1, which as stated above

increases the lifetime of ADP bound stacks and decreases the lifetime of ATP bound stacks. This observation can be verified by observing the extent of positive and negative CD signals of transient cycles by Alkaline Phosphatase and Apyrase. Alkaline Phosphatase mediated the CD signal changes from 6 to -4 mdeg whereas Apyrase shows a lower positive CD signal of 5 mdeg and increased negative CD signal of -8.5 mdeg (Figure 3.6 b, 3.9 c). Thus, there is a significant increase in lifetime of (*M*)-**NDPA**-ADP state as it can grow to a higher extent. Variation of enzyme units from 4.8 U/mL to 9.6 U/mL, increases the kinetics of enzyme and hence decreases the time of transient cycle. Doubling the enzyme units decreased the lifetime approximately 6 times from 1000 to 6000 seconds (Figure 3.9). The corresponding rates also accelerate from $9.9x10^{-3}$ s^{-1} to $1.6x10^{-2}$ s^{-1} for ATP to ADP whereas ADP to Pi decelerated from $2.3x10^{-4}$ s^{-1} to $3.7x10^{-3}$ s^{-1}. The rate constants calculated from absorption changes justify that ADP hydrolysis is the rate determining step reiterating the difference in hydrolysis rates. Next we investigated the efficiency of system to undergo refuelling. On subsequent addition of ATP in presence of 9.6 U/mL does not show any positive CD signal suggesting a fast ATP hydrolysis and hence a transient helical self-assembly from negative CD signal or (*M*)-**NDPA**-ADP to zero CD signal i.e. (*rac*)-**NDPA**-Pi (Figure 3.10).

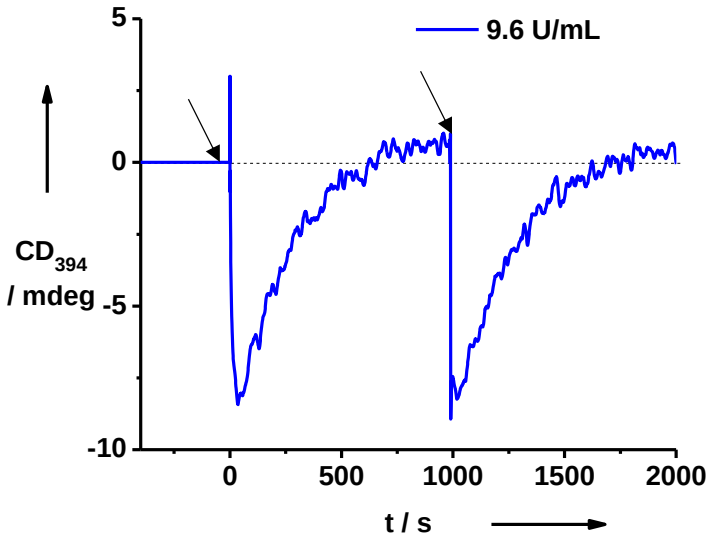

Figure 3.10. *Refuelling of transient self-assembly mediated by Apyrase: Time dependent CD changes at 394 nm shows an instantaneous ATP hydrolysis and thus no positive CD signal is observed depicting the rate of stereomutation showing an instantaneous P→M transition and a slow M→rac ([**NDPA**] = $5x10^{-5}$ M, [ATP] =10^{-3} M, 9.6 U/mL AP, 10 mM HEPES, T = 40 ℃).*

Thus, system can be successfully refuelled. Although no lifetime of (*P*)-**NDPA**-ATP is

observed, the transient self-assembly is still observed as (*M*)-**NDPA**-ADP is also equivalently aggregated state as suggested by DLS (Figure 3.3d). Therefore, a modular transient self-assembly mediated by Apyrase was investigated that shows enhancement in lifetime of negative CD signal corresponding to (*M*)-**NDPA**-ADP on compensation of lifetime of positive CD signal representing (*P*)-**NDPA**-ATP. Also, this justifies the fact that the transient self-assembly mediated by Alkaline Phosphatase and Apyrase are different.

3.6 Transient Conformational Switching Mediated by Apyrase

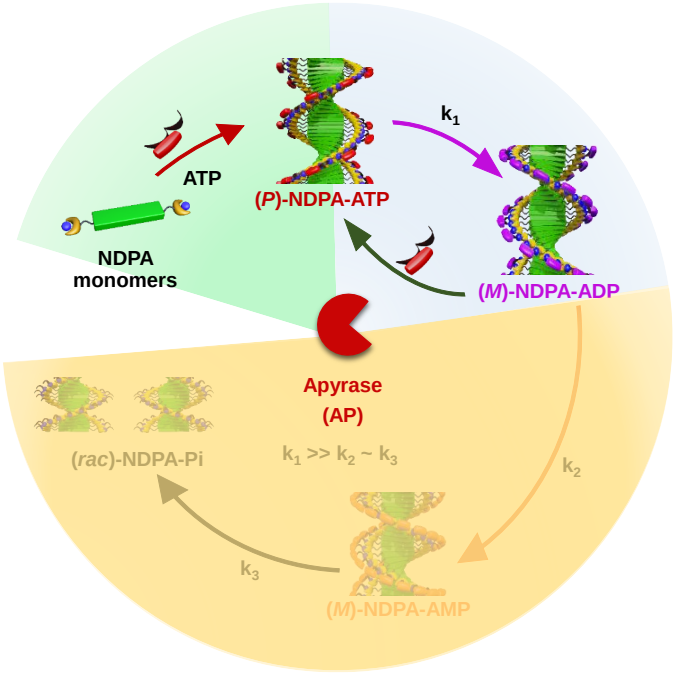

Scheme 3.5. *Schematic representation of transient conformational switching of* ***NDPA*** *assembly by intereference of higher valent guest ATP in the mid of transient self-assembly cycle mediated by Apyrase.*

Since **NDPA** self-assembly is highly selective and adaptive, we envisaged to see the effect of fuel addition in between the transient cycle. A highly dynamic and adaptive system should response to its fuel at any time during the transient cycle and the fuel addition should change the system's pathway (Scheme 3.5). For this, we utilized Apyrase enzyme which has 10:1 ratio of ATPase: ADPase. On subsequent addition of ATP, the bound ADP and AMP should get replaced by ATP. Then, the further slow hydrolysis of ADP and AMP should undergo only in solution and

thus, should not reflect in **NDPA** assembly. Furthermore, the system should show an instantaneous reverse conformational change from (*M*)-**NDPA**-ADP to (*P*)-**NDPA**-ATP state signified by change of CD signal from negative to positive. Subsequently, (*P*)-**NDPA**-ATP should convert into (*M*)-**NDPA**-ADP as ATP gets hydrolysed.

To examine the adaptiveness of system, a solution of $5x10^{-5}$ M **NDPA** and 4.8 U/mL Apyrase was taken and 1 eq. of ATP was added to it (Figure 3.11a,b). Monitoring the spectral changes at 394 nm showed a gradual *P*→*M* stereomutation and refuelling with 1eq. ATP was done once the negative CD signal seems to be in saturated state.

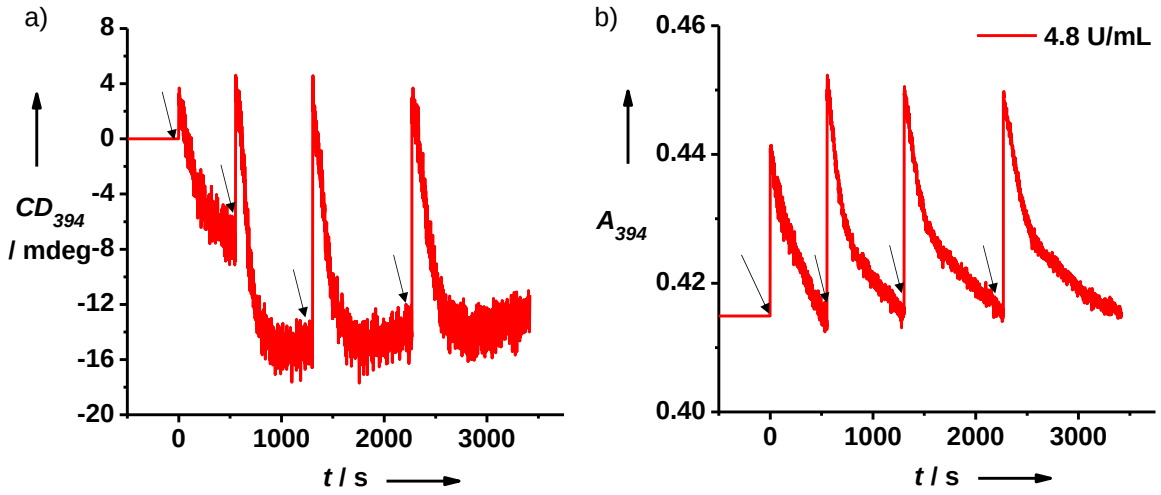

Figure 3.11. *Transient conformational switching of* ***NDPA*** *assembly mediated by Apyrase: Time dependent a) CD intensity, b) absorbance changes at 394 nm showing a fast P→M transition ([**NDPA**] = $5x10^{-5}$ M, [ATP] =10^{-3} M, 4.8 U/mL AP, 10 mM HEPES, T = 40 ℃).*

As hypothesized, system responded to ATP addition showing an immediate change of CD signal from negative to positive depicting *P*→*M* stereomutation. Successive refuelling of the system behaved similarly. Thus, preferential binding of ATP over ADP, AMP and Pi and lower rate of ADP hydrolysis than ATP, result in favoured conformational switching over disassembly. Hence we could successfully examine the adaptivity of the system to its chemical fuel and the environment (enzyme).

3.7 Transient Self-assembly with Palindromic Conformational Switching

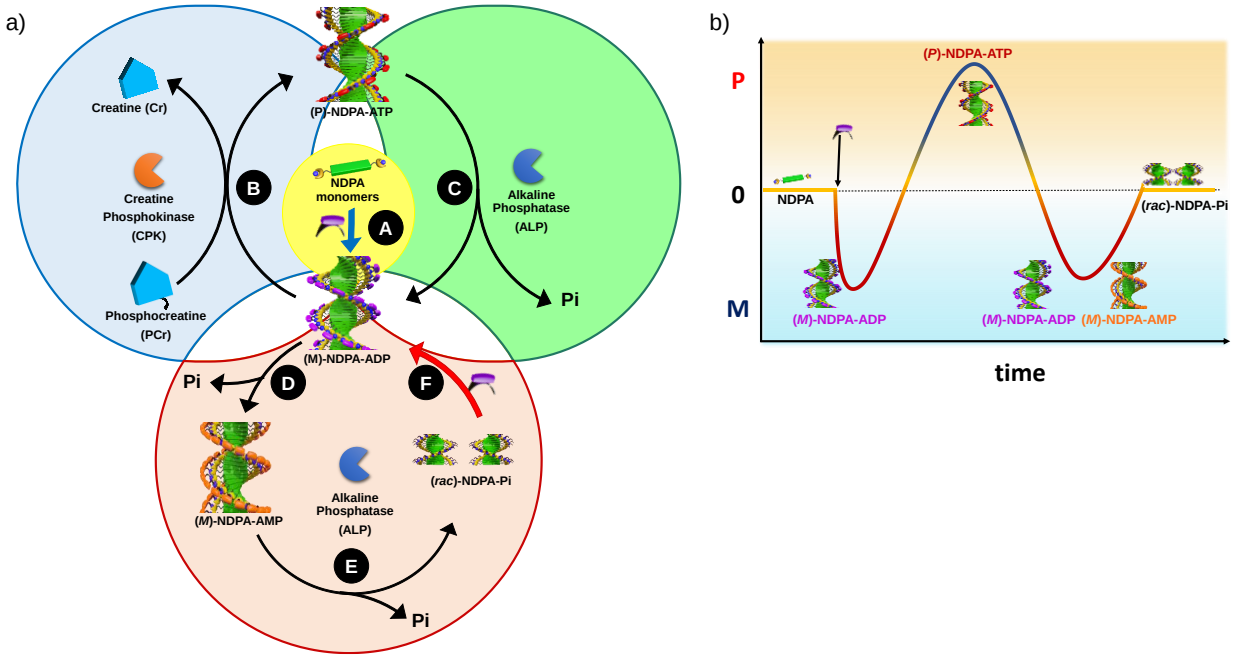

Scheme 3.6. *Schematic representation of transient self-assembly accompanied by transient conformational switching of* ***NDPA*** *assembly mediated by Alkaline Phosphatase and Creatine Phosphokinase in tandem. a) A to E represent the pathway followed by the system in alphabetical order. (M)-****NDPA****-ADP act as the connecting point for three different pathways. The four circles represent different reaction loops connecting (M)-****NDPA****-ADP. Thick blue arrow represent initiation of first cycle of transient process and thick red arrow represent the beginning of subsequent cycles. b) Schematic representation of the corresponding transient palindromic CD signal.*

Although the singluar enzymes also show a conformational switching in assembled state, in the present scenario, there shall be three non-equilibrium conformational states appearing in the following order (*M*)-**NDPA**-ADP→(*P*)-**NDPA**-ATP→(*M*)-**NDPA**-ADP/(*M*)-**NDPA**-AMP. Thus output of the system behaves as a palindrome in chiral conformations where CD signal follow 0→*M*→*P*→*M*→0(*rac*) (Scheme 3.6b)

Temporal control over transient systems are the key link between biological science and material science. It takes inspiration from complex natural systems to apply in materials for time regulated properties. So far in this chapter, singular enzymes with single loops were employed, on

the other hand, biological systems work with multiple loops in tandem to operate out of equilibrium.

To alleviate this, a synthetic manifestation was tried. We believed that using the tandem enzyme strategy in Chapter 2, Creatine Phosphokinase in presence of Phosphocreatine can be employed to *in situ* form (*P*)-**NDPA**-ATP from (*M*)-**NDPA**-ADP and simultaneously Alkaline Phosphatase can hydrolyse ATP and ADP to give (*rac*)-**NDPA**-ADP. Thus, a correct balance between the two enzyme should result in transient self-assembly, where the assembly state undergoes a reversible conformational switching *en route* to the disassembled state (Scheme 3.6a).

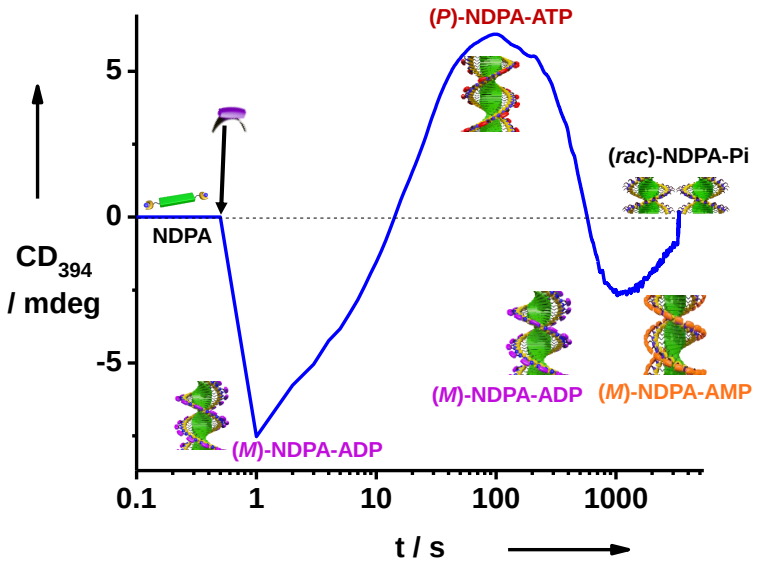

Figure 3.12. *Transient self-assembly and palindromic conformational switching mediated by Alkaline Phosphatase and Creatine Phosphokinase in tandem: Time dependent CD changes at λ 394 nm depicting 0→M→ P →M→0 transition ([**NDPA**] = 5x10^{-5} M, [ADP] = 2 eq., [PCr] = 5 eq., 9 U/mL CPK, 0.4 U/mL ALP, 10 mM HEPES, T = 40 ℃).*

To examine the proposed hypothesis, a solution of 5x10^{-5} M **NDPA**, 5 eq. PCr, 9 U/mL CPK and 0.4 U/mL ALP was taken, CD signal corresponding to monomeric NDPA was zero. 2 eq. of ADP, the chemical fuel in this case, was added to NDPA solution and CD signal at λ = 394 nm was monitored as a function of time. CD signal showed an instantaneous increase from zero CD signal to negative CD signal (Figure 3.12). This depicted the formation of (*M*)-**NDPA**-ADP and over time the **NDPA** assembly undergo a conformational switching from *M*→*P* resulting in formation of (*P*)-**NDPA**-ATP. Although ATP gets simultaneously hydrolysed, the P-type helical

conformation stays for some time at steady state due to presence of excess of PCr that regenerates ATP from ADP. As PCr gets consumed the (*P*)-**NDPA**-ATP then revert back to (*M*)-**NDPA**-ADP via *P*→*M* stereomutation. Further hydrolysis of ADP into AMP doesn't change signal of CD and hence M-type helical conformation is observed. Then a gradual change in CD signal to zero is observed signifying complete hydrolysis of ATP/ADP into Pi resulting in (*rac*)-**NDPA**-Pi

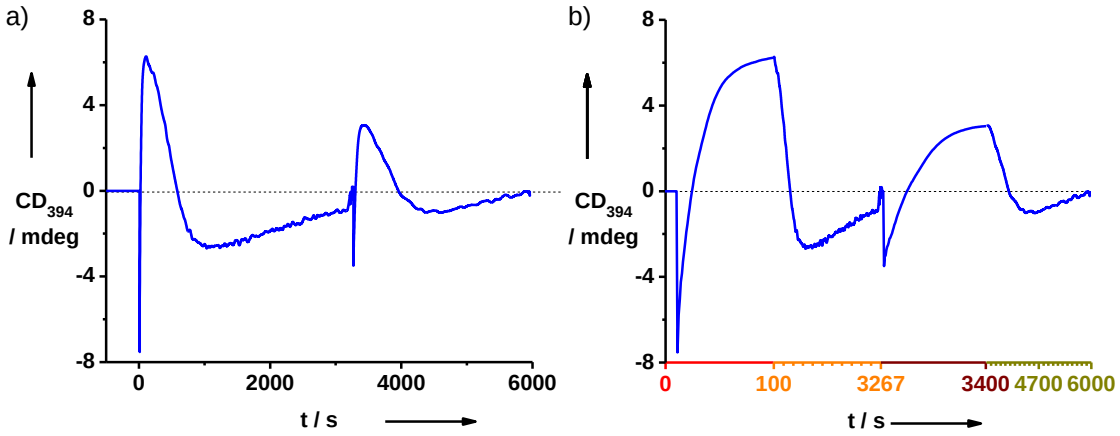

Figure 3.13. *Refuelling of transient self-assembly and reversible conformational switching mediated by Alkaline Phosphatase and Creatine Phosphokinase in tandem: a) Time dependent CD changes at λ = 394 nm depicting 0→M→ P →M →0 transition b) x-axis with different time ranges for clearer elucidation of cycle ([**NDPA**] = 5x10^{-5} M, [ADP] = 2 eq., [PCr] = 5 eq., 9 U/mL CPK, 0.4 U/mL ALP, 10 mM HEPES, T = 40 ℃).*

Addition of 2 eq. of ADP and 5 eq. of PCr reactivated the transient cycle which follows the same trend as the first cycle (Figure 3.13a,b). Hence, we have successfully demonstrated the transient self-assembly of **NDPA** by variation of enzymes to get different intermediate transient states, rates and lifetimes.

3.8 Conclusion

To conclude, we have presented chemical fuel-driven transient assembly of a highly dynamic and adaptive molecule **NDPA** which uses biological energy currency adenosine phosphates to induce supramolecular helical self-assembly. This system presents an interesting example, where the rate of stereomutation and disassembly can be modulated by an external stimulus such as enzyme. Hence, we have used three enzymes Alkaline Phosphatase, Apyrase and

Creatine Phosphokinase to obtain three different type of the transient self-assembly with change in number of transient states as well as their lifetimes. A clear understanding of the kinetics involved in various processes makes the present system unique for an adaptive self-assembled material.

3.9 Experimental Section

General Methods:

Optical Measurements: Electronic absorption spectra and Circular Dichroism measurements were performed on a Jasco J-815 spectrometer where the sensitivity, time constant and scan rate were chosen appropriately. Corresponding temperature dependent measurements were performed with a CDF – 426S/15 Peltier-type temperature controller with a temperature range of 263-383 K and adjustable temperature slope. Optical measurements were recorded in 10 mm path length cuvettes. CD spectra and time dependent CD changes were smoothened by adjacent averaging and fitted using first order kinetics to calculate rate constants. We are aware of the fact that enzymatic changes are not in theory first order changes, but a fit enables us to have a relative kinetic perspective between individual processes.

NMR Measurements: NMR spectra were obtained with a Bruker AVANCE 400 (400 MHz w.r.t. ^{1}H nuclei) Fourier transform NMR spectrometer with chemical shifts reported in parts per million (ppm).

Dynamic light scattering (DLS): The measurements were carried out using a NanoZS (Malvern UK) employing a 532 nm laser at a back scattering angle of 173°. A dead time (Time between sample loading and starting of measurement by the machine) of around 45 seconds is present in all measurements.

Sample Preparation:

All solutions were prepared in 10 mM HEPES except for NMR measurements. Stocks were prepared as $5x10^{-4}$ M **NDPA**, $5x10^{-2}$ M ATP, ADP and PCr, 1 U/µL ALP, 1 U/ µL AP, 0.25 U/µL CPK. Micropipette was used to transfer measured volumes of solution. Dead time (time between

fuel injection and starting of measurement by the machine) in all the measurements were less than 60 seconds. Temperature was maintained at 40 °C to have a sufficiently high enzyme activity throughout the measurements. The samples were measured in a 10 mm quartz cuvette.

Protocol for conformational switching:

i. For Alkaline Phosphatase mediated cycles: To a solution of **NDPA** and ALP, ATP was added and measurements were done.
ii. For Apyrase mediated cycles: To a solution of **NDPA** and AP, ATP was added and measurements were done.
iii. For Alkaline Phosphatase and Creatine Phosphokinase in tandem mediated cycles: To a solution of **NDPA**, PCr, ALP and CPK, ADP was added and measurements were done.

"*(P)*-**NDPA**-ATP" term used in main text refers to 5 x 10^{-5} M solution of **NDPA** (in 10 mM aq. HEPES buffer) with 1 eq. of ATP. "*(M)*-**NDPA**-ADP" term used in main text refers to 5 x 10^{-5} M solution of **NDPA** (in 10 mM aq. HEPES buffer) with 1.5 eq. of ADP. "ALP" refers to Alkaline Phosphatase, "AP" refers to Apyrase, "CPK" refers to Creatine Phosphokinase, "PCr" refers to Phosphocreatine

Materials: Calf Intestinal Alkaline Phosphatase (1.75 units/mg), Creatine Phosphate Disodium Salt Tetrahydrate (extrapure for biochemistry), Adenosine-5-Diphosphate Disodium Salt (extrapure for biochemistry) and Sodium Phosphate Dibasic Dihydrate (extrapure for biochemistry) were purchased from Sisco Research Laboratories Pvt. Ltd. India. Deuterated water (D_2O), Creatine Phosphokinase from rabbit muscle (150 U/mg), Apyrase from potato (18 U/mg), Adenosine-5-Triphosphate Disodium Salt (99%), Adenosine-5-Monophosphate Disodium Salt (99%), were purchased from Sigma Aldrich. HEPES (4-(2-hydroxyethyl)-1-piperazineethanesulfonic acid) was procured from SD fine chemical limited.

Synthesis: NDPA was synthesized following the reported procedure and was characterized accordingly.[5]

3.10 References

1. F. H. Westheimer, *Science* **1987**, *235*, 1173.
2. T. Mitchison, M. Kirschner, *Nature* **1984**, *312*, 237-242.
3. A. Nürnberg, T. Kitzing, R. Grosse, *Nat. Rev. Cancer* **2011**, *11*, 177-187.
4. a) J. Boekhoven, A. M. Brizard, K. N. K. Kowlgi, G. J. M. Koper; R. Eelkema, J. H. van Esch, *Angew. Chem. Int. Ed.* **2010**, *49*, 4825-4828; b) J. Boekhoven, J. M. Poolman, C. Maity, F. Li, L. van der Mee, C. B. Minkenberg, E. Mendes, J. H. van Esch, R. Eelkema, *Nat. Chem.* **2013**, *5*, 433-437; c) S. Debnath, S. Roy, R. V. Ulijn, *J. Am. Chem. Soc.* **2013**, *135*, 16789-16792; d) H. Thomas, A.-K. Steppert, C. M. Lopez, B. Zhu, A. Walther, *Nano Lett.* **2014**, *15*, 2213-2219; e) C. G. Pappas, I. R. Sesselli, R. V. Ulijn, *Angew. Chem. Int. Ed.* **2015**, *54*, 8119-8123; f) S. K. M. Nalluri, C. Berdugo, N. Javid, P. W. J. M. Frederix, R. V. Ulijn, *Angew. Chem. Int. Ed.* **2014**, *53*, 5882-5887; g) J. K. Sahoo, S. K. M. Nalluri, N. Javid, H. Webba, R. V. Ulijn, *Chem. Commun.* **2014**, *50*, 5462-5464; h) T. Heuser, E. Weyandt, A. Walther, *Angew. Chem. Int. Ed.* **2015**, *54*, 13258-13262; i) J. Boekhoven, W. E. Hendriksen, G. J. M. Koper, R. Eelkema, J. H. van Esch, *Science* **2015**, *349*, 1075-1079; j) C. Pezzato, L. J. Prins, *Nat. Commun.* **2015**, *6*, 7790; k) S. Maiti, I. Fortunati, C. Ferrante, P. Scrimin, L. J. Prins, *Nat. Chem.* **2016**, *8*, 725-781.
5. H. N. Lee, Z. Xu, S. K. Kim, K. M. K. Swamy, Y. Kim, S.-J. Kim and J. Yoon, *J. Am. Chem. Soc.* **2007**, *129*, 3828-3829.
6. a) A. Ojida, S.-K. Park, Y. Mito-oka, I. Hamachi, *Tetrahedron Lett.* **2002**, *43*, 6193–6195; b) O. Akio, Y. Mito-oka, K. Sada, I. Hamachi, *J. Am. Chem. Soc.* **2004**, *126*, 2454-2463; c) X. Chen, M. J. Jou and J. Yoon, *Org. Lett.*, **2009**, *11*, 2181; d) S. K. Kim, D. H. Lee, J.-I. Hong and J. Yoon, *Acc. Chem. Res.*, **2009**, *42*, 23; e) T. Sakamoto, A. Ojida and I. Hamachi, *Chem. Commun.*, **2009**, *2*, 141-152.
7. S. V. Bhosale, C. H. Jani, S. J. Langford, *Chem. Soc. Rev.* **2008**, *37*, 331.
8. J. Gawroński, M. Brzostowska, K. Kacprzak, H. Kołbon and P. Skowronek, *Chirality*, **2000**, *12*, 263.

Chapter 4

Transient Helicity: Temporally Modulated Helical Self-assembly

Chapter 4

Transient Helicity: Temporally Modulated Helical Self-assembly

Abstract

Supramolecular motifs are inspired from nature in their aspect of utilization of non-covalent and multivalent interactions, self-organization etc. An approach for temporal control brings us a step nearer to biological systems. To employ supramolecular polymer as a synthetic mimic to biological systems which have an inherent control over chirality, functions and time. We herein present dipicolylethylenediamine (DPA) appended supramolecular motif that grow as a helical self-assembly in presence of adenosine phosphate and then racemizes dissimilar to earlier cases where an opposite conformation is also obtained. A temporal control over the system is obtained by employing adenosine phosphate hydrolyzing enzyme. This shall be extrapolated for applications such as temporally modulated enantioselective catalysis and optoelectronic functions.

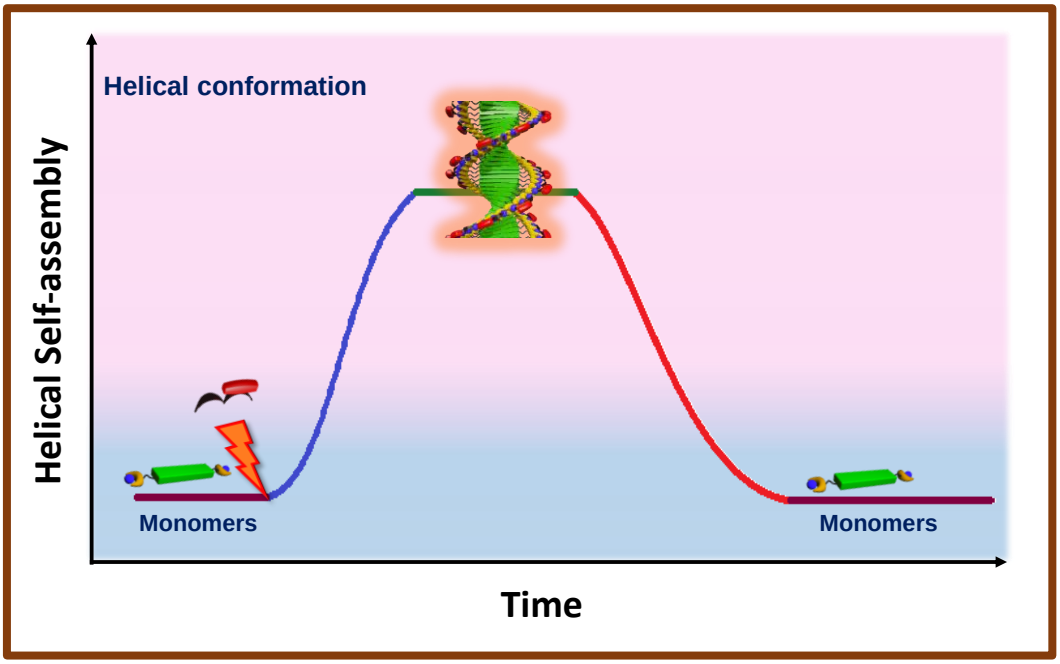

4.1 Introduction

Chirality is ubiquitous to nature from small molecules L-Amino acids and D-Sugars to assembled structures into α-helices in proteins and A/Z-DNA helices. Another important example is the right handed helix of actin filaments formed by self-assembly of G-actin proteins induced by chemical fuel adenosine triphosphate (ATP). F-actin proteins undergo chemical fuel-driven transient polymerization into right-handed helix and the hydrolysis of fuel ATP to ADP disfavours the assembled entropically unfavoured state.[1] In most cases, biological systems employ chemical fuel adenosine triphosphate (ATP), hence it's renowned as the biological energy currency.[2] This interesting fact inspires us to understand its importance and employ in synthetic systems for future advances.

In supramolecular chemistry, however, a thorough investigation of helical assemblies both with inherent chirality and guest-induced chiral organization is done over decades.[3] Most of these systems are passive in nature and thus, lack in temporal control. However, biological system have a perfect control on time for their functioning. Thus, there needs to be building of chemical fuel-driven transient system with temporally modulated helical organization under non-equilibrium similar to natural systems which can open key to many applications.

Additionally, transient systems addressed in the Chapter 2 and 3 are fundamental studies towards temporal control. We further want to extend these understandings and strategies for future prospective applications. To counter this, we need to visualize the system in real time for further insights into the mechanism of transiency which may act as a key link to build up systems with temporally programmed functions such as catalysis and optoelectronic applications.

In this chapter, we present core-substituted naphthalenediimide chromophore appended with zinc diethylenedipicolylamine that undergo adenosine phosphate induced transient helical assembly in presence of adenosine phosphate hydrolyzing enzyme with temporal modulation.

4.2 Design Strategy

Following a similar design as that of **NDPA** (Chapter 2-3) we have designed dipicolylethylenediamine–zinc complex (Zn-DPA) appended O-ethyl core substituted naphthalene diimide (NDI-OEt) derivative (**NDPA-OEt**) (Scheme 4.1) in the present Chapter.

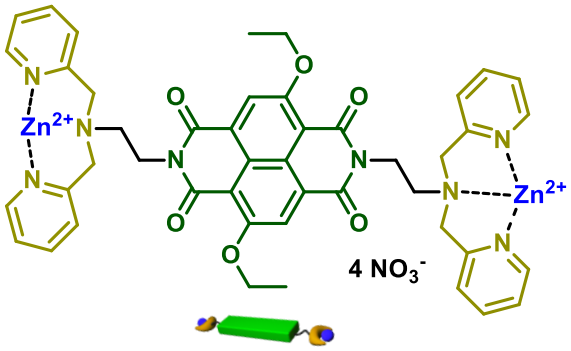

Scheme 4.1. *Structure and schematic representation of* ***NDPA-OEt****.*

The adenosine phosphate induced self-assembly driven by electrostatic interactions with the specific guest binding group Zn-DPA has been studied in the previous chapters. The naphthalenediimide derivative **NDPA** show that adenosine phosphates have preferential binding with Zn-DPA based on multivalent interactions. The chromophore provide π-π interactions to facilitate an efficient self-assembly and provides a spectroscopic readout to various transformations. The **NDPA** molecule lacks in fluorescence and hence can not serve the purpose of real-time visualization and further investigations under fluorescence microscopy. To address this, fluorescent analogue core-substituted naphthalenediimide derivative was synthesized. Core-substituted naphthalene diimides have been extensively studied by Matile and co-workers as fluorescent chromophores and hence we envisage that extending to similar chromophores would help us to monitor the self-assembly process in detail.[4]

4.2.1 Synthesis

NDPA-OEt was synthesized by the following Scheme 4.2 to 4.4 and the synthetic procedures are given below.

Synthesis of diBr-NDA (3), 4 and 5: Synthesis of molecules **4**-**6** was done following the literature procedure[5] (Scheme 4.2) and appropriately characterized.

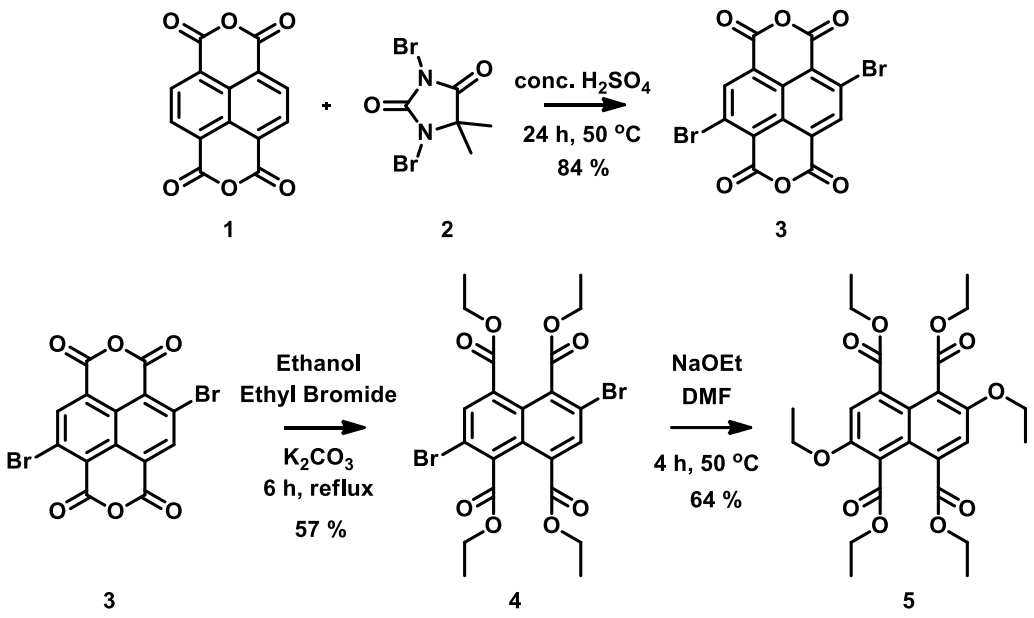

Scheme 4.2. *Synthetic scheme for the synthesis of diBr-NDA (**3**), **4** and **5** along with their structural representation.*

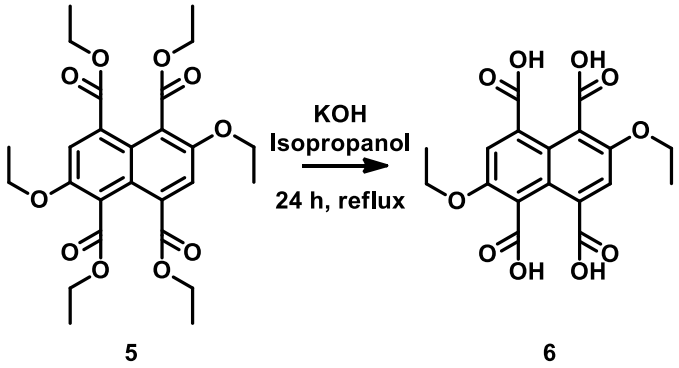

Scheme 4.3. *Synthetic scheme for the core-substituted tetraacid derivative synthesis of **6**.*

Synthesis of 6: 100 mg (0.198 mmoles) of **5** was added to 1 M KOH in isopropanol solution (16 mL) and refluxed for 24 h. The mixture was then evaporated to dryness to obtain grey residue as the product. The product was not subjected to any purification and used as obtained for the synthesis of **8**.

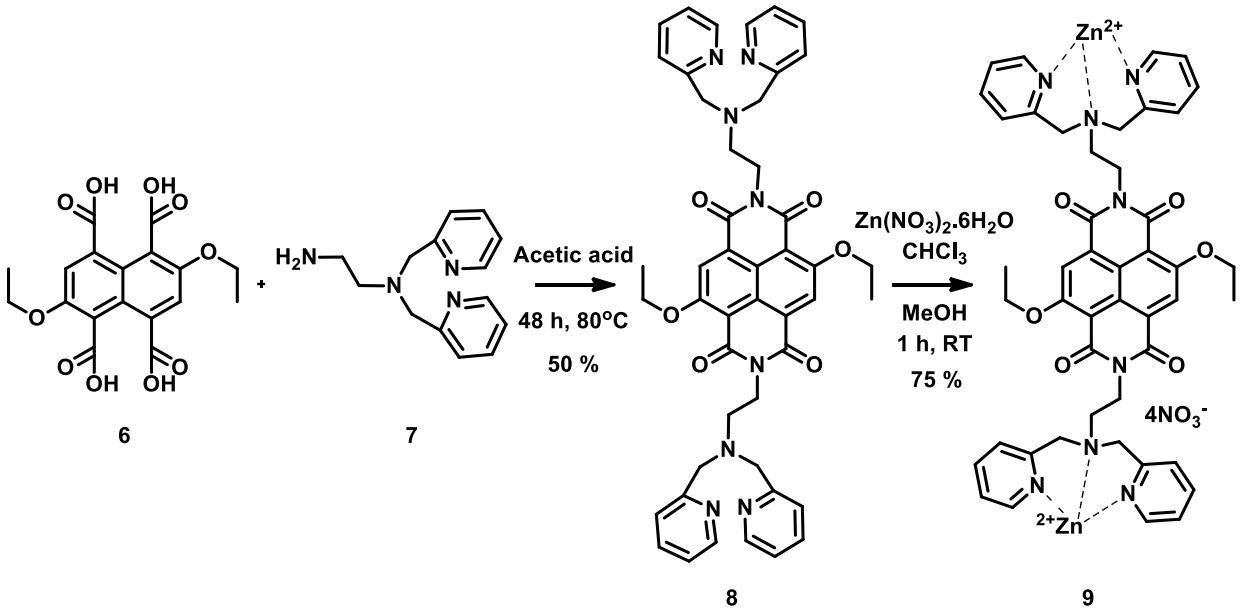

Scheme 4.4. *Synthetic scheme for the synthesis of* ***8*** *and NDPA-OEt (****9****).*

Synthesis of 7: Synthesis of molecule **7** was done following the literature procedure[6] (Scheme 4.2) and appropriately characterized.

Synthesis of 8: The synthesis was done following the literature procedure with slight modifications.[5] The crude residue obtained of **6** was dissolved in acetic acid (7 mL). **7** (48 mg, 0.198 mmoles) in acetic acid (1mL) was added to it and the mixture was heated at 80°C along with stirring for 24 h. Another batch of **7** (48 mg, 0.198 mmoles) in acetic acid (1mL) was introduced again and the heating was continued for additional 24 h to ensure completion of the reaction. After cooling to room temperature, the reaction mixture was neutralized to pH 7 with saturated Na_2CO_3 solution. The resultant solution was extracted with Ethyl acetate (3 x 50 mL) and the organic layer was dried over anhydrous Na_2SO_4. Solvent was evaporated and flash column chromatography with reverse phase silica (0-100% acetonitrile in water with 0.2 % TFA; R_f = 0.5 with 100% ACN with 0.3% TFA) gave the product (80 mg) in 50% yield.

^{1}H NMR δ_H (400 MHz; $CDCl_3$): 8.43 (s, 2H, ArH), 8.41(m, 4H, ArH), 7.40 (m, 8H, ArH), 7.03 (m, 4H, ArH), 4.49 (q, *J*=6.8Hz, 4H, OCH_2), 4.41 (t, *J*=6.4Hz, 4H, NCH_2), 3.93 (s, 8H, NCH_2Ar), 2.96 (t, *J*=6.4Hz, 4H, NCH_2CH_2) , 1.63 (t, *J*=6.8Hz, 6H, OCH_2CH_3).

HRMS (ESI): m/z: calcd for $C_{46}H_{44}N_8O_6$: 805.3456 $[M+H]^+$, found : 805.3457.

Synthesis of NDPA-OEt (9):

6 (47 mg, 0.058 mmoles) was dissolved in 1 ml of $CHCl_3$. To its stirring solution $Zn(NO_3)_2.6H_2O$ (38 mg, 0.058 mmoles) in MeCN (0.1 mL) was added and the solution was stirred for 2 h. A yellow precipitate was obtained. It was filtered and washed with $CHCl_3$. The precipitate was dissolved in minimum amount of MeCN and it was re-precipitated by $CHCl_3$. The solid was filtered and dried in vacuum at 50 °C. 52 mg (yield= 75%) of yellow compound was obtained.

^{1}H NMR δ_H (400 MHz; DMSO-d6): 8.65 (br, 4H), 8.33 (br, 2H), 8.12 (br, 4H), 7.65 (br, 8H), 4.47 (d+q, 8H), 4.37 (br, 4H), 4.18 (d, 4H), 2.8 (s, 4H), 1.46 (t, 6H). ^{1}H NMR peaks were broad due to strong aggregation tendency at high concentration. ^{13}C NMR has to be recorded. HRMS could not be measured as Zinc was cleaving under mass spectrometric conditions and futher attempts will be made.

4.3 Adenosine Phosphate Induced Helical Self-Assembly

The molecular design is of **NDPA-OEt** is similar to **NDPA**, the core-substituted naphthalene diimide fluorescent aromatic core is functionalised with the phosphate recognition unit Zn-DPA. The former assists the self-assembly by π-π interactions and the latter promotes the same by binding the phosphates. The bola-amphiphilic zinc salt, **NDPA-OEt** is soluble in polar solvents such as water.

The substitution at aromatic core do not alter much the vibronic fine structure of π-π* transition in absorption around 320-400 nm and corresponding fluorescence spectra. The origin of core-substituted NDI (cNDI) color is the presence of a new charge transfer band n-π* which undergo bathochromic shift with increasing push–pull character of the cNDI. There is substituent dependent change in ‘‘bandgap’’ with the donating ability of the substituents.[4] Although cNDI have been synthesized for optoelectronic properties, but limited investigations of their self-assembly behaviour has been done so far.[7] Thus, we synthesized the corresponding cNDI with DPA functionalised to understand its activities.

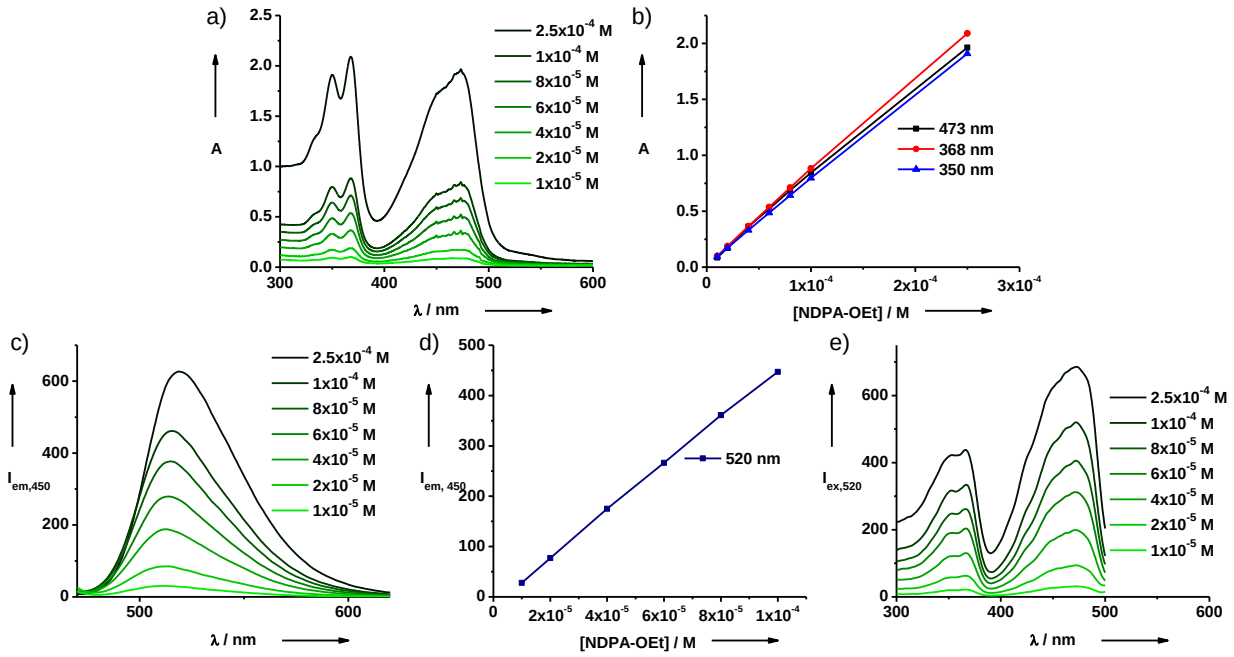

Figure 4.1. *Concentration dependent spectroscopic studies of* ***NDPA-OEt****. a) Absorption spectra, b) corresponding changes in absorbance at various wavelengths, c) emission spectra at* λ_{ex} *= 450 nm, d) corresponding changes in emission intensity at 520 nm and e) excitation spectra at* λ_{em} *= 520 nm (90% 10 mM aq. HEPES, T = 30 ℃).*

Prior to guest-induced self-assembly of **NDPA-OEt**, concentration dependent study was performed to understand its characteristics as a free chromophore. Increasing concentration of **NDPA-OEt** show no shift in λ_{max} and the sharp vibronic features of π-π* band, thus following linear increase, indicative of lack of any assembly in absence of guest (Figure 4.1a,b). The corresponding emission spectra at λ_{ex} = 450 nm show a decrease in emission with decreasing molecular concentration suggesting a linear accordance with absorption (Figure 4.1b-d). Excitation spectra at λ_{em} = 520 nm also matches well with the absorption spectra, thus reiterate the presence of molecularly dissolved **NDPA-OEt** in absence of any binding guests (Figure 4.1e).

4.3.1 Adenosine Diphosphate Induced Self-Assembly

For adenosine diphosphate induced self-assembly, titration of **NDPA-OEt** with ADP and was performed and the changes in absorption, CD and fluorescence were monitored (Figure 4.2). The absorption studies of **NDPA-OEt** (2.5 x 10^{-4} M, 10 mM aq. HEPES buffer) in absence of any

guest show sharp π-π* absorption band (368 and 350 nm) characteristic features of molecularly dissolved cNDI chromophores.[4] The addition of ADP resulted in broadening of absorption spectra, red shift in λ_{max} along with reversal of relative intensity of vibronic bands at 350 nm and 368 nm characteristic of cNDI chromophoric self-assembly (Figure 4.2a,b).

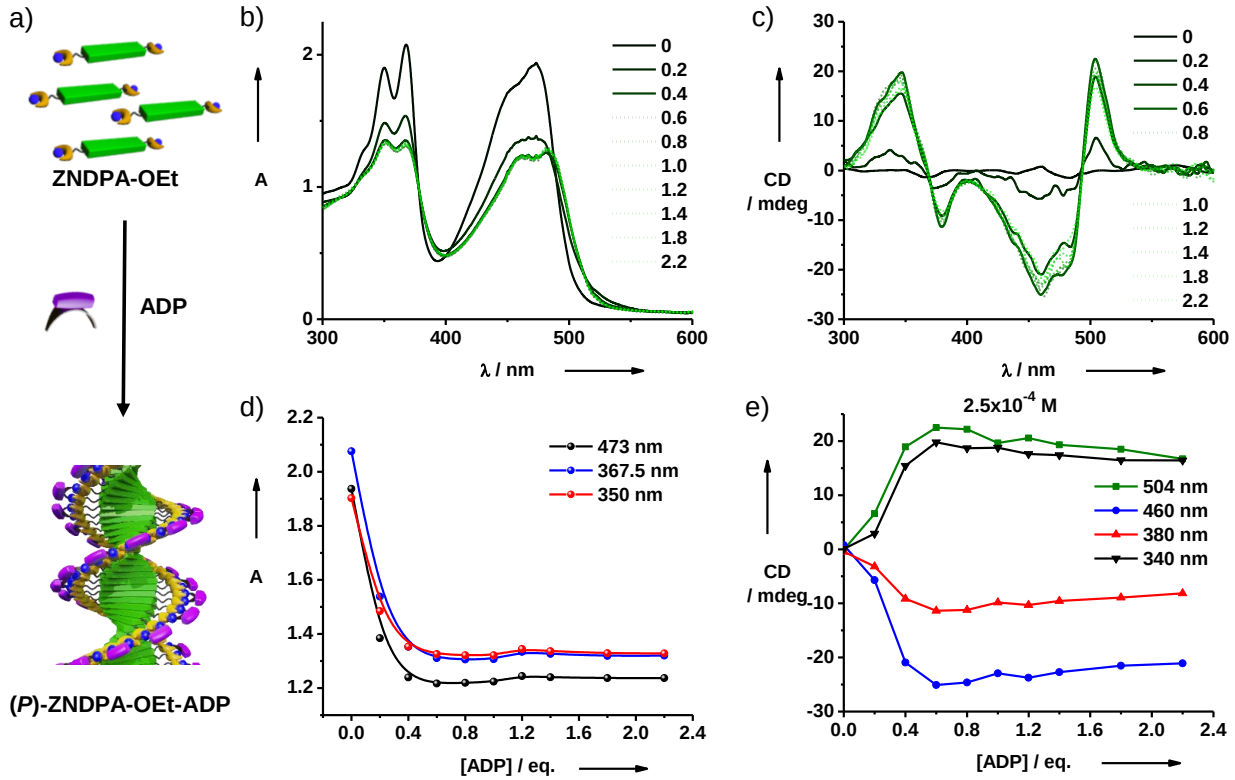

Figure 4.2. *ADP-induced self-assembly in* ***NDPA-OEt****. a) Schematic representation of formation of (P)-****NDPA-OEt****-ADP. Change in b) absorption spectra and c) CD spectra with addition of ADP depicting formation of P-type helical assembly. Corresponding changes in d) absorbance and e) CD intensity at various wavelengths with increasing equivalents of ADP ([****NDPA-OEt****] = 2.5 x* 10^{-4} *M, 10 mM aq. HEPES buffer, T = 30 ℃).*

Appearance of two bisignated CD signals centred around their respective absorption maxima of π-π* and n-π* bands, arising due to excitonic coupling between the chromphores suggest formation of chiral assemblies (Figure 4.2c). The CD spectra with dominant positive first CD signal and then negative CD signal centred on 500nm suggest a right handed (*P*)-**NDPA-OEt**-ADP chiral assembly (Figure 4.2b). The plot of changes in absorption and CD changes with equivalents of ADP saturates at 0.4 eq. and 0.6 eq. ADP, respectively (Figure 4.2d,e). Although, mathematically for complete binding the saturated equivalents required should be 1.0, but a lower

requisite equivalent propose probably an efficient one site clipping of ADP to DPA for resulting in aggregation of **NDPA-OEt**.

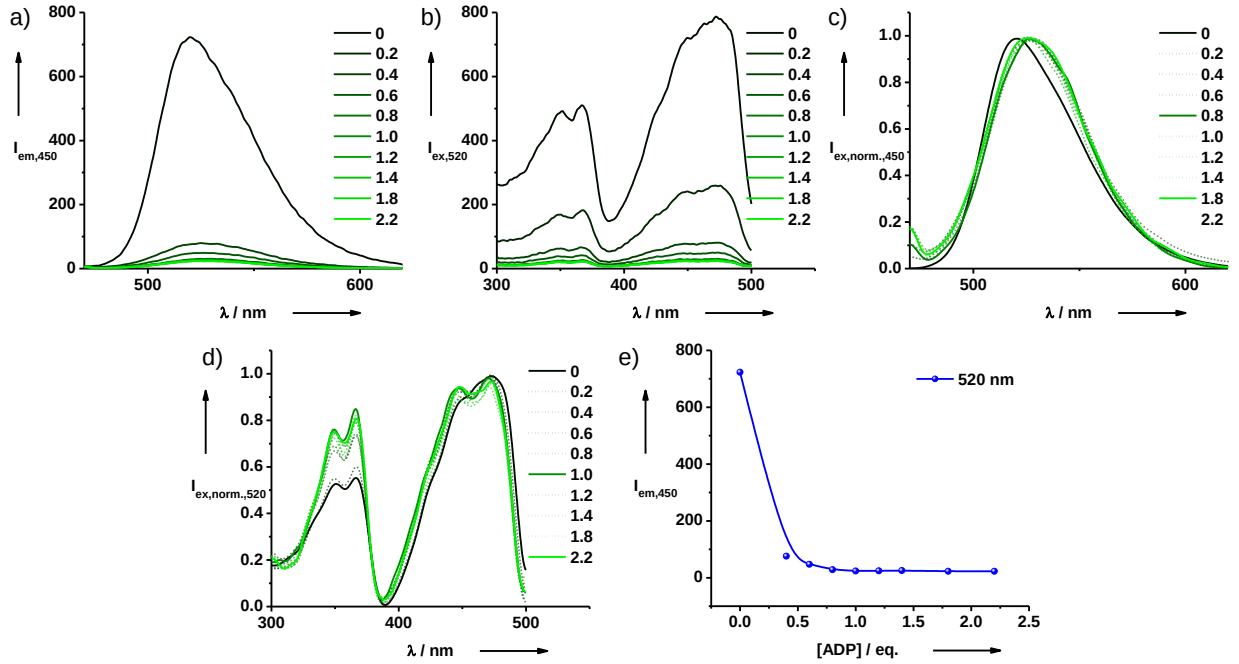

Figure 4.3. *ADP-induced self-assembly in* ***NDPA-OEt****. a) Emission spectra at* λ_{ex} *=450 nm, b) excitation spectra at* λ_{em} *=520 nm, c) and d) respective normalized spectra and e) emission changes with increasing equivalents of ADP ([****NDPA-OEt****] = 2.5 x* 10^{-4} *M, 10 mM aq. HEPES buffer, T = 30 ℃).*

Since cNDI are fluorescent in monomeric state with quantum yield of 22%, further investigations into the fluorescence changes on ADP-induced self-assembly in **NDPA-OEt** were done to find out the emissive nature of aggregate, if any, and thereby analyse the type of aggregation H or J. Excitation of molecule at 450 nm prior to ADP addition showed non-aggregated emissive state (Figure 4.3). On addition of ADP, aggregation caused quenching is observed with insignificant shift in λ_{max} on normalization, thus the residual fluorescence observed is due to monomeric emission. Reiterating this observation, excitation spectra at 520 nm on addition of ADP do not match with the corresponding absorption spectra, whereas it correlates to monomeric absorption spectra with sharp vibronic features and no reversal of vibronic bands. Thus, we conclude that ADP-induced self-assembly of **NDPA-OEt** form non-emissive H-aggregates which is further confirmed from the time-resolved fluorescence studies (vide infra).

Thus, **NDPA-OEt** on binding to ADP form non-emissive right handed helical (*P*)- **NDPA-**

OEt-ADP H-aggregates.

4.3.2 Comparison of Guest-Induced Self-Assembly

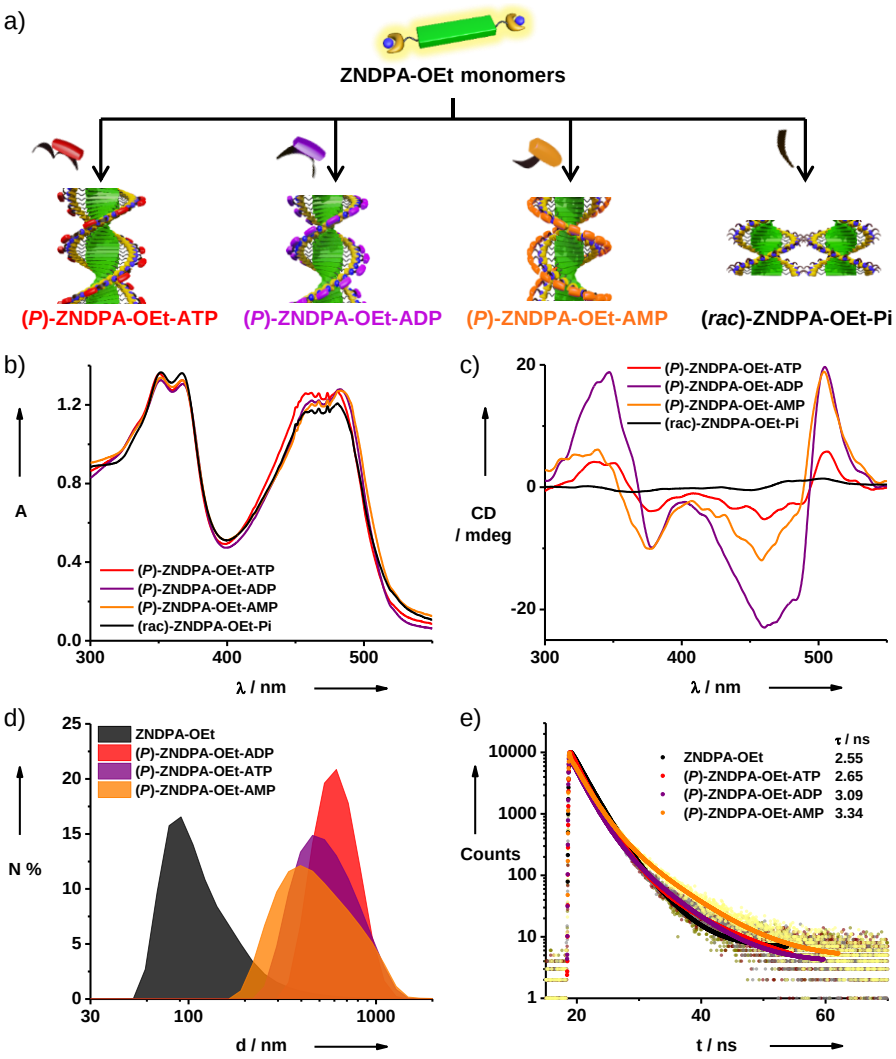

Figure 4.4. *Guest-induced self-assembly in* ***NDPA-OEt****: a) Schematic representation of formation of* ***NDPA-OEt*** *assembly. Saturated equivalent of guest-induced self-assembly b) Absorption spectra, c) CD spectra, d) Dynamic Light Scattering data, e) Lifetime data ([****NDPA-OEt****] = 2.5 x* 10^{-4} *M, 10 mM aq. HEPES buffer, T = 30 ℃).*

Similar titrations were done for other phosphate guests ATP, AMP and Pi (Figure 4.4a). The guest induced self-assembly of **NDPA-OEt** show that molecule is unselective to the adenosine phosphate. All the three adenosine phosphate form right handed helical self-assembly depicted by the reversal of vibronic bands in absorption spectra and bisignated CD spectra whereas inorganic

phosphate induces racemic self-assembly (Figure 4.4b,c). The DLS data depicted that all of the three adenosine phosphate form aggregates ranging from 300-800 nm size (Figure 4.4d). The lifetime of the resultant solution matches to that of monomeric **NDPA-OEt** ~2.5 ns, hence confirming the formation of H-type non-emissive aggregates (Figure 4.4e).

4.4 ATP-Fuelled Transient Helicity in NDPA-OEt Self-Assembly

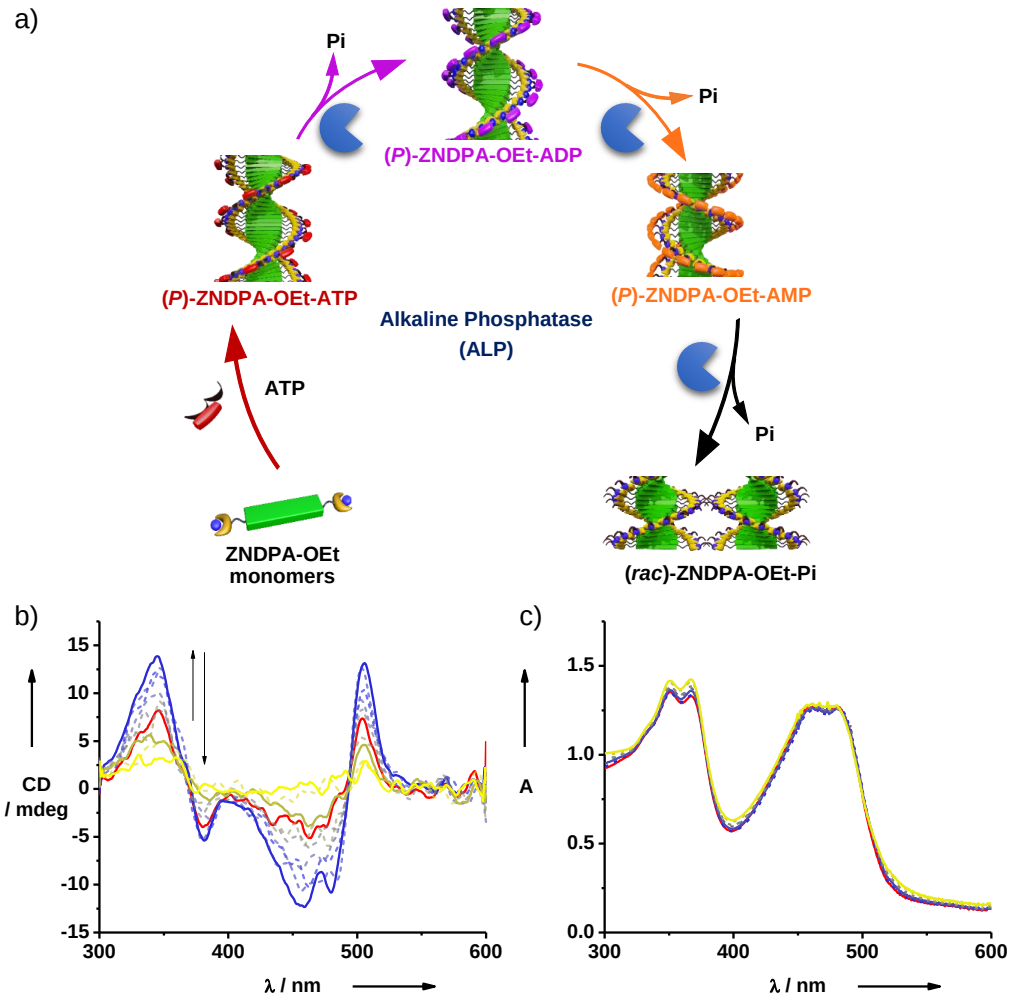

Figure 4.5. *ATP-fuelled transient helicity of* ***NDPA-OEt*** *self-assembly mediated by alkaline phosphatase: a) Schematic representation of alkaline phosphatase mediated transient helicity of* ***NDPA-OEt*** *self-assembly. b) Time dependent CD spectra depicting gradual evolution of CD signal followed by gradual decrease. c) Time dependent absorption spectra indicating insignificant change in extent of assembly (**[NDPA-OEt]** = 2.5 x 10^{-4} M, [ATP] = 0.5 eq., [ALP] = 0.5 U/mL, 10 mM aq. HEPES buffer, T = 25 ℃).*

Amongst these guests, the intensity of CD signal follows ADP>AMP>ATP>Pi=0. Additionally the CD signal of ADP and AMP saturate at a lower equivalents then corresponding ATP induced signal. Thus, we envisaged that *insitu* conversion of ATP to ADP should result in gradual evolution of CD signal and the hydrolysis of ADP to AMP to Pi should then slowly decrease to zero (Figure 4.5). Hence, we should observe transient helicity corresponding to helical assembly.

To observe transient helicity in **NDPA-OEt** assembly, a solution of **NDPA-OEt** (2.5×10^{-4} M, 10 mM aq. HEPES buffer) and 0.5 U/mL Alkaline phosphatase (ALP) was taken, to it 0.5 eq. of ATP was added and time dependent CD and absorption spectra was recorded. The CD spectra showed a gradual evolution of signal corresponding to the *in situ* hydrolysis of ATP to ADP till a saturation was observed. After which a gradual disappearance of signal was observed owing to further hydrolysis of ADP to Pi via AMP. The corresponding absorption spectra depicted no significant changes in vibronic features verifying that system is under assembled state. Thus, we could successfully obtain transient helicity in supramolecular polymer. Further investigations to modulate rate and lifetime of cycle is under study.

4.5 Conclusion

To conclude, we have presented a highly dynamic helical chromophoric assembly induced by phosphate guests. We then utilized to build a distinct transient system with temporally controlled evolution and disappearance of helicity of the self-assembly. This work mimics the formation of actin helical assemblies which do not undergo any conformational switching. The modularity of the system is under investigation.

4.6 Experimental Section

General Methods:

Optical Measurements: Electronic absorption spectra and Circular Dichroism measurements were performed on a Jasco J-815 spectrometer where the sensitivity, time constant and scan rate were chosen appropriately. Corresponding temperature dependent measurements were performed

with a CDF – 426S/15 Peltier-type temperature controller with a temperature range of 263-383 K and adjustable temperature slope. Optical measurements were recorded in 10 mm path length cuvettes. CD spectra and time dependent CD changes were smoothened by adjacent averaging and fitted using first order kinetics to calculate rate constants. We are aware of the fact that enzymatic changes are not in theory first order changes, but a fit enables us to have a relative kinetic perspective between individual processes.

NMR Measurements: NMR spectra were obtained with a Bruker AVANCE 400 (400 MHz w.r.t. ^{1}H nuclei) Fourier transform NMR spectrometer with chemical shifts reported in parts per million (ppm).

Dynamic light scattering (DLS): The measurements were carried out using a NanoZS (Malvern UK) employing a 532 nm laser at a back scattering angle of 173°. A dead time (Time between sample loading and starting of measurement by the machine) of around 45 seconds is present in all measurements.

Sample Preparation:

All solutions were prepared in 10 mM HEPES. Stocks were prepared as $2.5x10^{-3}$ M **NDPA-OEt**, $5x10^{-2}$ M ATP, $5x10^{-2}$ M ADP, $5x10^{-2}$ M AMP and $5x10^{-2}$ M Pi, 0.5 U/µL ALP. Micropipette was used to transfer measured volumes of solution. Dead time (time between fuel injection and starting of measurement by the machine) in all the measurements were less than 60 seconds. Temperature was maintained at 30 °C for **NDPA-OEt** to have a sufficiently high enzyme activity and clear CD signals throughout the measurements. The samples were measured in a 10 mm quartz cuvette.

Protocol for transient helicity:

For only ALP mediated cycles: To a solution of molecule, ALP was added, then fuel (ADP/ATP) was added and measurements were done.

"*(P)*-**NDPA-OEt**-ATP" term used in main text refers to 2.5 x 10^{-4} M solution of **NDPA-OEt** (in 10 mM aq. HEPES buffer) with ATP. "*(P)*-**NDPA-OEt**-ADP" term refers to 2.5 x 10^{-4} M solution of **NDPA-OEt** (in 10 mM aq. HEPES buffer) with ADP. "*(P)*-**NDPA-OEt**-AMP" term refers to 2.5 x 10^{-4} M solution of **NDPA-OEt** (in 10 mM aq. HEPES buffer) with AMP."*(rac)*-**NDPA-OEt**-Pi" term refers to 2.5 x 10^{-4} M solution of **NDPA-OEt** (in 10 mM aq. HEPES buffer) with Pi.

"ALP" refers to Alkaline Phosphatase.

Materials: Calf Intestinal Alkaline Phosphatase (1.75 units/mg), Adenosine-5-Diphosphate Disodium Salt (extrapure for biochemistry) and Sodium Phosphate Dibasic Dihydrate (extrapure for biochemistry) were purchased from Sisco Research Laboratories Pvt. Ltd. India. Adenosine-5-Triphosphate Disodium Salt (99%), Adenosine-5-Monophosphate Disodium Salt (99%), were purchased from Sigma Aldrich. HEPES (4-(2-hydroxyethyl)-1-piperazineethanesulfonic acid) was procured from SD fine chemical limited.

4.7 References

1. A. Nürnberg, T. Kitzing, R. Grosse, *Nat. Rev. Cancer* **2011**, *11*, 177-187.
2. F. H. Westheimer, *Science* **1987**, *235*, 1173
3. E. Yashima, N. Ousaka, D. Taura, K. Shimomura, T. Ikai, K. Maeda, *Chem. Rev.* **2016,** *116*, 13752–13990.
4. N. Sakai, J. Mareda, E. Vauthey, S. Matile, *Chem. Commun.* **2010**, *46*, 4225-4237.
5. R. S. Kishore, V. Ravikumar, G. Bernardinelli, N. Sakai, S. Matile, *J. Org. Chem.* **2008**, *73*, 738-740.
6. H. N. Lee, Z. Xu, S. K. Kim, K. M. K. Swamy, Y. Kim, S.-J. Kim and J. Yoon, *J. Am. Chem. Soc.* **2007**, *129*, 3828-3829.
7. a) S. Bhosale, S. Matile, *Chirality* **2006**, *18*, 849-856; b) H. Kar, D. W. Gehrig, F. Laquai, S. Ghosh, *Nanoscale* **2015**, *7*, 6729-6736; c) H. Kar, D. W. Gehrig, N. K. Allampally, G. Fernández, F. Laquai, S. Ghosh, *Chem. Sci.* **2016**, *7*, 1115-1120; d) H. Kar, S. Ghosh, *Chem. Commun.* **2016**, *52*, 8818-8821.

Outlook

Temporal Control on Supramolecular Assemblies and their Functions

Outlook

Temporal Control on Supramolecular Assemblies and their Functions

Abstract

Inspired from biological systems such as cytoskeleton proteins and transmembrane proteins to function out-of-equilibrium for spatio-temporal control, we urge towards utilization of the synthetic manifestations of the systems under study and their analogues into material applications. In this outlook Chapter, we summarize few future projects we would like to pursue in this direction.

Future and Ongoing Projects

Our first aim is real-time visualization of the transient cycle of these systems for further insights into the mechanism of growth and decay as well as the physical states of the molecule during the transient changes (Scheme 1a). We would like to monitor these processes with high resolution fluorescence microscopes.

To achieve this, two approaches are under study: firstly fluorescent analogues i.e core-substituted naphthalene diimide[1] of the molecule **NDPA** (Scheme 1b) is under synthesis and secondly fluorescent analogue of guest adenosine phosphates is also being targeted. For latter, single fluorescent tag ATP has been purchased (R_2 = H) to be used in a similar experiment (Scheme 1c). Additionally, Förster resonance energy transfer (FRET) pair is being synthesized (R_2 = Acceptor) that gives supplementary information differentiating ADP with ATP.[2]

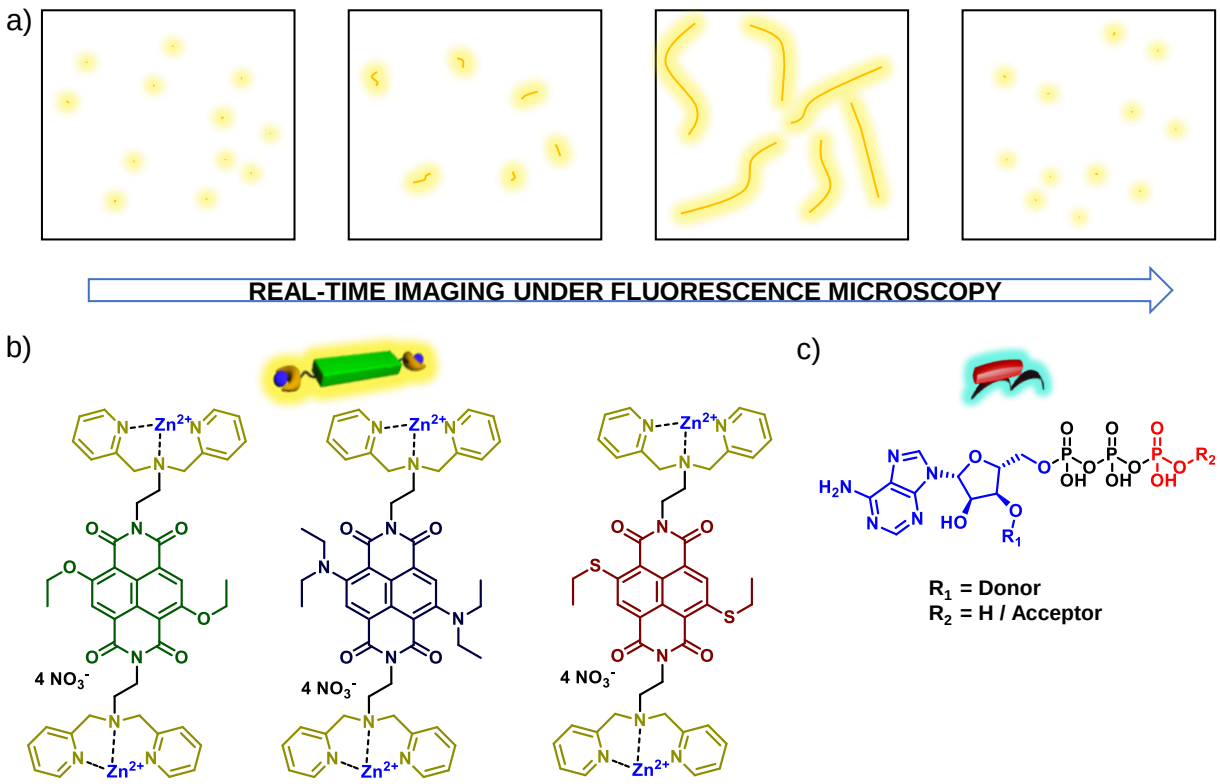

Scheme 1: *Real-time visualization of transient self-assembly: a) Schematic representation of real-time imaging under fluorescence microscopes depicting transient self-assembly. b) Structures of fluorescent core-substituted naphthalene diimide derivatives of* ***NDPA****, green aromatic core with ethanol substitution, blue with N,N-diethyl amine and red with ethane thiol. c) Fluorescent ATP analogue* R_1 *= Fluorescent molecule,* R_2 *= H, Fluorescent ATP analogue with FRET pair* R_1 *= Fluorescent Donor,* R_2 *= Fluorescent acceptor.*

Our second objective is for transient materials applications such as in catalysis and optoelectronics. To alleviate the transient catalysis, system is designed such that the catalytic activity is associated with the transient self-assembled state (Scheme 2a,b). For achieving this catalytic group-substituted naphthalene diimide of the molecule **NDPA** is under synthesis. Catalytic groups being used are carboxylates, guanidinium, imidazole etc., which are known in literature for catalysis (Scheme 2c).[3-5] Supramolecular polymers of such monomeric units can provide surface for catalysis through multivalent and hydrophobic interactions. Thus, we believe the present design should fulfill the required purpose.

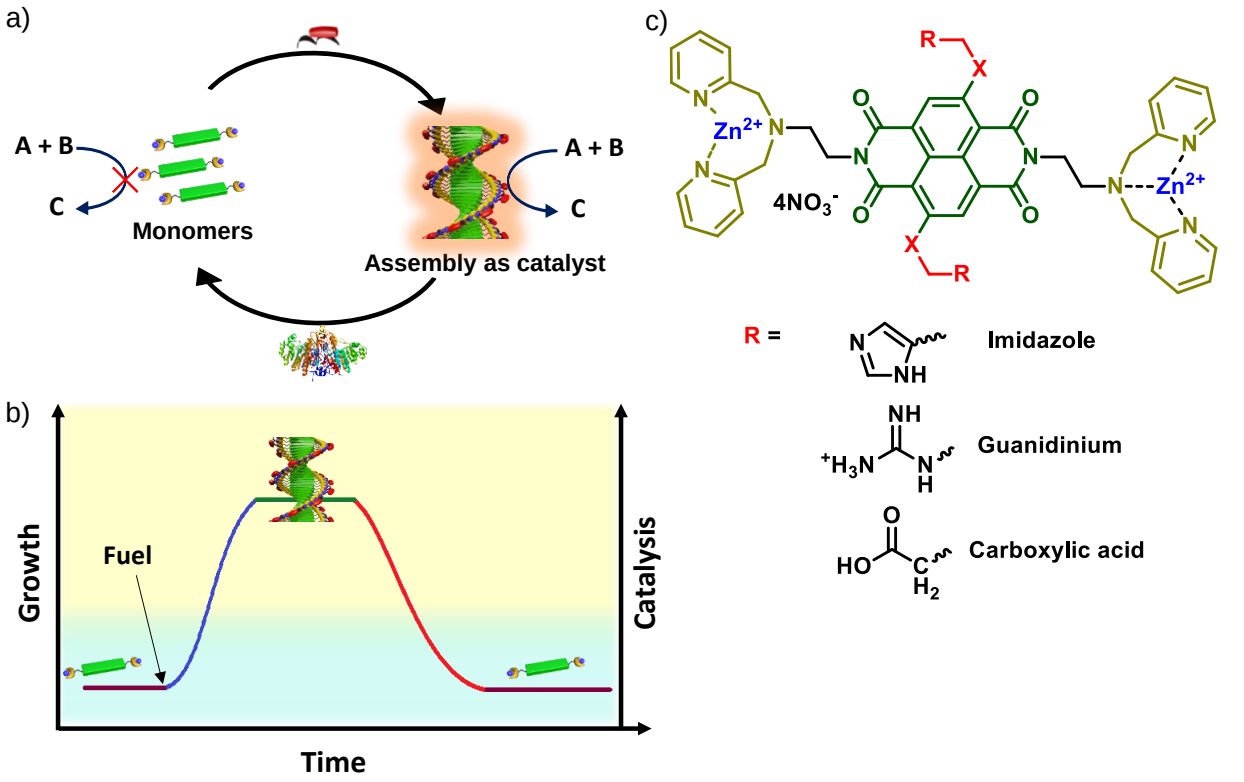

Scheme 2: *Transient catalysis: a) Schematic representation of transient self-assembly with catalysis mediated only by self-assembled transient state. b) Schematic representation correlating temporal changes in growth with catalysis. c) Structures of core-substituted naphthalene diimide derivatives of* ***NDPA****, X = -NH, -NR, -O or –S.*

For synthetic manifestation of temporally controlled electronic applications, we envisage the usage of semiconducting organic molecules and program their assembly characteristics. Our group has been working with methyl dodecyl viologen (**MV-12**) and coronene carboxylic acid salt (**CS**) that form linearly aligned fibers with high conductivity (Scheme 3a).[6] With the collaboration of Prof. Kulkarni's group, we have shown that these could be used in electronic devices.[7] Although, the system shows desirable properties, we take a step forward to temporally modulate the electronic systems, hence forming "transient electronics".

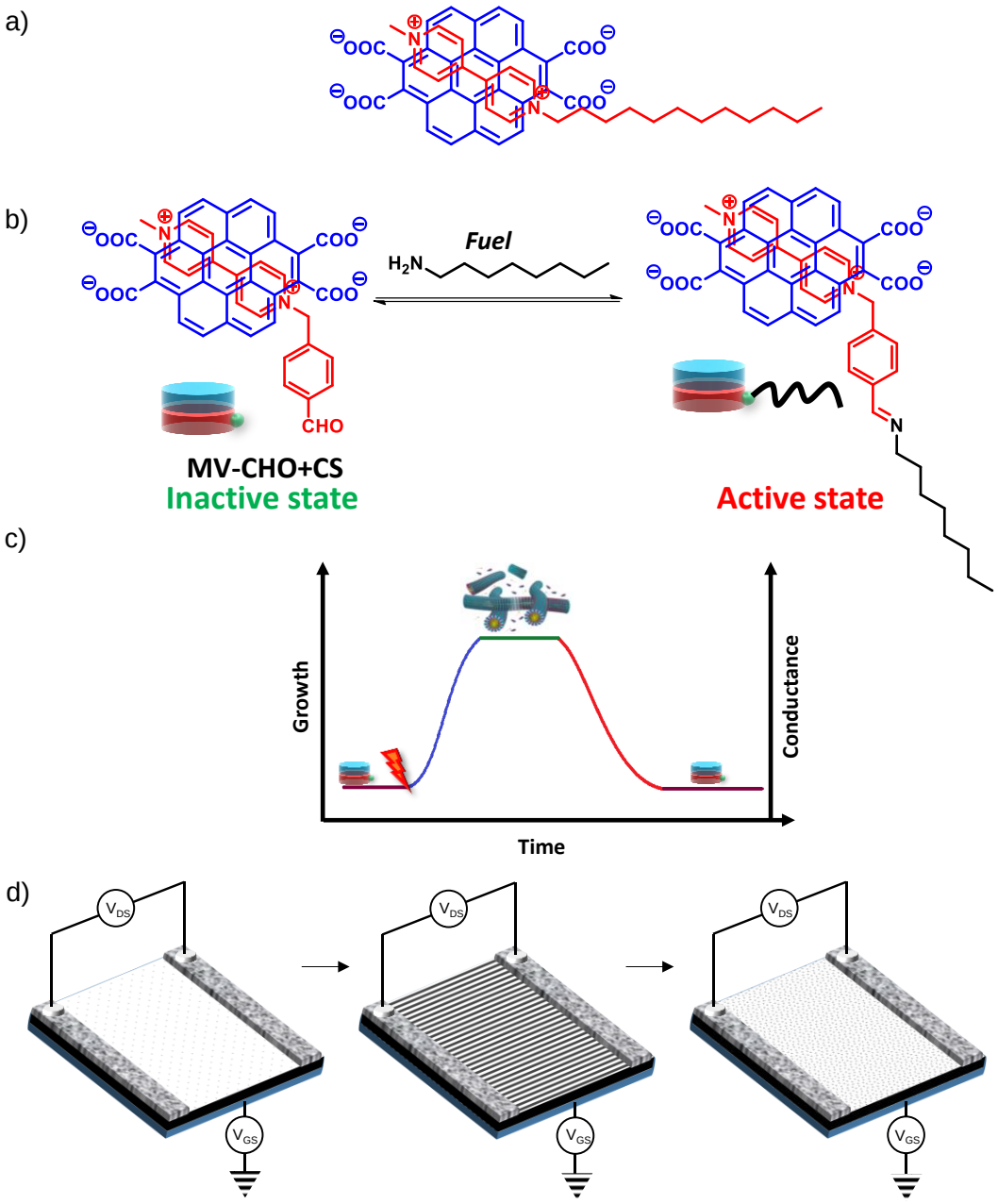

Scheme 3: *Transient electronics: a) Structure of* ***MV-12*** *and* ***CS*** *charge-transfer pair, b) Structure of* ***MV-CHO*** *and* ***CS*** *charge-transfer pair and schematic representation of transient self-assembly driven by imine bond formation. c) Schematic representation correlating temporal changes in growth with conductance across electrodes. d) Schematic representation of temporally controlled CT transient assembly between the electrodes on transistor.*

To alleviate this non-aggregating non-amphiphilic charge transfer derivatives have been synthesized. The hydrophilic methyl viologen benzaldehyde (**MV-CHO**) act as a receptor group to covalently attach hydrophobic amine forming imine bond. The resultant molecule is amphiphilic

in nature and hence capable of undergoing self-assembly (Scheme 3b). Different strategies for making it under transient conditions by breaking of dynamic imine bond is under investigations. Thus, forming these assemblies in between the electrodes shall result in transient electronics (Scheme 3c) and also serve as a technique to form highly aligned fibers across the electrodes for high performance transistors (Scheme 3d).

References

1. N. Sakai, J. Mareda, E. Vauthey, S. Matile, *Chem. Commun.* **2010**, *46*, 4225-4237.
2. N. Hardt, S. M. Hacker, A. Marx, *Org. Biomol. Chem.* **2013**, *11*, 8298-8305.
3. M. O. Guler, S. I. Stupp, *J. Am. Chem. Soc.* **2007**, *129*, 12082-12083.
4. C. Zhang, X. Xue, Q. Luo, Y. Li, K. Yang, Y. Jiang, J. Liu, G. Zou, X.-J. Liang, *ACS Nano,* **2014**, *8*, 11715 - 11723
5. N. Singh, K. Zhang, C. A. A. -Pach´on, E. Mendes, J. H. van Esch, B. Escuder, *Chem. Sci*. **2016**, *7*, 5568–5572.
6. K. V. Rao, K. Jayaramulu, T. K. Maji, S. J. George, *Angew. Chem.* **2010**, *122*, 4314-4318.
7. U. Mogera, M. Gedda, S. J. George, G. U. Kulkarni, *ChemNanoMat.* **2017**, *3*, 39–43.

List of publications:

From Thesis:

1. S. Dhiman, A. Jain, S. J. George, Transient Helicity: Fuel-Driven Temporal Control over Conformational Switching in a Supramolecular Polymer, *Angew. Chem. Int. Ed.* **2017**, *129*, 1349-1353 (Hot paper). Highlighted in Nature Nanotechnology.
2. S. Dhiman, A. Jain, S. J. George, ATP-Fuelled Multistate Transient Self-assembly *(Manuscript under preparation)*

Other works:

1. R. Jana, S. Dhiman, S. C. Peter, Facile solvothermal synthesis of highly active and robust Pd1. 87Cu0. 11Sn electrocatalyst towards direct ethanol fuel cell applications, *Materials Research Express* **2016**, *3*, 084001.
3. K. Jalani, S. Dhiman, A. Jain, S. J. George, Temporal Switching of an Amphiphilic Self-assembly by a Chemical Fuel-Driven Conformational Response *(Manuscript under review)*